POSITRON ANNIHILATION IN METALS

FATHI A. EL KHANGI
B.Sc.(Hons.), Khartoum; M.Sc.(London)

A Thesis Submitted for the Degree of
DOCTOR OF PHILOSOPHY
in the
University of London

Physics Department
Bedford College
London
1980

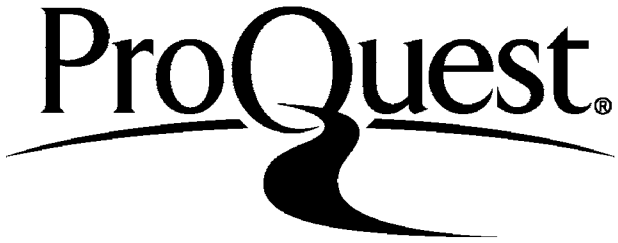

TO HIM.

A HUMBLE GESTURE OF INFINITE GRATITUTE.

ABSTRACT

The Doppler broadened annihilation gamma ray line Shape (511-kev) resulting from the interaction of thermalized positrons with a metallic lattice has been measured for a number of metals — Cadmium, Indium, Tin, Aluminium and Lead; either as single crystals, or in polycrystalline form between 4.2° K and their melting temperature by means of a high resolution germanium detector.

Application of the trapping model to parameters derived from changes in the annihilation line profiles provides monovacancy formation energies for thermally generated vacancies.

Other phenomena and their possible effects - e.g. thermal expansion, meta-stable self trapping of positrons, positron zero point motion, di-vacancies-are explored in order to achieve a better understanding of the overall temperature-or defect concentration-dependance of the line profile and thus a better estimate for the vacancy formation energies of the metals studied.

A positron can be demonstrated to be an extremely sensitive probe of the environment in which it annihilates. By using the Convolution technique the probability of positron annihilation with Core and Conduction electrons can be calculated throughout the temperature range-or defect concentration in question.

Inclusion of zero point motion of trapped positrons in the analysis of these line shape profiles lends a possibility to estimating the trapping probability in a more direct fashion for some metals, and therefore an alternative method of testing some of the assumptions and conclusions of the conventional way in which the trapping model is currently, and widely, applied.

ACKNOWLEDGEMENTS

I would like to express my deep and sincere gratitude and debt to Dr. P. Rice-Evans for his able supervision, constant encouragement, and valuable suggestions during the course of this research; and to Professor E.R. Dobbs for his interest in the work.

The author would also like to thank Dr. M. Lea for his help and advice with the cryogenic system.

It is a pleasure to acknowledge and thank Dr. I. Chaglar, Mr. A. Berry, Mr. McGetrick and Mr. A. Moghimi for their generous help, willing cooperation, numerous and valuable discussions, and above all infinite patience. My special thanks in particular to Dr. I. Chaglar and Mr. A. Berry for their kind assistance with the diagrams and drawings preparation.

I would like to thank Messrs. W.A. Baldock, A.K. Betts, S. Sen, T. Le Mottee, J. Sales, F. Grimes, A. King and D.J. Gower for all the technical assistance which is much appreciated.

The invaluable help of the Computer Unit Staff, Dr. P. Pal, Mr. P. Taylor, Mr. M. Datko, Mr. D.J.Waddell, Mr. R.C. Rogers, Mr. C.R. Kirton and also the staff of the University of London Reactor Centre, Mr. E.A.Y. Caesar and Dr. G.D. Burholt is gratefully acknowledged.

I would also like to express my gratitude and thanks to Mrs. S. Pearson, Mrs. S. Casey and above and beyond all to Miss A. Withers for generously saving a desperate situation at the later stages of typing.

Finally, I would like to thank the Government of the Democratic Republic of Sudan for the financial support and the staff of Sudan House in London for their help. A special thanks to all those members of the Physics Department who have made my stay at Bedford College a pleasant and an interesting experience.

TABLE OF CONTENTS

1. INTRODUCTION

1.1 General Introduction

Positrons were first predicted by Dirac. If all the negative energy states for electrons are filled then the "sea" of occupied states is not detectable because all transitions are forbidden by Pauli's principle. An electron could make a transition to a vacant positive energy state if it obtained at least $2m_0C^2$ energy when it would be observable as would the "hole" or positron left in the negative state.

In 1932 Anderson [1] verified experimentally the existence of the positron by the observation of tracks in a cloud chamber exposed to cosmic radiation at Pasadena. Positrons can be produced when photons interact with matter. Pair creation is forbidden in free space by conservation of energy and momentum and usually occurs in the field of an atomic nucleus which recoils with the excess momentum imparted by the photon. Loss of kinetic energy to the nucleus is small because of the relative masses. Small differences in the energies of the positron and the electron are due to the potential energy differences in the field of the positive nucleus.

The positron is entirely stable in vacuo but annihilates with an approaching electron, the exact reverse of pair production. On interaction with matter, positrons annihilate with electrons into gamma - quanta. Several early reviews [2] [81] highlight some of the activities during the initial period, the 1950's and early 1960's, in the history of positron annihilation.

First attempts to correlate the difference between angular correlation curves at room temperature and very near the melting temperature with positron - defect interaction in metallic lattice are credited to Mackenzie [11]. Convincing evidence of the role played by defects was established when large similar effects on positron lifetimes were found [12]. A further piece of this puzzle fell in place when it was recognized that the temperature dependence of positron lifetimes and nuclear magnetic resonance line widths appeared remarkably similar. The nuclear magnetic resonance experiments had already been satisfactorily explained on the basis of vacancy - controlled diffusion process [3].

The issue had been obscured for a while because of the temperature independance in some metals like mercury and the alkali metals, which were nevertheless known to have large vacancy concentrations below their melting points. This is partly cleared now by predictions claiming the positron vacancy binding energies in these metals to be small [4].

Deformation or heating of the sample to elevated temperatures causes remarkable changes in the annihilation characteristics. Since these changes were too big to be attributed to bulk properties , they were explained in terms of positron trapping by crystal imperfections. The classification and description of various defect types is considered at length in any of a number of references on the subject [5], [6],[7],[8]. In defects, where atoms are missing or their density is locally reduced, the repulsion between the positron and ion cores is decreased. Also the redistribution of electrons causes a negative electrostatic potential at this type of defect. Thus positrons see defects like vacancies, voids and dislocations as strongly attractive centres in the crystal.

The localization of positrons at the defect sites has three important consequences broadly speaking:-

(a) The concentration of defects can be deduced from the ratio of trapped and free positrons which can be then utilized. The result of such positron trapping measurements in metal samples, containing an equilibrium concentration of vacancies is currently being used successfully to determine mono-vacancy formation energies [9], [10], [26]. It is similarly applicable to divacancies and even larger clusters that will trap positrons [13], [14].

(b) The annihilation characteristics of trapped positrons reflect local properties of defects, giving thus unique information on their internal electronic structure [27].

(c) The annihilation characteristics of trapped positrons are to some extent different for different defect configurations. Thus the positron technique can be a valuable tool in the study of plastic deformation [15], [16], vacancy migration and agglomeration in irradiated materials and thus information about the interpretation of annealing stages [23], [24], surface deformation [25], fatigue [18], recovery and recrystallization [17], edge dislocations [15], volume defects such as voids [19], [20], [22], with a sensitivity that is capable of differentiating between the type of defects produced in irradiated and rolled samples [21]. A classic demonstration of the versatility of the technique is provided by Lengeler etal [25] where information about trapping of hydrogen by vacancies and vacancy-hydrogen binding energy are extracted.

The work embodied in this thesis is part of an ongoing programme concerned with defect formation and deformation - annealing studies in pure metals by positron annihilation undertaken in this physics department under the supervision of the Dr. P. Rice-Evans. Previous members of this group included D. Rees [94], T. Hlaing [95], and I. Chagler [96] each taking the programme a step further as far as experimental technique improvement and computer programming sophistication are concerned. This should be stated from the outset since this work should be seen as a link in a chain, so to speak.

1.2 Thermalization and mobility

1.2.1 Thermalization

According to Brandt [45] when positrons are injected into a solid from an external source composed of radioactive isotope with positron-energy spectrum reaching up to a maximum value E_{max}, they are stopped in the sample with an implantation profile given to a good approximation by

$$\delta P(x) = \alpha_+ \exp(-\alpha_+ x)\ \delta x \qquad 1.1$$

where $\delta P(x)$ is the probability that a positron thermalizes at a distance between x and $x+\delta x$ from the entrance surface. The mass absorption coefficient α_+ depends on the density of the solid, d, and on E_{max} as

$$\alpha_+(d,E_{max}) = R_+^{-1} = (16 \pm 1)\ \frac{[d\ g\ Cm^{-3}]}{E_{max}^{1.43}\ [Mev]}\ [Cm^{-1}] \qquad 1.2$$

Na-22, with halflife of 2.58 years and E_{max} of 0.54 Mev, has a surface density d/α corresponding to the 37% positron range of 24 [mg/Cm^2]. Thus the typical implantation range R_+ is a fraction of millimeter in solids, and is little influenced by channelling conditions.

The positrons lose their energy via ionizing collisions, plasmon and electron-hole generation and finally by phonon scattering coming to thermal equilibrium with the host material. Brandt [45] argues that positron-positron interactions need not be considered in today's standard experiments and that results obtained by positron methods should be understood as representing statistical averages of many consecutive trials performed with single positrons.

The threshold energy E^{th} for relativistic positrons to displace atoms in solids through knock-on collisions is [45]

$$E^{th}\ [\text{Mev}] = 0.5\ [(1+0.05A)^{\frac{1}{2}} - 1] \qquad 1.3$$

where A is the atomic mass number of the target atoms. Most of the positrons injected from sources like the ones shown on the table below have energies less than E^{th} and, therefore, create no radiation damage in metals. Positrons in non-metals can leave radiation effects through electronic excitation and ionization.

Source	Halflife	E_{max} [Mev]	Surface Density [mg/cm^2]
Na-22	2.58y	0.54	24
Co-55	18.2h	1.50	105
Co-58	71.3d	0.48	21
Cu-64	12.9h	0.65	32
Ge-68	275d	1.90	147

The slowing down and thermalization times are usually assumed to be short compared to mean positron lifetimes in solids. Lee-Whiting [37] first performed an analytic calculation on the positron lifetime in a conduction electron gas of a metal by assuming a screened Coulomb potenial for the interaction of a positron with electrons. He estimated the thermalization time of positrons to be 3×10^{-12} seconds. A more refined formalism shows that within 10^{-15} seconds the positron energy drops from several hundred Kev to below the average valence electron energies and by 10^{-12} seconds it is at about 0.1 ev or is very nearly in equilibrium with the lattice. The main reason for this very low energy, is that, in contrast to the electron case, there is only one positron in the sample at a time and hence the exclusion principle does not prevent it from going to its lowest energy state [46].

Carbottle and Arora [38] pointed out that most of the thermalization time occurs toward the end of the positron range and to reach thermal equilibrium from 0.1 ev may require times much larger than 10^{-12} seconds in certain cases. These calculations and the exprimental results of Kim etal (39) indicated that it was only in metals of low electronic density at temperature near $100^{\circ}K$ that thermalization was not complete within a typical lifetime of 200 p seconds. It was also predicted that the thermalization time increased with increasing electron density due to increased screening which weakens the coupling of positrons to electrons. The high resolution angular correlation expriments by Kubica and Steward [35] do show that positrons in metals thermalize down to nearly liquid helium temperatures before annihilation. This indicates that phonon scattering must play a major role

in the final stages of thermalization as was argued theoretically by Perkins and Carbotte [36].

The apparent effective mass m^* of thermalized positrons in metals can be deduced from the smearing of the angular correlation curve near the Fermi cutoff. The effective mass has contributions arising from the static positron-lattice interaction (band mass), from positron-phonon scattering [61], and from positron-electron interactions (many-body mass) [62], [63]. The theoretical estimates for these effects combined yield values of $m^* = 1.2m$ in alkalis [36],[40], [41].

1.2.2 Mobility:-

The motion of a thermalized positron in solids is limited by positron-electron interaction, described by electron-hole pair generation, by positron lattice interaction and by scattering off impurities. An understanding of the mobility and its temperature dependence is important for a proper interpretation of the trapping process at defects.

Owing to the experimental difficulties, there exist few direct measurements of the positron mobility in condensed matter. Mills and Pfeiffer [42] determined the mobility of positrons in Ge, observing the Doppler shift of the annihilation gamma as a function of the bias electric field across an intrinsic Ge detector. A similar technique was employed to measure the mobility in Si [43]. Estimates of the mobility U_+ and the diffusion constant, defined via the Einstein relation

$$D_+ = U_+ \frac{KT}{e} \qquad 1.4$$

are given by Brant and Paulin [34]. The mobilities in

insulators seem to be a few percent of the electron mobilities at comparable temperatures. In semiconductors, the positron mobility is limited by acoustic phonons [42].

A few workers have tried to estimate the positron mobility and diffusion constant indirectly from defect trapping. However this is a tricky approach, because the results depend crucially on what specific trapping model is used. If the mobility of positrons is high, the trapping process is not diffusion limited and the extraction of diffusion - related parameters is not meaningful.

In metals the measurement of positron mobility is obviously prohibitively difficult, and one has to rely on theoretical estimates. Bergersen etal (44] have calculated the various contributions in a number of simple metals. The inverse relaxation time due to scattering off conduction electrons near the Fermi surface is

$$\tau_e^{-1} = \frac{\pi}{4} \frac{m^*}{m} \frac{(KT)^2}{h\varepsilon_F} \qquad 1.5$$

where ε_F is the Fermi energy. Acoustic phonon scattering contributes a relaxation time τ_{ph} and the relaxation time due to impurity scattering is proportional to $(KT)^{-\frac{1}{2}}$. Bergersen etal [44] calculated the deformation potenial constants

$$E_d = \Omega \frac{\delta E(\Omega)}{\delta \Omega} \qquad 1.6$$

where E is the energy of the lowest positron state in the crystal of volume Ω . They find that at T = 300°K in pure metals:

τ_e ranges between (1.5 - 8.2) x 10^{-12} S
τ_{Ph} ranges between (1.3 - 2.7) x 10^{-14} S
U_+ [cm^2 V^{-1} S^{-1}] ranges between 13 - 26
D_+ [cm^2 S^{-1}] ranges between 0.3 - 0.7
The mean free path defined as

$$\tau = \left(\frac{3KT}{m^*}\right)^{\frac{1}{2}} \left(\frac{1}{\tau_e} + \frac{1}{\tau_{ph}}\right)^{-1} = \frac{3D_+}{V_+} \qquad 1.7$$

where V_+ is the thermal velocity, ranges between (11 - 26) A°

The average diffusion length before annihilation, L, defined as

$$L = (6\, D_+\, \tau)^{\frac{1}{2}} \qquad 1.8$$

ranges between 2100A° to 3800A°.

1.3 Positron distribution in solids and Annihilation characteristics:-

In a perfect rigid lattice of ions and its related electronic configuration a positron will be in its lowest energy Bloch state with nearly zero thermal momentum. As it is a light-mass positively charged particle it is strongly repelled from the ion cores and consequently its wave-function amplitude is small in these regions, increasing rapidly to become largest in the interstitial space between the ions. The spatial distribution of the thermalized positron has somewhat of a "swisscheese" character, the density distribution being relatively uniform apart from the "holes" around each ion due to the strong repulsion. The solution of this is achieved using Stott's pseudopotenial theory [47], [48], [49].

The construction of a single-particle potenial for a positron in a metal is somewhat simpler than electrons. There is no exchange repulsion, and calculations based on a positron in a uniform electron gas [50] indicate that the positron-electron correlation potential is a slowly varying function of density, and will be swamped out by the electrostatic potential near ions. To a good approximation the positron in a perfect metal moves in the Hartree potential of ions and the conduction electrons.

In defected systems, the electron-positron correlation contribution may have to be included, in many cases a local density approximation will suffice [46]. The positron wave function for States near the bottom of the lowest energy band is separated into two factors. One reflects the strong repulsion of the positron from the ion core, and is insensitive to the positron energy or the environment of the core. The other is a smooth envelope, which is energy dependent, sensitive to the environment and reflects the positron distribution in the interstitial regions and/or between atomic cells in the crystal.

In a homogenous electron gas of density n the positron annihilation rate can be written as

$$\lambda(n) = \lambda_o(n)\ \gamma(n) = \pi\ r_o^2\ nC\ \gamma(n) \qquad 1.9$$

where λ_o is the Sommerfeld free-electron formula, r_o the classical electron radius and C the velocity of light. γ is a density dependent enhancement factor caused by the strong electron-positron correlation which increases the electron density at the site of the positron. Brandt and Reinheimer [51], [45] suggested a practical interpolation formula for the enhancement

factor and give

$$\lambda(n) = \frac{12}{r_s^3}\left(1 + \frac{10 + r_s^3}{6}\right) \times (nS)^{-1} = (2 + 134\ n)(nS)^{-1} \qquad 1.10$$

where r_s is the density parameter

$$r_s = \left(\frac{3}{4\pi n}\right)^{\frac{1}{3}}$$

given in units of a_o, the Bohr radius of 0.529A. This reproduces within a few percent the results of most many-body calculations [52], [53], [54] for $2 < r_s < 6$ i.e. for the metallic density range. However the formula fails at the high-density limit $r_s < 1$, where the leading term is

$$\lambda(n) = \frac{12}{r_s^3}\ (1 + 1.23\ r_s)(nS)^{-1} \qquad 1.11$$

Most theoretical and experimental values of λ for metals fall in the range $2 \times 10^9 - 6 \times 10^9\ S^{-1}$

In real metals a positron has a non vanishing overlap with the more tightly bound "core" electrons, and consequently a faster annihilation rate than what would be predicted by the conduction electron gas alone. Especially large is the core contribution in transition and noble metals, which have an extrusive d-shell.

West [55], [56] has suggested that the annihilation with the core electrons can be calculated using the electron gas theories by renormalizing the valence electron density n according to the description

$$n_{eff} = n\ (1 + \frac{\Gamma c}{\Gamma v}) \qquad 1.12$$

where Γ_C and Γ_V are the partial annihilation rates with the "core" and "valence" electrons respectively. The ratio Γ_c/Γ_V can be estimated from the angular

correlation curves, which consist of a clearly separable gaussian core electron part and free electron-like parabola. This separation is best done in simple metals, whereas it may not be so easy in some transition metals. The ratio Γ_C/Γ_V is simply A_C/A_V where A_C and A_V are the areas under the gaussian and the parabolic parts of the angular correlation curve. Because of the uncertainty as to the higher momentum components from valence electron annihilations and the way in which the broad component should be extrapolated back to the origin, West [55] has once suggested that A_C should be taken, arbitrarily, to be 80% of the measured area of the gaussian portion of the angular distribution.

West [56] also makes the point that the relative intensity of the broad component will depend, very largely, on the extent to which the positron is able to penetrate the ion cores. Thus in cases like (Na, Mg, Al, Si) the compensating effects of increasing valence and relative ion volume cause core distributions of small and similar intensity. In the periodic sequences (Cu, Zn, Ga, Ge), (Ag, CD, In, Sn, Sb) and (Au, Hg, TI, Pb), the combined effects of volume and charge result in a progressive decrease of the core intensity.

The angular correlation and Doppler line-shape experiments measure the momentum distribution of the annihilating electron-positron pair. If the electrons and the positrons are treated as independent particles the many-body wave function is a Slater determinant and the momentum distribution of the annihilation quanta is

$$\Gamma o(\underline{P}) = \frac{\pi r_o^2 C}{(2\pi)^3} \sum_i \left| \int d\underline{r} \exp(-i\underline{p}.\underline{r})\, \psi_i(\underline{r})\, \psi_+(\underline{r}) \right|^2 \qquad 1.13$$

where ψ_+ is the ground-state positron wave function

and where the sum goes over the occupied electron states ψ_i . The conventional long-slit angular correlation apparatus measures only one component, P_z, of the momentum distribution, so that the angular correlation curve is

$$I(P_z) = \int dp_x \int dp_y \; \Gamma_o(\underline{P}) \qquad 1.14$$

which reduces in the isotropic case to

$$I(P_z) = 2\pi \int_{P_z}^{\infty} dp \; p \; \Gamma_o(P) \qquad 1.15$$

In a two-dimentional angular correlation measurement the average is of course taken only over one momentum component.

For a homogeneous electron gas the independent partical approximation (1.10) gives the 2-gamma angular correlation curve

$$I(P_z) = \frac{r_o^2 C}{2\pi} (P_F^2 - P_z^2)(P_F - |P_z|) \qquad 1.16$$

which is an inverted parabola the width of which is proportional to the Fermi momentum P_F. The independent-particle approximation does not take into account the strong electron-positron correlation and thus by integrating (1.16) over P_z one recovers the Sommerfeld formula for the total annihilation rate. The effect of the electron positron correlations on the momentum distribution in the homogeneous electron gas can be included through a momentum dependent enhancement factor [52], [56], [57] $\epsilon(P)$, so that

$$\Gamma(\underline{P}) = \epsilon(P) \; \Gamma_o(\underline{P}) \qquad 1.17$$

$\varepsilon(P)$ can be written in the form

$$\varepsilon(P) = a + b\,(P/P_F)^2 + C\,(P/P_F)^4 \qquad 1.18$$

where a, b, c, depend on the electron density, b and c being in metallic densities much smaller than a. Since the core electrons are tightly bound to the nucleus, they are expected to be less perturbed by the presence of the positron than will be the valence electrons, which are to a large extent free. Some theoretical effort has been made to estimate the enchancement of the valence-electron density around the positron within the jellium model of a metal [51], [54], [58], [59]. Gupta and Siegel [57] argue that the enhancement factors for different shells of electrons in the core will be different owing to their different degrees of localisation. This may be taken into consideration by assigning a different enhancement factor for each shell, which may then be determined by a least-square fit to the S(r) curve in the small-r region -(where S(r) is defined in real space as the Fourier transform of $\Gamma(P)$ the momentum distribution of the annihilating pair in momentum space). It would then be possible to determine the anistropy of the momentum dependence of the enhancement factor for valence electrons if the angular correlation curves obtained using either point or long-slit geometry detectors were used instead of spherically averaged angular-correlation or Doppler broadened spectra.

1.4 Positronium Formation and Annihilation

A positron in a molecular substance can capture an electron from the surrounding medium and a positronium atom (PS), the bound state of the positron-electron pair, is formed. As the size of positronium is twice that of the hydrogen atom, positronium formation occurs

mainly in molecular media which have relatively open structures.

The energetics of positronium formation is usually described by the so-called Ore gap model. It states that positronium formation is most probable when the positron energy during its slowing down lies within a gap where no electronic energy transfer process is possible. To capture an electron from a molecule of the medium with ionization energy E_i, the kinetic energy E of the positron must be greater than $E_i - E_{ps}$, where E_{ps} is the binding energy of positronium. In vacuum E_{ps}, is 6.8 ev but may be smaller in the medium. When the positronium atom is formed with kinetic energy greater than its binding energy it will rapidly break up in collisions. Furthermore inelastic collisions will compete with positronium formation until the positron kinetic energy is less the E_{ex}, the lowest electronic excitation energy. Thus positronium formation is most probable with the energy in the range

$$E_i - E_{ps} < E < E_{ex}$$

which is the ore gap. Its width can be used to estimate the positronium yield, the fraction of positrons which have formed positronium.

The ground states of the positronium atom are the singlet ^1S state or parapositronium, in which the orbital angular momentum L and the total spin are zero, and the triplet ^3S state, ortho positronium, in which L=0 and the total spin is unity. Since a system of two photons cannot have states of angular momentum equal to unity it follows that the triplet state cannot decay into two photons. Additional constraints are supplied by the requirements of conservation of parity.

The charge parity of the electron plus positron system is [33]

$$C = P_i \, P_L \, P_S \qquad 1.19$$

Where P_i is the instrinsic parity which is negative for a particle - anti-particle pair, $P_L = (-1)^L$ is the spatial parity, $P_S = (-1)^{s+1}$ is the spin parity.

Thus for positronium $C=(-1)^{L+S}$ is +1 for the singlet state and -1 for the triplet state. The charge partity of the photon is negative and for a system of n photons $C=(-1)^n$. It follows from conservation of charge parity that para positronium decays into an even number of photons and ortho positronium into an odd number of photons.

The probability of two-photon annihilation is considerably greater than that for one or three photons; the ratios of the cross sections for the respective processes being [56].

$$\sigma_{(3)}/\sigma_{(2)} \approx \alpha, \quad \sigma_{(1)}/\sigma_{(2)} \approx \alpha^4 \qquad 1.20$$

where $\alpha = 1/137$ is the fine structure constant.

The cross section for the two-photon annihilation of a free positron and a stationary electron was shown by Dirac [83] to be

$$\sigma_{(2)} = \frac{\pi r_o^{\,2}}{\gamma + 1}\left[\frac{\gamma^2 + 4\gamma + 1}{\gamma^2-1} \; ln[\gamma + (\gamma^2-1)^{\frac{1}{2}}] - \frac{\gamma + 3}{(\gamma^2-1)^{\frac{1}{2}}}\right] \qquad 1.21$$

where $\gamma = (1-v^2/C^2)^{-\frac{1}{2}}$ and $ro = e^2/m_o c^2$ is the classical electron radius. At low positron energies, one obtains a cross section inversely proportional to the positron

velocity v and consequently the annihilation probability

$$\Gamma_{(2)} = \sigma_{(2)}\ v\ n_e = \frac{\pi r_o^2}{v}\ v\ n_e = \pi r_o^2 C n_e \qquad 1.22$$

is independent of the positron velocity and simply proportional to the density of electrons n_e.

The ground-state positronium wave functions have the form

$$\psi(r) = (\pi\ a^3)^{-\frac{1}{2}} \exp\ (-r/a) \qquad 1.23$$

where r is the relative coordinate and $a = 2\ \hbar^2/m_o e^2$ is the Bohr radius of positronium which is twice that for hydrogen (the reduced mass is $m_o/2$).

It can be deduced then that the decay rate of parapositronium is

$$\Gamma_{para} = 4\pi\ r_o^2\ C\ |\psi(0)|^2 \qquad 1.24$$

Here $|\psi(0)|^2 = (\pi\ a^3)^{-1}$ is the electron density at the positron and the factor four arises because equation (1.22) corresponds to the initial state averaged over spins, whereas in positronium only one of the four possible spin states can undergo two-photon decay. Substituting the values for r_o and a, we obtain a parapositronium lifetime of 123 p sec. In like manner, when the expression for spin average cross section for three-photon annihilation [33].

$$\sigma_{(3)} = \frac{4(\pi^2 - 9)\ r_o^2\ C\alpha}{3v} \qquad 1.25$$

is used the orthopositronium lifetime is found to be 140 n sec.

A comparison between the decay rates

reveals that the ratio of three photon to two photon annihilations for slow unbound pairs is about 1/370.

If however positronium is formed, the fraction of three photon events will be larger. Nevertheless since the normal decay of the orthopositronium atoms must compete with more rapid processes arising from the interactions of these orthopositronium atoms with other electrons and atoms in the system, this fraction will be reduced. These interations often result in the annihilation of the positron with an antiparallel spin electron from the surrounding; the so called "pick off" annihilation.

1.5 Temperature Effects

1.5.1 Effect of temperature on Annihilation Characteristics

There are three main possible thermal effects to be considered aside from the temperature -dependent smearing of Fermi breaks due to positron thermal motion:

(1) Thermally generated lattice defects can trap positrons.

(2) Thermal expansion of the crystal lattice causes a corresponding contraction of the reciprocal lattice and an increase of the momentum density in order to preserve normalization.

(3) The temperature also affects the intensity of the high momentum components of the momentum density.

Stott and West (49) argue that as the temperature is raised changes in the positron distribution, and thus in the core contribution rate, are mainly due to:-

(a) Anharmonic thermal expansion of the crystal which leads to a uniform decrease of the positron amplitude and thus diminishes the core rate.

(b) Anharmonic thermal expansioin leads to a redistribution of the positron density from the core to the interstitial regions because of the large interstitial space and thus a further decrease in the core overlap.

(c) Lattice vibrations cause an increase in positron density in any interstitial region which is momentarily enlarged by the thermal motion of the ions around their equilibrium positions.

Thus understanding how a free positron in a lattice behaves as the temperature is raised is a must if one is to draw any sensible conclusions about positron trapping at defects which will be treated in the next section. The reason is that such thermal dependence of the annihilation rate will also be present in the high-temperature region where thermally activated defects may act as positron traps, and it has to be properly subtracted if one wants to focus on the changes in annihilation characteristics induced by an equilibrium defect concentration. The state of things as they stand now, leaves a few points in need of further clarification.

1.5.2 The trapping rate

A problem that has caused considerable discussion is the correct temperature dependence of the

positron-vacancy trapping rate to be used in the analysis of experiments to determine vacancy formation energies in metals by positron annihilation. The possible temperature dependence of this quantity which always appears multiplied by C_v, the concentration of vacancies, seems to be an interesting problem from the theoretical point of view; since different assumed temperature dependences lead to only minor modifications in the deduced vacancy formation energies.

Theoretical predictions of specific trapping rate in vacancies proportional to $T^{\frac{1}{2}}$ [97] [98], T^0 [71] [99] [100] and $T^{-\frac{1}{2}}$ [70] [87] [101] have all been suggested, while the experimental evidence for positron-vacancy trapping rate proportional to from $T^{\frac{1}{2}}$ to T^1 [102] and T^0 [103] is both scarce and contradictory. At the present time it would appear that the magnitude of the specific trapping rate for mono vacancies, as well as for other multi vacancies, is an open question. However, the theoretically suggested temperature dependences for the trapping rate are all rather weak when compared with the exponential temperature dependence of C_v and, hence, can probably be neglected until more concrete experimental or theoretical knowledge regarding this problem is developed.

1.6 Self-trapping

Self-trapping in metals was first suggested by Lichtenberger et all [88] [93], Seeger [70] and others in the context of any anomalous temperature dependence of annihilation characteristics e.g. in cadmium [88], gold [31], and indium [92]. Seeger [70] used an elastic continuum model with the positron coupled to

the lattice dilation by a deformation potential, and suggested that a metastable self-trapped positron state would account for the observed behaviour in cadmium [88]. The idea has been examined in more detail by Trinkaus and Hodges [89] [90] and Leung et al [91].

A positively charged particle in a metal tends to localize about an interstitial site by displacing the neighbouring metal ions because of its repulsive interaction wih them. The relaxation of the lattice leads to a lowering of the potential energy of the system whereas the localization of the particle results in an increase of its kinetic energy. Whether a particle favours either a Bloch-wave type state or localized, self-trapped state depends upon the particle-lattice coupling and particle mass.

Seeger [86] argues that a particle with mass m_+ and elementary positive electric charge may be self-trapped in a metal if

$$2\pi \frac{K h^2}{\varepsilon_d^2 m_+} \equiv K_{max} < K_o \qquad 1.26$$

Here ε_d is the positron deformation constant [86] K is an elastic constant of the matrix and K_o of the order of magnitude 2×10^7 cm $^{-1}$. If the stronger condition

$$K_{max} < 2 K_o/3 \qquad 1.27$$

is satisfied, the binding energy in the self trapped state is positive ie. the self-trapped configuration is stable relative to a free or quasi-free (Bloch-wave type) particle. If however

$$2 K_o/3 < K_{max} < K_o \qquad 1.28$$

the self-trapped state lies above the Bloch-wave state by an energy

$$\varepsilon_o \equiv \varepsilon_o(K_o) = \frac{2\pi\hbar^2}{2m_+} K_o\left(1 - \frac{2K_o}{3K_{max}}\right) > 0 \qquad 1.29$$

In this situation, which may be realized for positrons in metals, the self-trapped positron state is metastable with respect to the Bloch-wave state. It is virtually unpopulated at temperatures $T \ll \epsilon_o / K_B$. At temperatures $T \gg \epsilon_o / K_B$ practically all positrons are in the self-trapped state.

At intermediate temperatures the probability that a positron is self-trapped is given by

$$f_{st} = [\, 1 + A^{-1}\, T^{1.5} \exp\,(\epsilon_o / K_B T)]^{-1} \qquad 1.30$$

According to Trinkaus and Hodges [89] positron self-trapping should occur, if it ever does, in high-valence metals like Pb, In, and Al.

1.7.1 Equilibrium concentrations and formation energies and entropies

The formation of a vacancy can be described as the removal of one interior atom from the crystal and replacement of the atom on the crystal surface. The vacancy formation energy is defind as the corresponding energy change for the whole crystal. Since the configurational entropy of vacancy formation is determined solely by the number of different ways in which n vacancies and N atoms may be distributed among (N + n) sites, the total change of the Gibbs free energy of the system when n vacant lattice sites are

created can be written as

$$n\,G^f_{1v} = n\,(E^f_{1v} - TS^f_{1v,th}) + KT\left(N \ln \frac{N}{N+n} + n \ln \frac{n}{N+n}\right) \quad 1.31$$

where T, K, S^f are the absolute temperature, the Boltzmann's constant and thermal or vibrational entropy respectively [72].

The introduction of vacancies therefore lowers the free energy of the crystal until an equilibrium concentration is reached; after which G again increases. The equilibrium number of vacant sites is obtained when $dG/dn = 0$

Differentiating (1.31) leads to

$$C_{1v} = n/N = \exp\,(S^f_{1v,th}/K)\,\exp\,(-E^f_{1v}/KT) \quad 1.32$$

For $n \ll N$ where C_{1v} is the atomic concentration of vacant sites. For all metals studied to date, since the equilibrium vacancy concentrations are indeed rather small, the ensemble of vacancy defects present under conditions of thermodynamic equilibrium can be more than adequately described by a system including only mono, di, and sometimes tri-, vacancies. However, if the primary concern is with systems of mono and divacancies, the total equilibrium vacancy concentration C_v is given by

$$C_v = C_{1V} + C_{2V} = \exp\,(S^f_{1V}/K)\,\exp\,(-E^f_{1V}/KT) + 2g_{2V}\exp\,[(2S^f_{1V} - S^B_{2V})/K]\,\exp\,[(E^B_{2V} - 2E^f_{1V})/KT] \quad 1.33$$

where S^B_{2v} and E^B_{2v} are the entropy and enthalpy of binding of the divacancy and where g_{2v} is a constant related to the geometric configuration of the divacancy [73]. The entropies and enthalpies in equation (1.25) may be slightly temperature dependent [28] [72] [85] due to an aparent "softening" of the interatomic potential caused by the change in the interatomic distances associated with thermal expansion.

While it would be most desirable to be able to measure the individual C_{nv}, in most experiments only C_v or a property proportional to it can be measured as a function of temperature in order to obtain information regarding the vacancy concentrations in metals. The effective vacancy formation enthalpy is given by

$$E^f_v = \frac{\delta \text{ Ln } C_v(T)}{\delta (1/KT)} \qquad 1.34$$

The thermal expansion measurements cover, with reasonable accuracy, the concentration range 10^{-3} to 10^{-4} where the effective formation enthalpy is likely to contain a significant contribution from divacancies. On the other hand the range of measurements of C_v with positron techniques extends from about 10^{-4} to 10^{-7} with maximum accuracy about 3.5×10^{-6} [9] [10]. The contribution of divacancies to the effective formation enthalpy in this range is indeed negligible except, maybe, towards the top of it.

1.7.2 Experimental determination of formation energies

Perhaps the most reputable method of determining formation energies is differential dilatometry. The technique, based upon the difference betwen the dilatations of the macroscopic crystal volume and the

average microscopic lattice volume (i.e. average unit cell volume) caused by the presence of a uniform random distribution of point centres of dilatation (e.g. vacancies), established itself in a series of classic papers [104] [105] [106] by Simmons and Balluffi on the FCC metals Al, Ag, Au and Cu. The temperature range over which the difference in the fractional change in the length and the lattice parameter of a thin specimen can be determined with useful accuracy is reasonably narrow since one is considering a small difference between large quantities. The C_v determination is poor for concentrations as low as 10^{-5}.

A second technique capable of providing absolute vacancy concentrations is the measurement of specific heat as a function of temperature using calorimetric techniques.

Nevertheless, since for most metals the main part of the high temperature rise of the specific heat is considered due to lattice anharmonicity and not due to vacancies, this technique is considered less suitable for the study of formation energies.

Another method involves measurements of electrical resistance at high temperature. The main drawback of this technique however is the fact that, because of anharmonic effects, the temperature dependance of the electrical resistivity due to phonon scattering is not well known.

Quenching experiments to study non-equilibrium concentrations of vacancies by studying the quenched-in resistivity is a fourth technique [107]. Seeger [28], in arguing the merits and shortcomings of non-equilibrium techniques, points out that in this method the sample

history itself plays an important role in addition to other difficulties like the unknown degree of association of vacancies to form clusters, high sensitivity to impurities and, in general, a more involved theoretical approach.

A more comprehensive review of all of these techniques and others can be found in several recent surveys discussing self-diffusion, equilibrium and non-equilibrium studies [72] [73] [108].

1.8 The Trapping Model

A simple rate theory [66] describing the trapping of positrons [67], [68], [45] has been applied with great success to the results from experiments using lifetime, angular correlation and Doppler-broadening techniques. A rate equation approach involving time-independent transition rates K_{ij} ($K_{ij} \neq K_{ji}$, $K_{ii} = 0$) is used to describe the decay of a positron population. In a general case where positrons may exist in a spectrum of quasi-stationary states s, each characterized by a particular annihilation rate $\lambda(s)$, with relative probabilities given by a suitable normalized distribution fuction P(s), any initial positron population decays as

$$n(t) = \sum_{i}^{N} n_i(t) \qquad 1.35$$

where $n_i(t)$ are determined by a set of coupled differential equations

$$\frac{d\, n_i(t)}{dt} + (\lambda_i + \sum_{j \neq i}^{N} K_{ij}) n_i(t) = \sum_{j \neq i}^{N} k_{ji}\, n_j(t) \qquad 1.36$$

if $k_{ij} >> \lambda_i$ for all i,j approximate solutions of the form

$$\bar{\lambda} = \int \lambda(S)\ P(S)\ dS \qquad 1.37$$

can be obtained. For the case N=2 [64], [65]

$$n(t) = n_o \exp\left[- \frac{(\lambda_1 K_{21} + \lambda_2 K_{12})}{K_{21} + K_{12}} \right] t \qquad 1.38$$

The simple trapping models [66], [67], [68] assume that at sometime t=0 ($<< \lambda_i^{-1}$) all the positrons exist in a common delocalized state in which they can either annihilate or make transitions to other states in or around structural or other defects. If the probability of further transitions (ie. escape from the traps) is negligibly small we can rewrite (1.36) as

$$\frac{d\, n_1(t)}{dt} + (\lambda_1 + \sum_{j \neq 1} K_{1j})\, n_1(t) = 0 \qquad 1.39a$$

and

$$\frac{d\, n_j(t)}{dt} + \lambda_j\, n_j(t) = K_{1j}\, n_1(t) \qquad 1.39b$$

for all $j \neq 1$.

Application of the appropriate boundary conditions, $n_j(o) = n_o \delta_{i,j}$, yields a discrete spectrum

$$n(t) = n_o \left[1 - \sum_{j \neq 1} \frac{K_{ij}}{\lambda_1 - \lambda_j + \varepsilon} \right] \exp -(\lambda_1 + \varepsilon)t + \sum_{j \neq 1} \frac{n_o K_{ij}}{\lambda_1 - \lambda_j +} \exp(-\lambda_j t) \qquad 1.40$$

where $\epsilon = \sum_j K_{1j}$

This is normally translated into formulae like

$$I(t) = \sum_i^N I_i \exp(-\lambda_i t) \qquad 1.41$$

when used in positron lifetime spectra analysis, where I_i refers to a component's intensity. Observable effects of positron trapping will occur in lifetime spectra whenever the corresponding K_{1j} is of the same order as λ_1, and the λ_j is sufficiently different from λ_1. Should the first of these conditions be satisfied at a sufficiently low concentration of traps, C_j, the relation

$$K_{1j} = \nu_{ij} C_j \qquad 1.42$$

will be applicable, where ν_{ij} is the appropriate trapping rate. A change in the concentration of traps can then be followed through the consequent changes in an annihilation characteristic or the appropriate component intensity.

If the specific case of vacancy trapping is considered with the notation that the number and decay rate of free positrons is denoted by n_f and λ_f respectively, the atomic concentration of vacancy traps is $C_v(T)$, the positron trapping rate per lattice vacancy is ν and the number and decay rate of trapped positrons at vacancy sites is given by n_d and λ_d ; the rate equations for the trapping model describing the time dependence of the number of free and trapped positrons are

$$\frac{d\, n_f(t)}{dt} = \lambda_f\, n_f(t) - \nu\, C_v(T)\, n_d(t) \qquad 1.43a$$

$$\frac{d\, n_d(t)}{dt} = -\lambda_d\, n_d(t) + \nu\, C_v(T)\, n_f(t) \qquad 1.43b$$

$$\frac{d\, n\ (t)}{dt} = -\lambda_f\, n_f(t) - \lambda_d\, n_d(t) \qquad 1.43c$$

initially $n_f(0)$ positrons are injected into the defective sample and $n_d(0)=0$. Therefore

$$n(t) = \frac{n_f(0)\,(\lambda_f-\lambda_d)}{\lambda_f-\lambda_d+\mu C_v} \exp\,[-(\lambda_f+\mu C_v)t] + \frac{n_f(0)\,\nu C_v\, \exp(-\lambda_d t)}{\lambda_f-\lambda_d+\nu C_v} \qquad 1.44$$

which indicates that positrons annihilating in a material containing defects will do so with two distinct lifetimes $(\lambda_f + \nu C_v)^{-1}$ and λ_d^{-1}. Since the total annihilation rate is found from

$$R(t) = \frac{1}{n_f(0)} \frac{d}{dt}\Big(n_f(t) + n_d(t)\Big) \qquad 1.45$$

The mean lifetime is given as

$$\bar{\tau} = -\int_0^\infty R(t)\ t\ dt = \frac{\lambda_d + \nu C_v}{\lambda_d\,(\lambda_f+\nu C_v)} \qquad 1.46$$

The connection with vacancy formation parameters is made via equations of the form

$$C_{1v} = \exp\,(S^F_{1v}/K)\ \exp\,(-H^F_{1v}/\,KT) \qquad 1.47$$

Where C_{1v}, S^F_{1v}, H^F_{1v} and K are the monovacancy concentration, entropy of formation, enthalpy of formation and the Boltzmanns constant respectively.

More comprehensive treatments of the trapping model describing multiple trapping phenomena, effects of impurities and dilute alloys, possibility of thermal detrapping are to be found in Seeger's work [28], [69] and Brandt's [45], [66].

1.9 Positron Techniques

1.9.1 Introduction

While differential dilatometry is the only equilibrium technique presently available for the generally reliable determination of C_v in metals, positron annihilation spectroscopy has become in recent years a new and sensitive method for investigating the temperature dependence of vacancy concentrations in metals. The behaviour of positrons in metals must be studied through the gamma irradiation emitted during the annihilation process. There are three types of measurements that may be performed:

1) Measurement of the positron lifetimes or, more precisely, of the positron decay spectrum.

2) Measurement of the angular correlation of the two-quanta annihilation radiation.

3) Measurement of the Doppler broadening of the 0.511 Mev. photon annihilation line.

1.9.2 Positron Lifetimes

For lifetime measurements one has to use positron sources which emit a fairly strong gamma radiation in coincidence with positrons, such as ^{22}Na. The coincidence radiation is used to trigger an "electronic clock" at the birth of a positron. It is triggered off at its death by the subsequent detection of the 0.511 Mev. photon when the positron annihilates with a lattice eletron. The technique is reviewed in detail by Bell [74] and Gedcke et al [75] , [76]. A fast-slow delayed coincidence system records the annihilation time spectrum. The detectors consist of fast plastic scintillators coupled to fast photomultiplier tubes. The energy windows of the single-channel analysers in the slow channels are adjusted so that one of the detectors is assigned, exclusively, to registering the birth gamma ray, while the other, exclusively, registers the annihilation gamma ray; of individual positrons. The fast signals from the anodes of the photomultipliers are fed to timing discriminators to produce time signals. The output pulses from the time-to-amplitude converter are then transferred to a multichannel analyser through a linear gate driven by the coincidences in the slow channel ie. the output pulses are accepted only if the corresponding start and stop signals have correct energy values determined by the windows of the single-channel analysers.

The lifetime of the positron gives a measure of the electron density at the positron position. If positrons annihiliate from different states in the sample the result is a multi exponential lifetime spectrum. The two principal methods for analysing the measurements are:

a) A sum of exponential decay functions is convoluted with the instrumental time resolution function and then fitted to the experimental data in order to find the lifetime values and relative intensities associated with the different components. The resolution function is determined by measuring the pulse height distribution from a source such as ^{60}CO that emits two coincident gamma rays.

b) If the positron decay may be described by a single lifetime as is the case for annealed metals, the difference in the centroids of the time resolution function and the positron decay function is equal to the positron lifetime in the free state.

For (a), in cases where individual components have rather close decay values, the result of the curve fitting is quite ambiguous; whereas for (b) adequate precision requires a very high degree of time stability of the electronics [78].

1.9.3 Angular Correlation

If both members of an annihilating electron-positron pair are at rest, the conservation of energy and linear momentum demands that in two-photon annihilation the two gamma rays are emmited with exactly the same energy $E_\gamma = m_o C^2$ where m_o is the electron or positron rest mass) and in exactly opposite directions with linear momentum $P_\gamma = m_o C$. If the annihilating pair has a non vanishing linear momentum $\underline{P}$, this symmetry is lost, and the direction of the gamma rays differs from 180° by a small angle.

$$\theta = P/m_o C \qquad 1.48$$

Measurements of the angular correlation of the directions of the photons resulting from a 2-gamma annihilation furnish thus information on the linear momentum and hence on the velocity of the annihilating pair. Since it is usually assumed that the positron is thermalized and essentially at rest, what is being measured in effect is the distribution of electron momenta. Measurements by Stewart [79] have shown that electron-positron correlation does not appreciably disturb the momentum distribution of the annihilation photons. This is a result of the fact that the operator corresponding to the centre of mass momentum commutes with the Coulomb energy operator of the electron-positron pair.

If the direction of observation is chosen as the Z-direction and the conventional long slit geometry is used [79], the counting rate into the momentum region $m_o C\theta$ and $m_o C(\theta+d\theta)$ is given by [80].

$$N_Z(\theta) = A \int_{-\infty}^{\infty}\int_{-\infty}^{\infty} \Gamma(p_x, p_y, m_o C\theta)\, d\, p_x\, d\, p_y \qquad 1.49$$

where A is a constant .

The total area under the angular correlation curve is proportional to the total annihilation rate (which is equal to the reciprocal lifetime). If the geometrical conversion factor is known, the positron lifetime may thus be obtained from angular correlation experiments.

It can be shown that annihilation with a gas of free electrons [28] leads to

$$N_Z(\theta) = B(P_F^2 - P_Z^2) \qquad 1.50$$

where P_F is the Fermi momentum and B a constant.

Experimentally one finds that in most metals such an inverted parabola $N_Z(0)$ is superimposed on a much broader, more slowly varying background, which is often approximated by a gaussian. The main contributions to this background come from deviations of the Bloch waves of the conduction and valence electrons from plane waves, from positron annihilation with core electrons, and from excluded volume effects.

When positrons are trapped in bound states, the part of the angular correlation curve associated with core electrons is suppressed relative to the approximately "free-electron contribution". Measurements of the changes in peak counting rate as a function of temperature have been used to determine vacancy formation energies [10] [26].

Angular correlation experiments are performed by measuring the counting rate as a function of angle for coincidence between 2-photon annihilation. The techniques are considered in detail in literature [81] [82]. Although the coincidence count rate is rather low, it is offset by the superb angular resolution of less than half a milliradian that can be easily obtained.

1.9.4 Doppler-broadening

A non vanishing velocity component of the annihilating electron-positron pair in the x-direction (i.e along the direction of emmitted photons) cannot be resolved in an angular correlation experiment and hence the integration over P_x in equation (1.49). Nevertheless such a velocity component gives rise to a Doppler

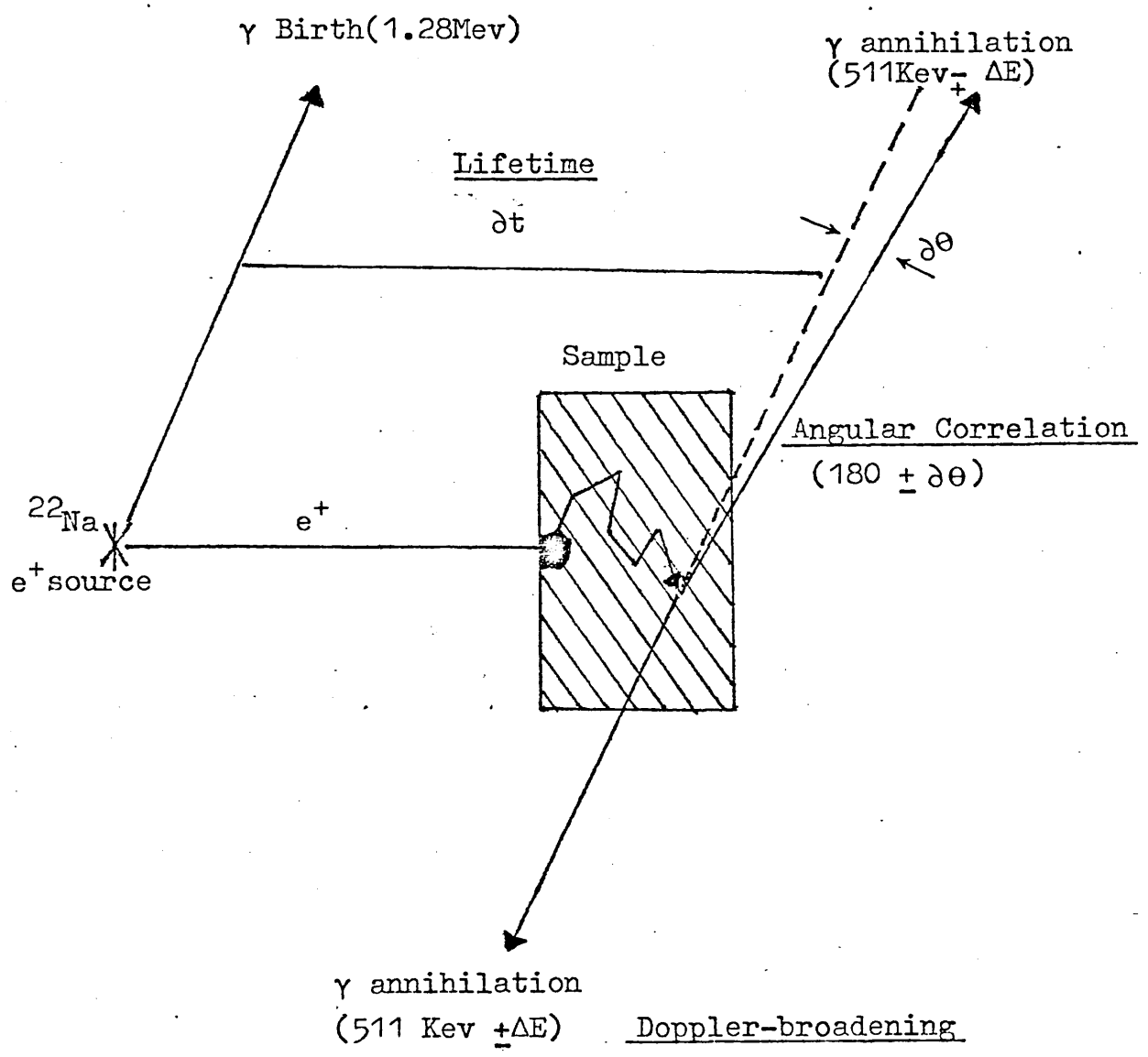

FIG.1.1 Schematic representation of positron annihilation indicating the bases for the three experimental techniques : lifetime, angular correlation, and Doppler-broadening

broadening of the annihilation line at 511 Kev. The longitudinal Doppler shift formula is

$$E = E_o \ (1 \pm V_x/C) \qquad 1.51$$

where V_x is the centre of mass velocity and E_o is the rest energy of an electron. Assuming the positron to be at rest $V_x = \frac{1}{2} V_{ex}$, where V_{ex} is the electron velocity. For an isotropic medium all of the momentum components are equivalent and we can write

$$P_x = P_z = m_o C\theta \qquad 1.52$$

where P_x, P_z are the x and z components are of electron momentum in these directions respectively. Therefore

$$E-E_o = \Delta E = \pm \frac{E_o V_{ex}}{2C} = \pm \frac{p_x E_o}{2m_o C} = \pm \frac{m_o C\theta}{2m_o C} E_o = \pm \frac{1}{2} E_o\theta \qquad 1.53$$

So, in principle, the Doppler-broadening of the annihilation line, due to motion of the annihilating pair, provides the same information about the distribution of electrons as angular correlation measurements. However there is a considerable difference in the resolutioin which can be achieved. The Doppler broadening resolution, even with the best available Ge and Ge (Li) detectors, is a factor 10 to 20 larger than that achievable in angular correlation. Because of the addition of the normal line width of the detector-amplifier combination to Doppler-broadening effects, only a very high resolution system will show annihilation broadening effects in measurable quantities [81] [84].

Annihilation of positrons at rest with a gas of free electrons with Fermi velocity V_F yields an annihilation eneregy spectrum which is an inverted parabola centred at $m_o c^2$ and extending from $m_o c^2 (1-V_F/2c)$ to $m_o c^2(1+V_F/2c)$. The velocities of core electrons are, on the average, larger than those of conduction electrons and therefore their contribution to the energy distribution is much broader. Similar to the angular correlation case it is usually represented by a Gaussian function centred at $m_o c^2$. The distinct advantages of the Doppler-broadening technique, when compared with angular correlation experiments, are basically due to its simplicity. It requires only one detector, no coincidence circuitry, a small source strength and permits very rapid data collection. The counting statistics are therefore very good and may, for certain applications, more than compensate the disadvantages connected with poor resolution.

2. Experimental Techniques and Equipment

2.1 Description of the measuring system

The original pulse shape at the detector terminals is modified by the chain of electronic processing components through which the signal passes before analysis. The two basic reasons for this processing are firstly to shorten the response time of the detector so that pulses do not overlap and create errors in amplitude measurements and secondly to enhance the signal - to - noise ratio.

Figure (2.1) shows a block diagram of the system. The heart of the system is a high resolution Princeton Gamma - Tech (PGT) intrinsic germanium detector. It is mounted at the end of a cold finger in a cryostat and has an active area of 200 mm^2 and its thickness is 10 mm. It is powered by a Tennelac TC 941 high voltage power supply. The recommended operating bias is - 2200 volts. Coupled to the detector is a preamplifier the heart of which is a field-effect transistor. The preamplifier uses optical feedback and there is a reset pulse (8 micro second rise time) that is generated periodically to compensate for: (a) leakage current in the detector and (b) detector currents caused by absorbed radiation. The output pulses from the preamplifier are of positive polarity. Simultaneously with the optical reset pulse there is a positive inhibit pulse generated by the preamplifier. This is used to gate the analyser off during the amplifier recovery from the optical reset.

The output from the preamplifier is fed into a Tennelac main amplifier (model TC 205). The pulse shaping

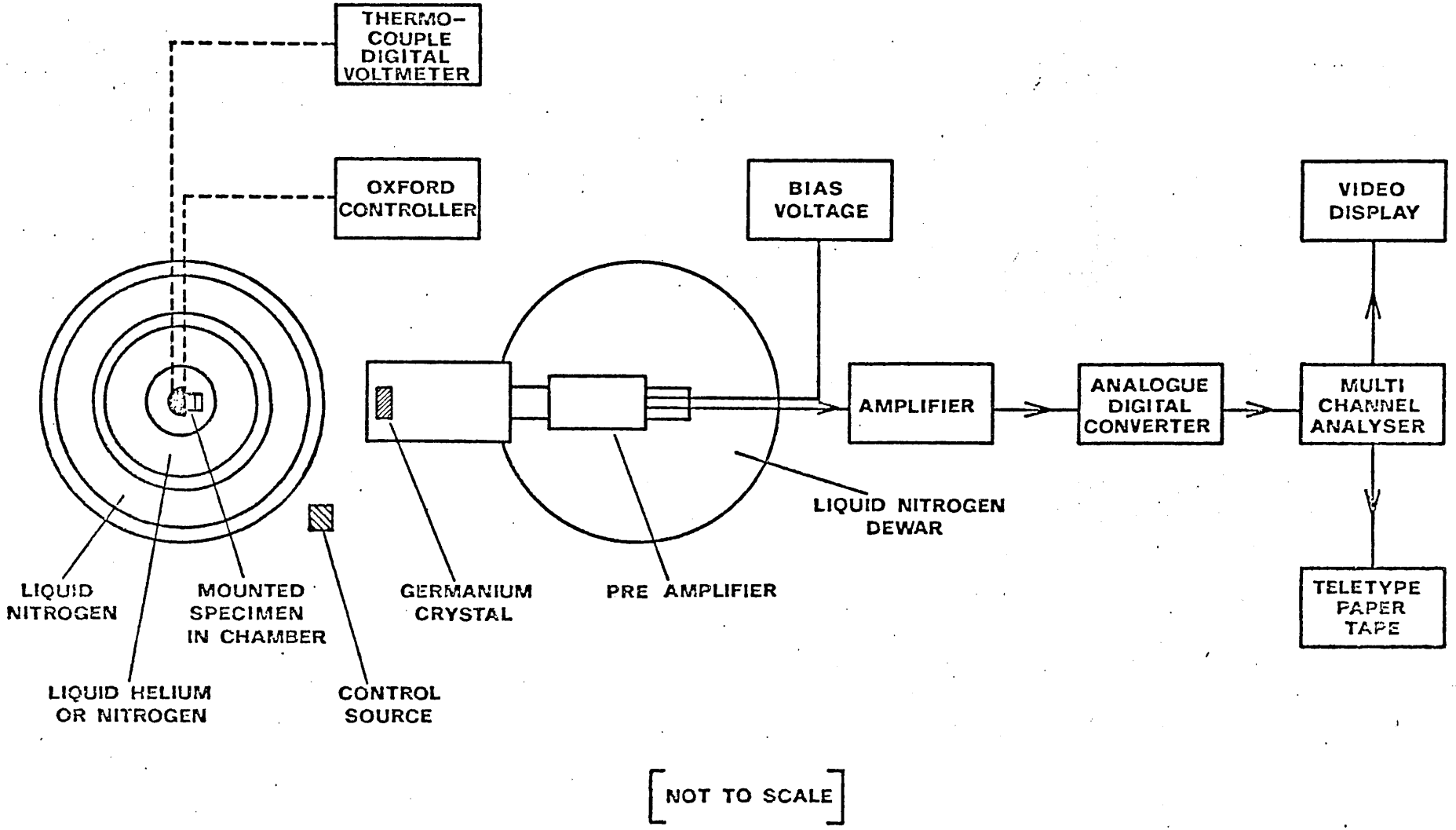

FIG. 2.1 The schematic illustration of the Doppler-broadening system, employed throughout the work.

circuits in the main amplifier operate with time constants much shorter than the decay of the preamplifier signal and much larger than its rise time. Typical values of these R-C time constants are 2 to 4 microsecond. The output from the main amplifier is fed to a Laben 8215 Analog to Digital Converter. The ADC has a conversion constant of 1 mv per channel and a conversion time of (4.5 microsec + Rise Time Protection). At 5K CPS the average dead time is about 10%.

The ADC is connected to a Nova Computer provided by Link Systems for data storage. Instructions to the computer are entered using a control keyboard. A video screen displays the spectrum in histogram form and a hard copy of the spectrum is obtained as a list of channel contents by coupling the computer to a Data Dynamic teletype

2.2 Low Temperature cryostat design and operation

2.2.1 Design

The study of positron behaviour in metals at temperatures between 4.2° K and room temperature necessitated the design and construction of a low temperature cryostat, a schematic diagram of which is shown in Fig (2.2), that would enable such measurements to be performed, T.Hlaing [95] and I.Chagler [96].

The dewar Fig (2.3) would be positioned in front of the detector and the distance between the two adjusted in order to obtain the desired counting rate which would normally be 5K CPS. The outer pyrex dewar will always be filled with liquid nitrogen, while the

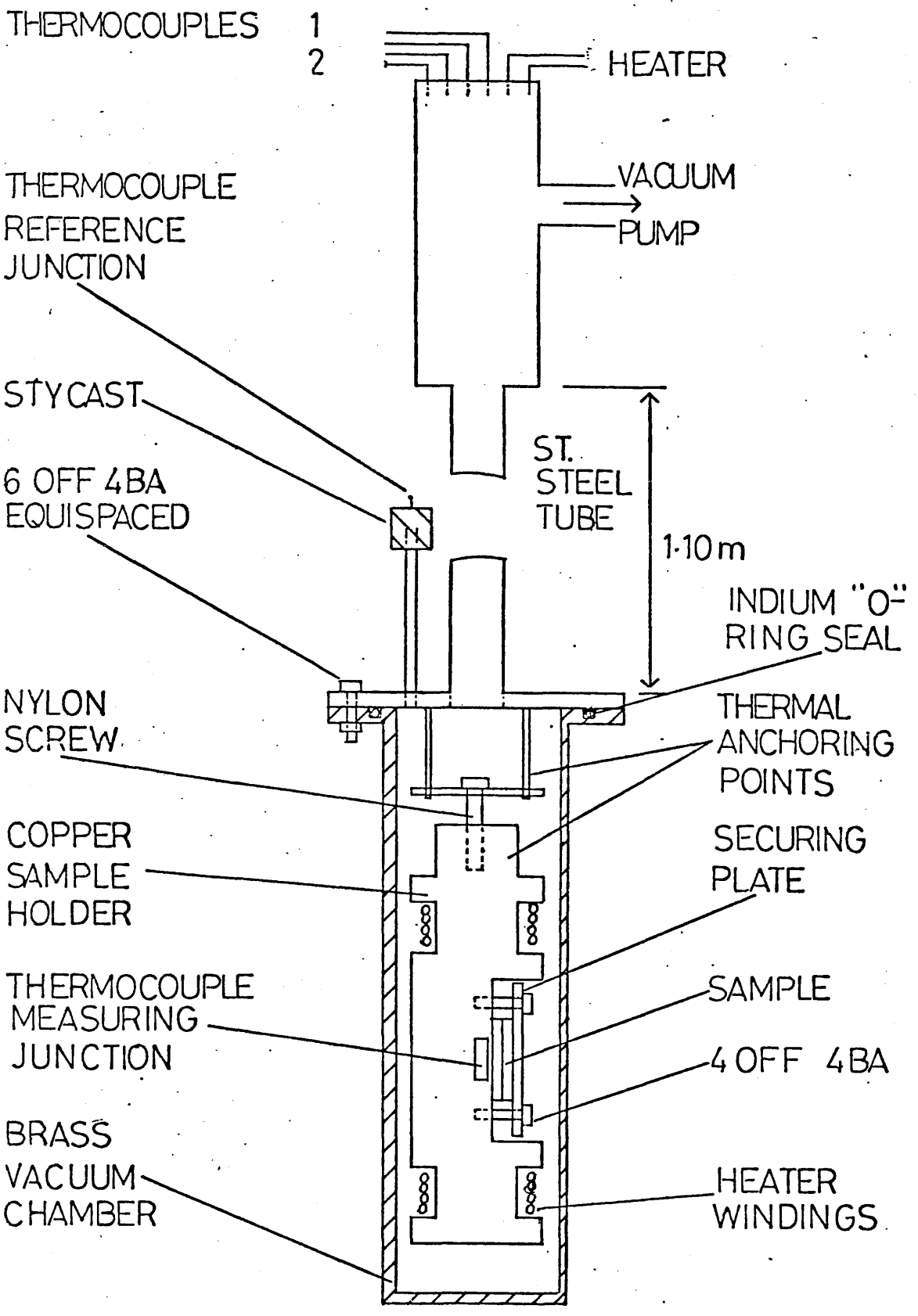

FIG. 2.2 A cshematic drawing of the low temperature cryostat.

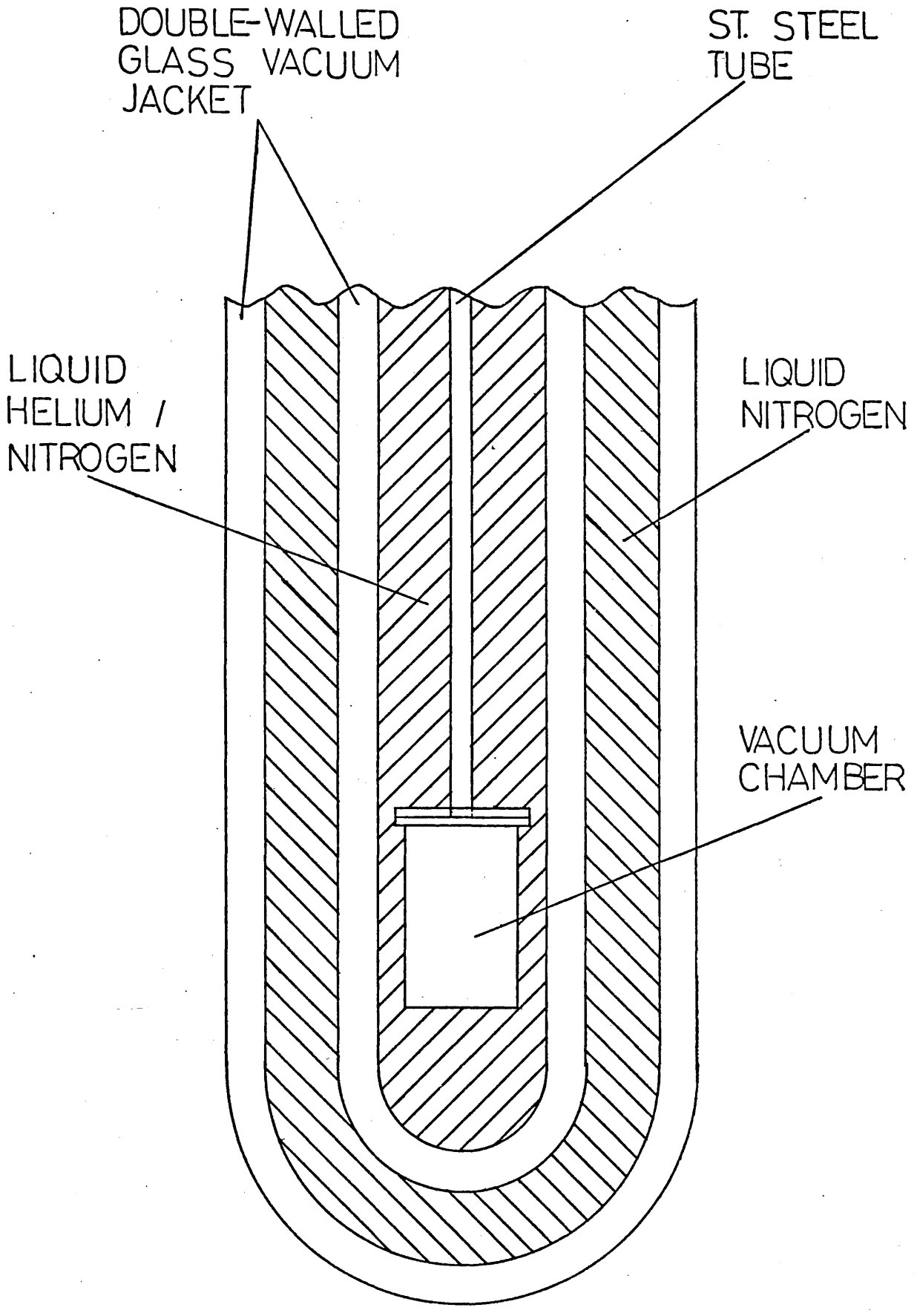

FIG. 2.3 Cross-section of the pyrex liquid nitrogen or liquid helium dewar.

inner dewar would be filled with either liquid nitrogen (if the desired lower limit is 77°K) or liquid helium (if the desired lower limit is 4.2°K).

The sample holder shown in Fig (2.2) was made of 4N pure copper.

Ideally a pumping system should employ large piping, and avoid bends which reduce the pumping speed and the ultimate vacuum that can be achieved. The vacuum chamber after being lowered into position in the inner dewar would normally be connected to an Edwards high power vacuum pump and evacuated at room temperature to about 10^{-5} torr prior to any cooling down. All the joints on the brass vacuum chamber, as well as the steel tube, were hard soldered. 1 mm diameter indium wire which was embedded in a 0.5 mm deep groove made a good vacuum tight seal to the chamber even at the lowest temperatures.

2.2.2 Cooling down

The standard cooling down procedure starts normally by filling the outer dewar with liquid nitrogen as a pre-cooling stage for the inner dewar. When a good vacuum condition exists in the chamber, the inner dewar would be gradually filled up with liquid nitrogen and then both dewars would be topped up from time to time. For measurements below 77°K, the same procedure would be followed until the sample temperature is ensured to be 77°K and then liquid nitrogen would be expelled from the inner dewar and replaced by liquid helium. In either case a small amount of helium gas would be allowed in the chamber to speed up the cooling and to maintain the sample temperature at 77°K or 4.2°K whatever the case might be.

In the temperature region 4.2°K to 77°K pumping on the chamber at intervals was found to achieve the desired result of warming up the sample when the temperature needed to be varied; as opposed to actual heating up by passing a current through the heater element which was the normal practice above 77°K.

Heat Leakage through the thermocouple and heater element is always a problem. Good temperature stability at low temperatures requires the minimization of this heat injection. It was found that this could best be achieved by thermally anchoring the wires before they reached the sample holder.

2.2.3. Temperature control and measurement

To achieve temperature cycling above 4.2°K a 70 ohm Enamel-Constantan heater wire was used. It was wound on the sample holder inside the grooves on either side of the sample.

Two different thermocouples were used. A pure Au + 0.03 at % Fe versus Chromel thermocouple was normally employed in the temperature region 4.2°K, while temperatures above 300°K were measured by a Chromel-alumel thermocouple. This arrangement aforded an adequate accuracey in the temperature measurement. In order to cycle the sample temperature and maintain it automatically at a required value, and Oxford Instrument Temperature Controller (DTC - 2) was used in conjunction with the thermocouples. The temperature stability in the range (4.2 - 420)°K with this arrangement was better than 0.5°K.

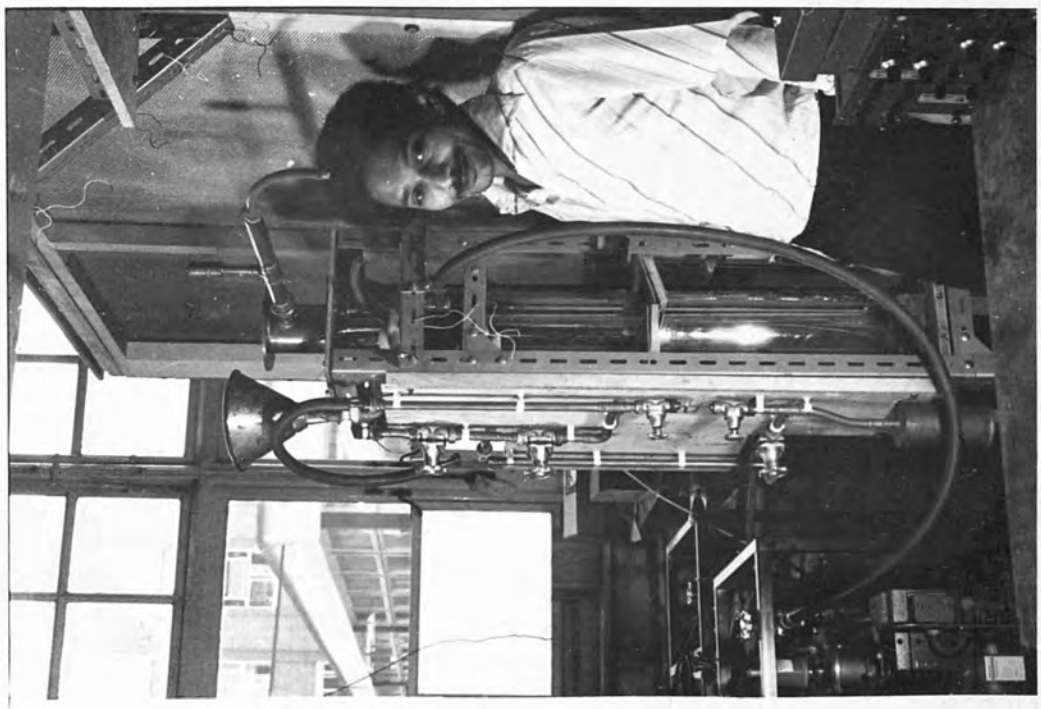

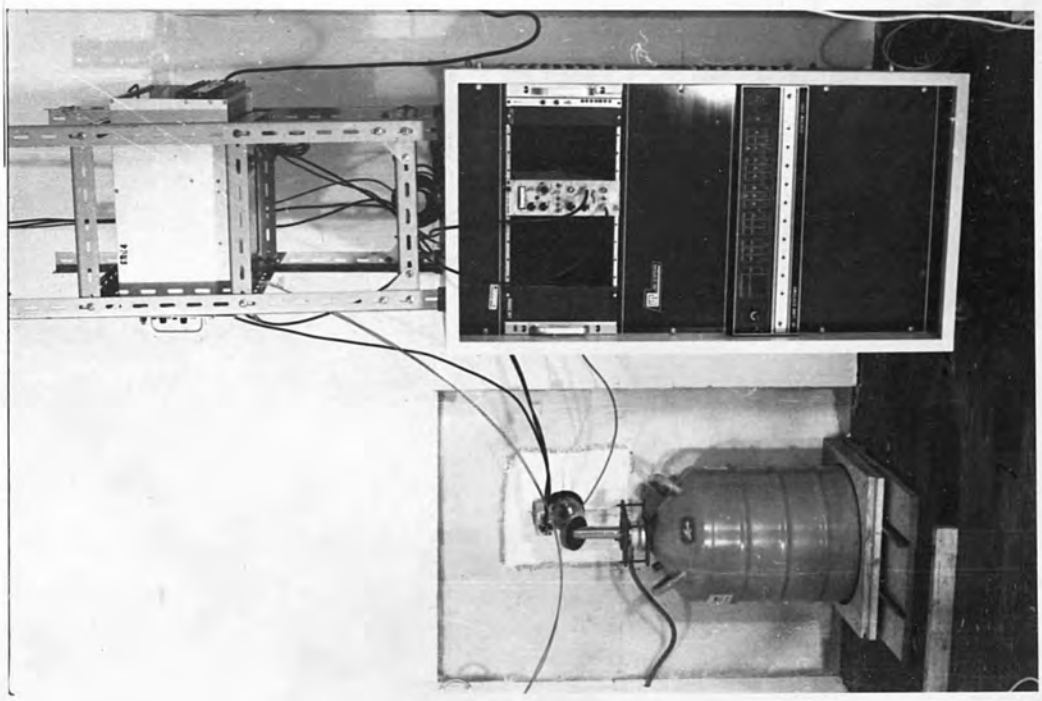

2.3. High temperature furnace

2.3.1. Design

When designing a furnace for the use in positron studies, in general a small furnace, with a heating zone that is sufficiently long so as to minimize thermal gradients, is best. Firstly it requires a smaller amount of power to reach high temperatures and secondly it is portable, easy to insulate and cool and is much easier to evacuate. Coupled with the fact that the sample under study would generally be small it proves desirable to have a compact furnace - detector arrangement that would enable reasonably high counting rates to be achieved.

To facilitate the study of positron behaviour in metals at elevated temperatures (above 400°K) a tubular high temperature furnace was designed and constructed. Fig (2.4) shows a schematic drawing of the furnace. It was made of a 60 cm long thermal aluminous porcelain tube with nominal bore 22.5 mm. An aluminous porcelain tube was chosen because it is a good electrical insulator that can withstand temperatures up to 1900°C as well as being impervious to gases thus minimizing the danger of sample contamination at high temperatures. It also can support a vacuum less than 10^{-6} torr. A heavy piece of stainless steel sample holder attached to the end of a 3 mm diameter alumina twin bore, was used to maintain a fairly homogeneous temperature distribution on the sample. The insulating layer of asbestos cloth that was wrapped round the heater element as well as the 1 mm thick aluminium enclosure which made the supporting frame provided good thermal insulation to the detector at high temperatures.

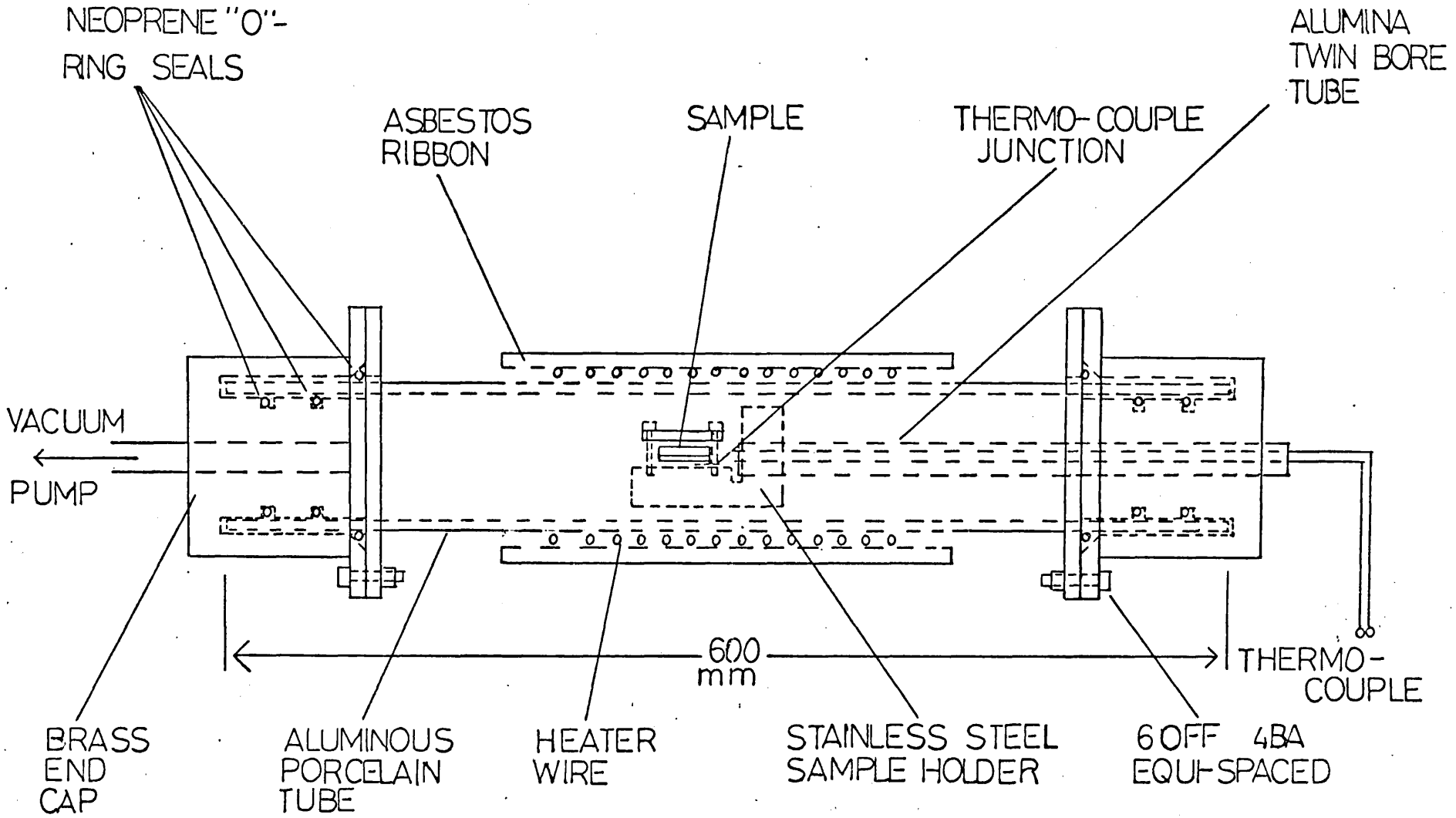

FIG. 2.4 A schematic drawing of the high temperature furnace.

2.3.2. Vacuum conditions and temperature measurement

To minimize the danger of sample oxidation and contamination at elevated temperatures, it was necessary to perform these experiments under very high vacuum conditions. One end of the aluminous porcelain tube was connected to the high power vacuum pump through a brass piece while the other end of the tube was used for the chromel-alumel thermocouple wires, these being passed through the alumina twin bore where one end was open to the atmosphere and sealed with araldite. The brass pieces at each end of the tube were specially made with high precision. The three rubber "O" rings at each end enabled a tight fit of the brass pieces to the tube, thus providing a high vacuum in the tube. The vacuum achieved was better than 10^{-6} torr.

A high power 40 ohm nichrom heater wire was wound directly on the central 20 cm of the aluminous porcelain tube thus providing a heat zone with a very small heat gradient. Sample temperature control was maintained automatically by the temperature controller DTC - 2, supplemented by an Oxford Instrument external high power unit. In view of the high vacuum that was maintained in the tube, the temperature stability, monitored by the Chromel-alumel thermocouple which was attached to the sample holder, was better than 0.25°K.

3. Line-Shape analysis

3.1 Introduction

The apparent simplicity of the conventional approach of deriving a sensible parameter to characterize changes in Doppler broadened line shapes, and thus monitor positron behaviour (e.g. trapping) is highly deceptive.

First attempts are credited to Mackenzie [111] who tried to use the full width at half maximum of the 511 kev peak. This parameterization, although it has certain merits, was found incapable of providing quantitative description of the physics involved.

Deconvolution of the line had been attempted by several groups, Hotz etal [84], Ramma Reddy etal [112], Jackman etal [109], but the deconvolution technique has always been too involved and complicated an approach to afford simple and easy parameters that can be correlated with the phenomena at hand to yield sensible conclusions.

The most popular parameter that is widely employed nowadays is the F-parameter, which was originally proposed by Mackenzie [16]. It is defined as the sum of counts over a fixed number of channels in the centre of the annihilation line divided by the total counts in the line. It is therefore a parameter that relies on the fact that the line narrows as the defect concentration increases regardless of why it narrows.

The F-parameter seems to be a reasonably convenient parameter to use provided decent stability is ensured. There are of course more sophisticated parameters available nowadays that, while employing an approach

similar to that of the F-parameter, involve the line profile in their definition e.g. the N-parameter [113], and the parameters extracted from Running Integrated Difference Curves used by the Harwell group [114].

3.2 The F and W parameters

In a well annealed specimen it is assumed that all positrons annihilate in the free state. That results in a characteristic line shape or a "signature" of free annihilation. As defects are introduced the line begins to narrow. This primarily reflects more annihilation with valence electrons at the expense of high momentum core electrons. The limit to the narrowing of the line is when all positrons annihilate in defects. The narrowest possible line is again a "signature"; this time of saturation trapping [113].

The F-parameter reflects the narrowness of the annihilation line. It is the ratio of the intensity n_1 of the central segment of the peak to the total intensity N, Fig (3.1)

$$F = n_1/N \qquad 3.1$$

If various modes of annihilation occur with frequency f_i each having a line shape parameter Fi, then the observed F is a linear combination

$$F = \frac{\Sigma f_i F_i}{\Sigma f_i} \qquad 3.2$$

i.e. F has a superposition property.

If such a definition of the F-parameter is adopted then the binomial distribution is applicable

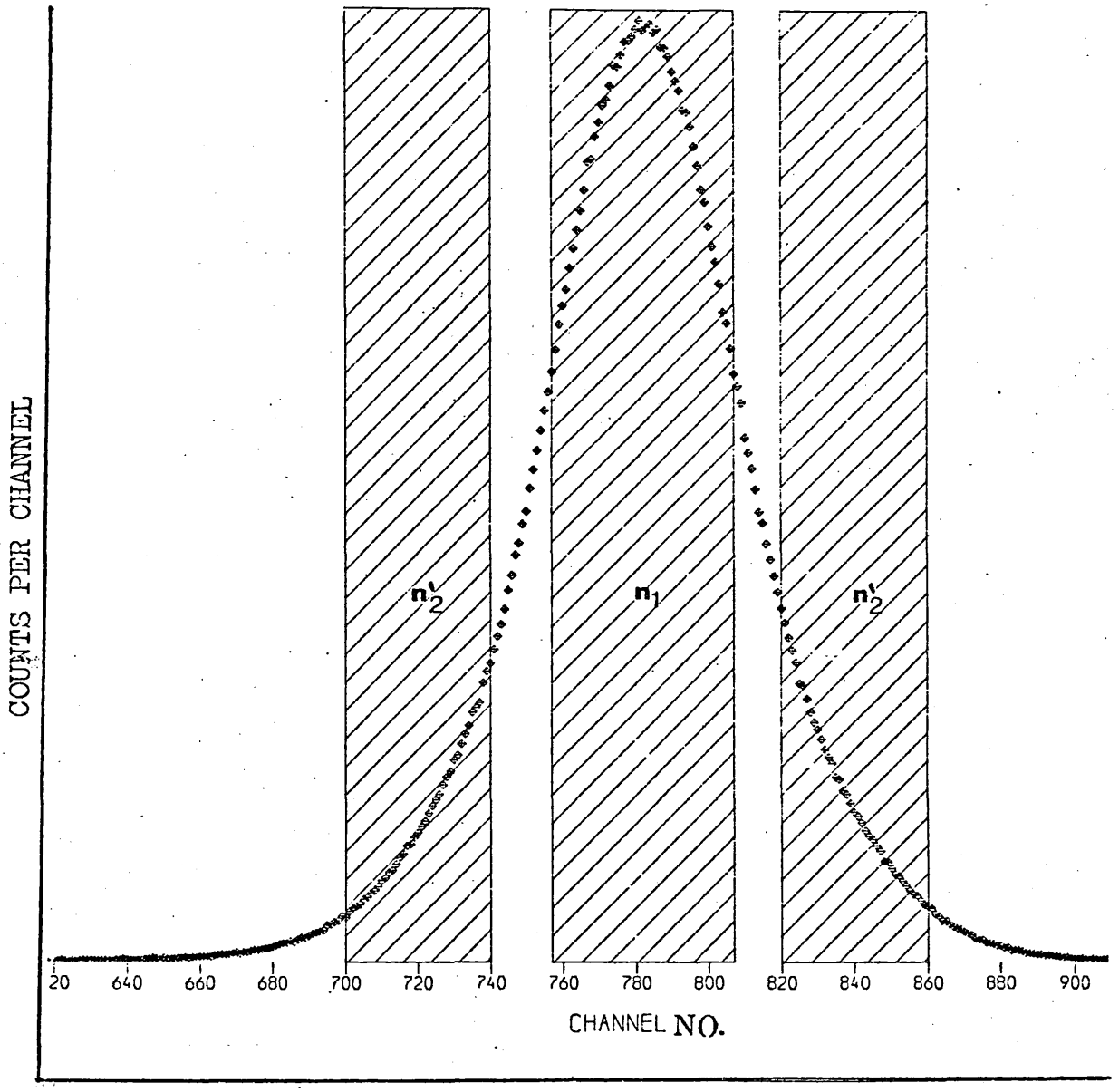

FIG.3.1 The F and W parameter definitions when $n_2=n'_2+n'_2$.

$$P(n_1) = \binom{N}{n_1} \quad p^{n_1} (1 - p)^{N-n_1} \qquad 3.3$$

where $n_1 = 0, 1, \ldots\ldots, N$ and $0 < P < 1$

The variance in the measured central intensity n_1 is therefore

$$V(n_1) = Np(1-p) \qquad 3.4$$

The standard deviation of the line shape parameter F is then

$$\sigma(n_1/N) = N^{-1.5} [n_1 (N-n_1)]^{\frac{1}{2}} \qquad 3.5$$

which is much lower than the one that would result from the invalid addition of independent counting errors in n_1 and N.

Since F reflects annihilation with valence electrons, it increases as the defect concentration increases and more positrons are trapped. Conversely the intensity in the outer, higher momentum, regions of the line is depleted as annihilations with core electrons diminish. A parameter W can be defined as the probability (n_2/N) that an event falls in wing regions. If considered independently this parameter has variance of the form as the F parameter.

3.3 Precision and optimization

If the binomial distribution is assumed the standard deviation of F is

$$\sigma(F) = N^{-1.5} [n_1 (N-n_1)]^{\frac{1}{2}} \qquad 3.6$$

which is smaller than the one we get if the binomial property is ignored i.e.

$$\sigma(F) = [(1/N) + (1/n_1)]^{\frac{1}{2}} \qquad 3.7$$

The ratio between the standard deviations in the two different approaches is of the order of

$$[(1+F)/(1-F)F^2]^{\frac{1}{2}}$$

For a commonly used value of F of about 0.5 this is $(12)^{\frac{1}{2}}$.

The same argument applies to the W-parameter except that the optimum values for W are usually in the region of 0.1 - 0.2. This fact strengthens the view that the binomial property of these definitions ought to be exploited more fully, since otherwise one would have to rely totally upon poor statistics - in the W parameter case - as the determining factor for the standard deviation.

In order to qualify a particular choice of definition of the F parameter or the W parameter two main considerations are taken into account. Upon these considerations the definition of a series of F or W values across a temperature range or a defect concentration can be regarded as sensible parameterization.

The main aim is a compromise that achieves two things:-

(a) The largest possible percentage change in F or W over the temperature range - or defect concentration.

(b) The highest possible statistical stability per point

We will define a sensitivity parameter Z as

$$Z = \frac{\text{percentage change in F (or W) over the range considered}}{\text{standard deviation characteristic of F (or W) in that range}} \qquad 3.8$$

There are a few remarks however concerning optimization:-

(1) This treatment has to be applied to any data in order to ensure that one is extracting as much information as possible prior to the deployment of these F or W values in any subsequent model fittings.

(2) Improvement of data collection is directly reflected on the sensitivity parameter ie. increased counting rate or counting time will improve the quality of the parameter.

(3) Resolution worsening at high counting rates or temperature instability of the electronics over long counting times has to be guarded against once an optimum choice has been made.

3.4 Determination of monovacancy Energies:-

The conventional method of applying the trapping model to angular correlation and lifetime data is discussed in [9], [10], [28].

The application to doppler-broadened data is outlined as follows:-

If P_f and P_t represent probabilities for annihilation in the free and the trapped states respectively such that

$$P_f + P_t = 1$$

then the trapping model leads to

$$P_f = \lambda_f \exp[-(\lambda_f+\mu C_v)t]dt = \frac{\lambda_f}{\lambda_f+\mu C_v} \qquad 3.9$$

$$P_t = 1 - P_f = \frac{\mu C_v}{\lambda_f+\mu C_v} \qquad 3.10$$

Under the assumption that a parameter F, which is linear in the trapping fraction, can be defined of the annihilation spectrum, and that this parameter takes on the values F_f and F_t for the free or trapped positron states, we can write

$$F = F_f P_f + F_t P_t \qquad 3.11$$

i.e. F is given by the weighted mean of the characteristics of the two states.

Substituting 3.9 and 3.10 in 3.11 we get

$$C_v = \frac{\lambda_f}{\mu} (F-F_f)/ (F_t-F) = A \exp [-E_v/KT] \qquad 3.12$$

In practice the use of 3.12 is quite a headache since there are a few temperature dependences floating around and one needs to allow for them sensibly, if there is to be any hope of extracting a reliable E_v value. It is common practice to allow a linear temperature dependance for both F_f and F_t, nevertheless the sign of the F_t temperature dependence is debatable. A positive sign implies that the vacancy is expanding as the

temperature increases, an assumption that has got quite a following recently [29] [30]. On the other hand a negative sign in the temperature assumes that the vacancy contracts, or at least that the trapped positron sees more of the neighbouring ions at high temperature than at low temperature [31] [32]. Possible temperature dependences on the trapping rate, E_v and the entropy factor are still to be settled [71], [72], [97], [28].

The standard form of the two-state trapping model when applied to Doppler broadened data is

$$F(T) = \frac{F_f(1 + \beta T) + F_{1v}(1 + \alpha T) A_{1v} \mathrm{Exp}(-E_v/KT)}{1 + A_{1v} \mathrm{Exp}(-E_v/KT)} \qquad 3.13$$

Extending (3.13) to include divacancies [13] one can write

$$F = F_f P_f + F_{1v} P_{1v} + F_{2v} P_{2v}$$

where F_{2v} characterizes saturation trapping in divacancies. For programming purposes this is written more explicitly as

$$F = \frac{F_f(1+\beta T)+F_{1v}(1+\alpha T)A_{1v}\mathrm{Exp}(-E_{1v}/KT)+F_{2v}(1+\gamma T)A_{2v}\mathrm{Exp}(-E_b/KT)}{1+A_{1v}\mathrm{Exp}(-E_v/KT)+A_{2v}\,\mathrm{Exp}(-E_b/KT)} \qquad 3.14$$

where E_b is the divacancy binding enthalpy defined by

$$E_b = 2\,E_{1v} - E_{2v} \qquad 3.15$$

The case of self-trapping is treated by assuming Seeger's [70] expression for the probability (Pst) of self trapping

$$P_{st}(T) = \frac{1}{1 + B^{-1} T^{1.5} \exp(\varepsilon(K_o)/KT)} \qquad 3.16$$

where $\varepsilon(K_o)$ is an energy given by

$$\varepsilon(K_o) = \frac{3\hbar^2 K_o^2}{2m_+} - \frac{1}{2}\frac{\varepsilon_d^2 K_o^3}{K} \qquad 3.17$$

where Ko is an upper cut-off of the wave number, m_+ is the band mass, K is a combination of elastic constants, ε_d is the positron deformation potential parameter; and where

$$B = \pi_j \frac{\nu_j}{\nu'_j} \left[\frac{2\hbar^2}{m_+ K}\right]^{3/2} \Omega^{-1} \qquad 3.18$$

Ω is the atomic volume and ν_j, ν'_j are the vibrational frequencies of the crystal with free or self-trapped positrons. Under the assumption that trapping by vacancies will always predominate; the F parameter is related to P_{st} by

$$F = F_{1v} P_{1v} + [F_f (1-P_{st}) + F_{st} P_{st}] [1-P_{1v}] \qquad 3.19$$

The inclusion of divacancies in the model analysis of the F curve requires the introduction of the additional parameters F_{2v}, A_{2v} and E_b in a similar fashion to 3.14

3.5 The resolution function

The primary effects of gamma radiation is to release electrons which travel at high velocities initiating showers of free electrons and holes, the final members of which travel at low energy in the lattice. The processes by which the energy of this radiation is

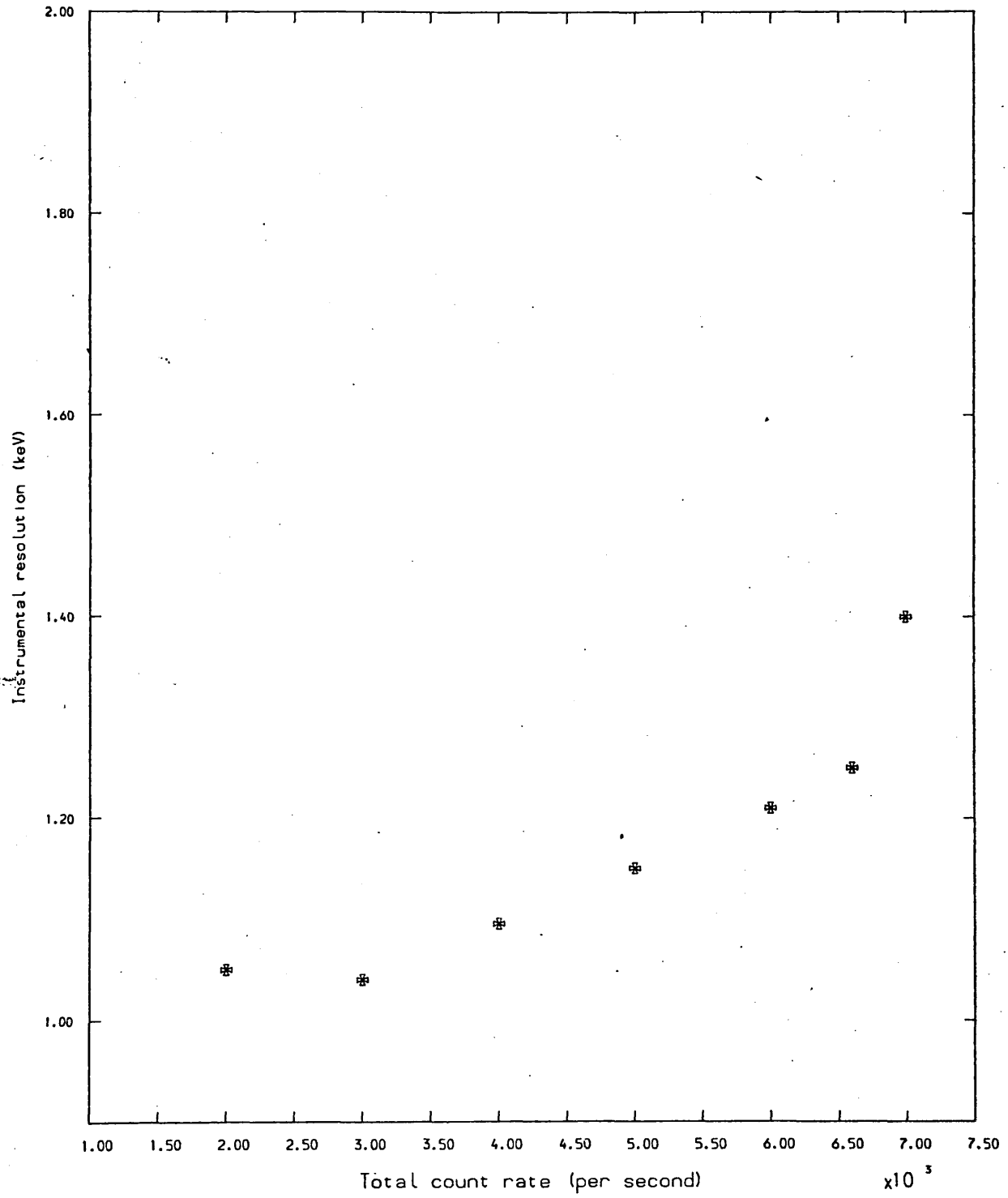

FIG. 3-2 Change of resolution with count rate

expended in generating free electrons are the photo-electric effect, Compton effect, and pair production.

In practical terms the energy resolution of a detector is specified as the full width at half maximum (fwhm) of a peak in a pulse-height spectrum resulting from interaction of a primary photon by the photo-electric effect and is usually given in terms of energy measured in electron volts. By assuming Poisson statistics, modified by a Fano factor F since multiple events that occur in the energy-loss are correlated [115], if the line shape can be represented by a Gaussian then

$$\text{fwhm} = 2.36\ (FWE)^{\frac{1}{2}} \qquad 3.20$$

where W is the average electron-hole pair creation energy resulting from the detection of energy E.

The system performance obtained here is 1.15 Kev fwhm at 514 Kev. This is found by measuring the response of the system to the mono energetic 514 Kev gamma ray from ^{85}Sr. Contributions from incomplete charge collection and from noise arising in the electronic circuitry and system are additional limitations to the one imposed by the Fano factor. There is a variety of analytic functions in literature [116] [117] [118] that are used to describe the resolution function. They generally employ the same approach, namely that of a modified Gaussian distribution in order to allow for tailing effects at the low energy side of the peak. Further details can be found in a Thesis by I. Chagler [96].

Like all analytic functions that are used to approximate a real situation this approach is a complicated one in addition to the fact that since the

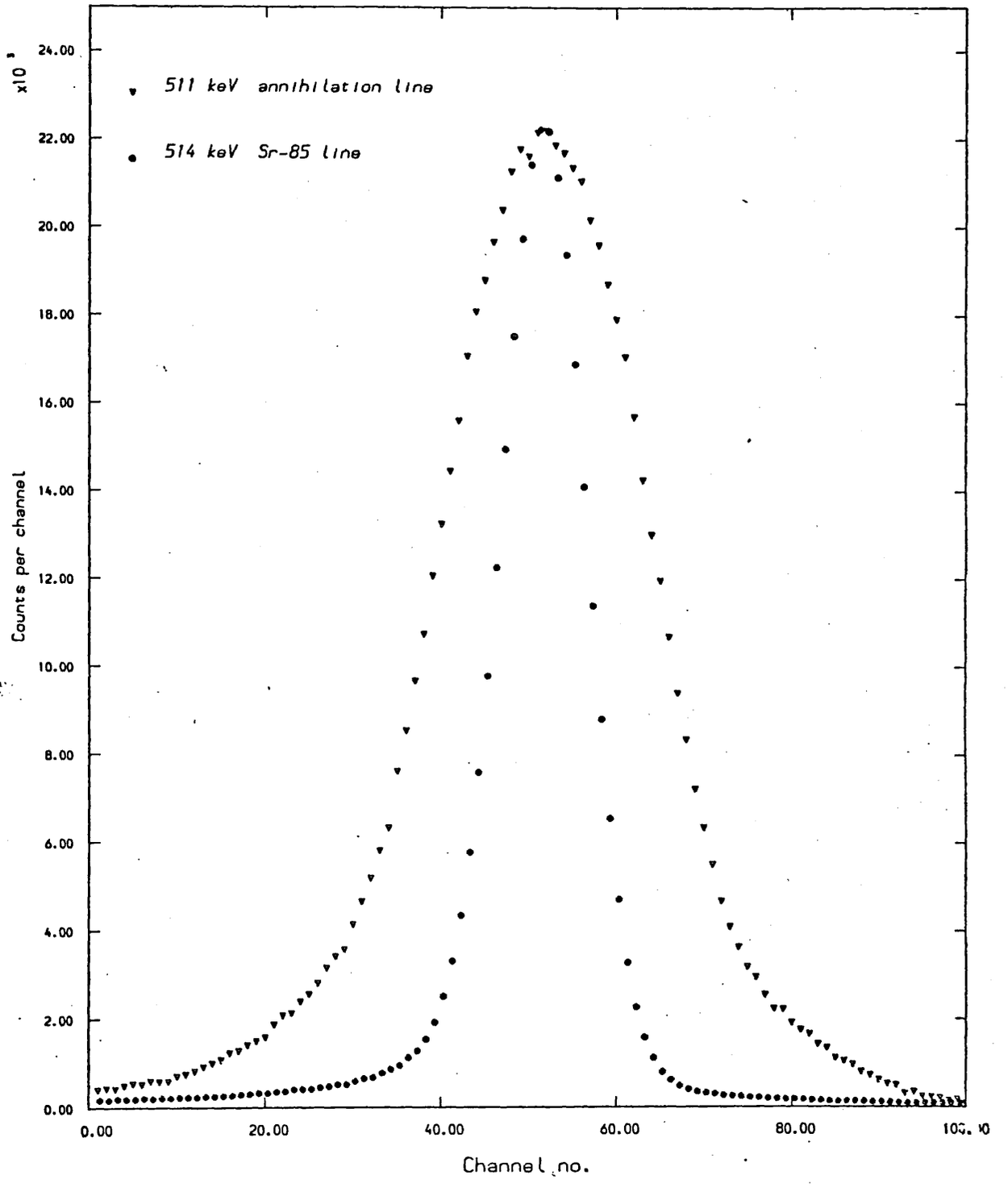

FIG. 3.3 Annihilation line in annealed lead compared to 514 keV gamma-ray line in ^{85}Sr .

resolution function arises as the end result of a sum of several distinct contributions of different parts of the system and since these contributions are capable of varying independently, the reproducibility of this function will be doubtful. A more attractive alternative, suitable for convolution purposes, is that once the resolution of the detector is determined very accurately by recording the lineshape from the 514 kev gamma ray of the isotope ^{85}Sr (typically 2.5 x 10^6 counts per peak), a resolution row vector R (X_i) is formed by assigning to each element of the vector the number of counts in the corresponding channel of the resolution spectrum and then normalizing that vector to unity. This has two main advantages. Firstly it is a more genuine representation of the system response and secondly it is easier to acquire, check, and use in any subsequent convolution.

3.6 Convolution

The observed annihilation spectrum is not the intrinsic (true distribution) of the annihilation radiation, but a spectrum folded with the response function of the detector system. The folded function is expressed as

$$D(E) = \int_0^\infty T(E')\ R\ (E - E')\ dE' \qquad 3.21$$

Where E is the energy of the radiation and is directly related to the channel number of the spectrum. The intrinsic distribution T (E) is extracted by unfolding the observed spectrum D (E) with the response function R(E).

The problem of how to remove the effect of finite spectrometer resolution from experimental data is a

difficult one. It is further complicated by the existence of noise in the data. It is basically a deconvolution problem which is best viewed in terms of Fourier transforms. It can be shown that if d(y), t(y), and r(y) are the Fourier transforms of D(E), T(E) and R(E) respectively then

$$t(y) = d(y)/r(y) \qquad 3.22$$

If the data were free of noise this would be an exact solution. However, the inclusion of noise causes the value of t(y) to become large at high y so that T(E) oscillates wildly. The object of various deconvolution schemes is to attenuate t(y) at high values of the transform variable in order to damp the oscillation in T(E) and still retain some of the resolution. This attenuation leads to what is commonly referred to as the residual instrument function (RIF) which may be viewed as the function which would be obtained after convolution if the apparatus were set to measure a profile which was a delta function. When the data is Fourier transformed it is usually seen that at the lower frequencies the signal dominates the noise and at high frequencies the signal decreases and disappears into the noise. Deconvolution is conceptually as well as computationally a demanding problem to tackle.

Hortz etal [84], Jackman etal [109], Shizuma [116], Dauwe etal [117], and Dannefaer and Kerr [118] [146] have all tried to develop an unfolding technique that would render the recovery of the true distribution possible. In a model-dependent unfolding programme, analytical functions are assumed for the intrinsic distribution T(E) and the optimum parameters of them are determined by means of the least squares method. In the case of annihilation in metal T(E) is usually

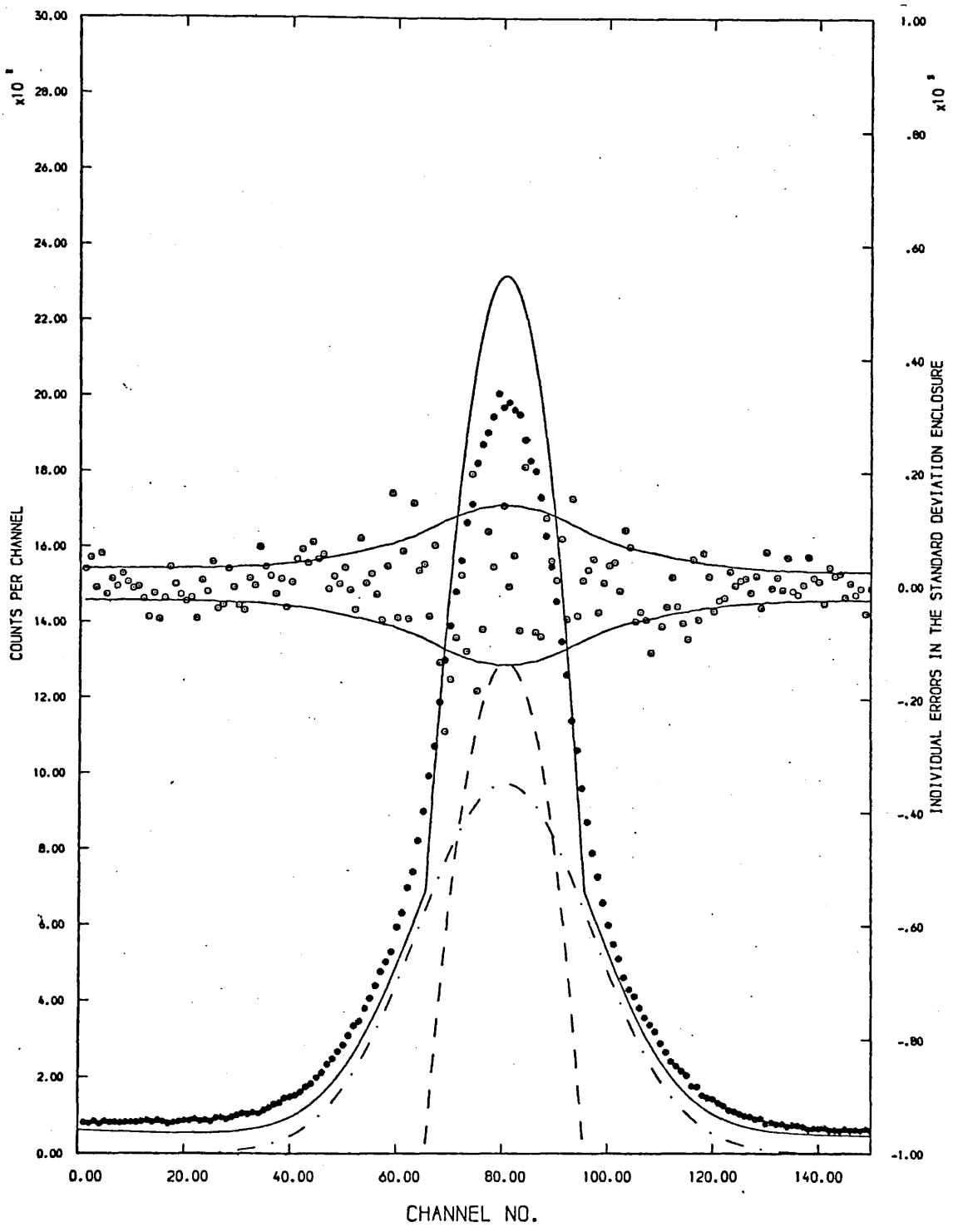

FIG. 3.4 Application of the convolution technique to seperate the two components of the annihilation gamma-ray line in cadmium at 80 K .

assumed to be the sum of an inverted parabola for conduction electrons and a Gaussian for core electrons. That is, the intrinsic distribution is written as

$$T(x) = H_g \exp\left[-\frac{(x-\bar{x})^2}{2w_g^2}\right] + H_p\left[1 - \frac{(x-\bar{x})^2}{2w_p^2}\right] \qquad 3.23a$$

for $|x - \bar{x}| \leq 2^{\frac{1}{2}} w_p$

and

$$T(x) = 2 H_g \exp\left[-\frac{(x-\bar{x})^2}{2w_g^2}\right] \qquad 3.23b$$

for $|x-\bar{x}| > 2^{\frac{1}{2}} w_p$

where x is the channel number, $\bar{x}$ is the common centroid of the parabola and the Gaussian and H_g, W_g, H_p, W_p are the Gaussian height, Gaussian width, parabola height and parabola width respectively. The folded function is calculated as

$$A(i) = \frac{1}{G} \sum_{j=1}^{n} T(i)\, R(i-j), \quad i = 1, \ldots, n \qquad 3.24$$

with

$$G = \sum_{i=-n}^{n} R(i) \qquad 3.25$$

The optimum parameters $\bar{x}$, H_g, W_g, H_p, W_p are obtained from fitting A(i) to D(i). Fig (3.4) shows such a fitting. The actual minimization used required nine free parameters; four of which are used to approximate the background by employing a third-order degree polynomial.

Using the optimum values of the parameters, the area under each analytical expression can be integrated to get the percentage contribution of conduction and core

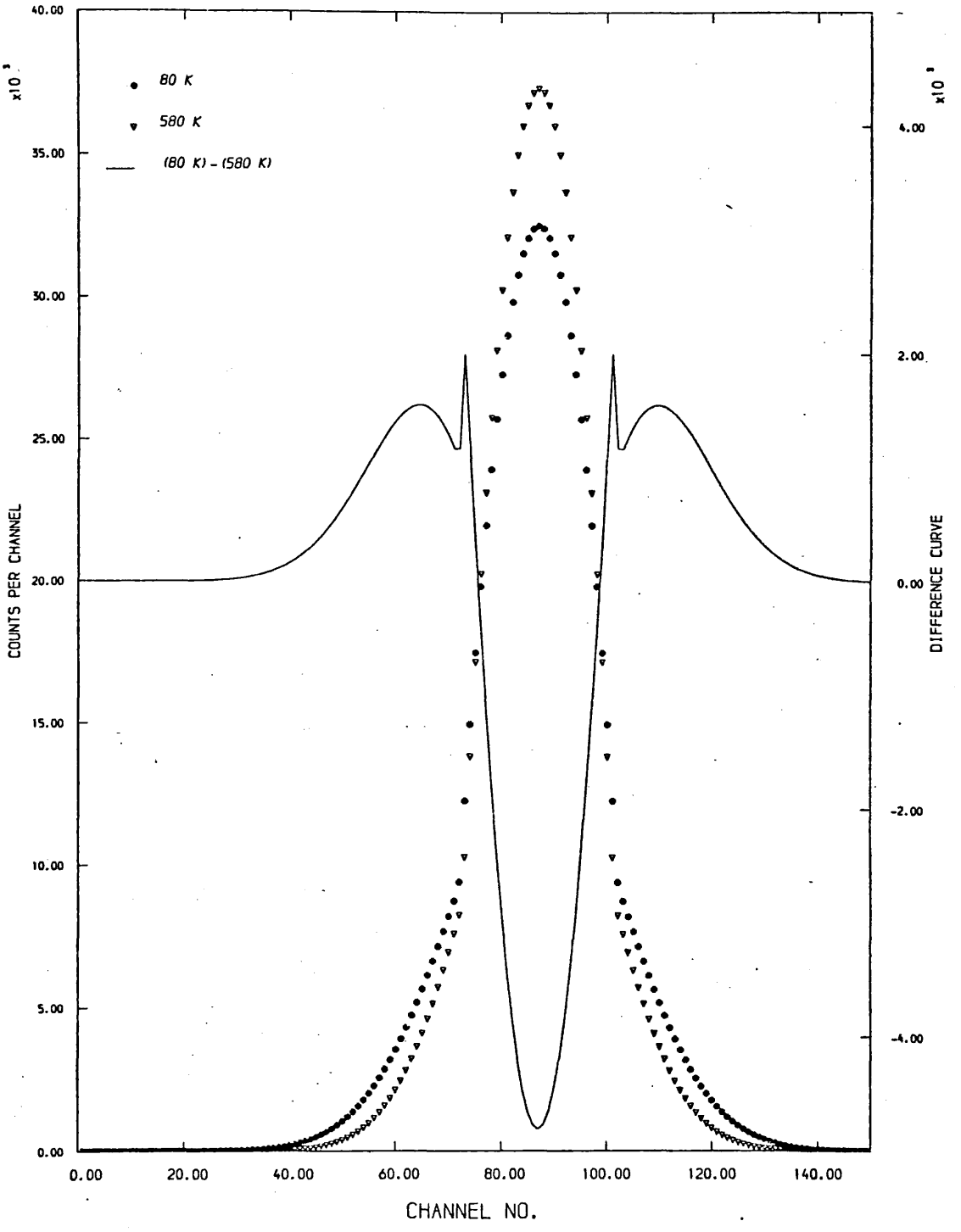

FIG. 3.5 Annihilation line shapes in polycrystalline annealed cadmium at two different temperatures. The solid line represents the deviation between the two lines on an enlarged scale.

electrons to the annihilation line. The percentage contribution can thus be monitored as the sample temperature is changed. The parabolic contribution generally shows an increase, similar to that shown by the F-parameter, as the trapping probability increases.

It should however be mentioned that the convolution technique is not as powerful as the model-independent deconvolution technique. Its main limitations are exposed when the intensity of one component dominates or when the width of one component becomes comparable to that of the response function. In either case the fitting becomes insensitive to the finer details of the model and shows a marked dependency on the initial value of the parameters.

As pointed by Shizuma [116] it is possible to get a good fit using two Gaussians, instead of a parabola and a Gaussian, when one of them is weaker than 10% of the total intensity.

The reduced-chi squared values one obtains are normally in the range 0.9 - 1.3. This is reasonable considering the crudity of the model since it ignores high momentum components in the conduction electrons contribution and assumes the core contribution to be strictly Gaussian.

3.7 Positron zero-point energy

It was observed that when convolution is attempted in metals that show strong trapping effects like cadmium and indium the reduced chi-squared showed systematic worsening, coupled with marked narrowing of the electron Gaussian, as the trapping probability increased. This was taken to be indicative of the trapped positron zero-point energy.

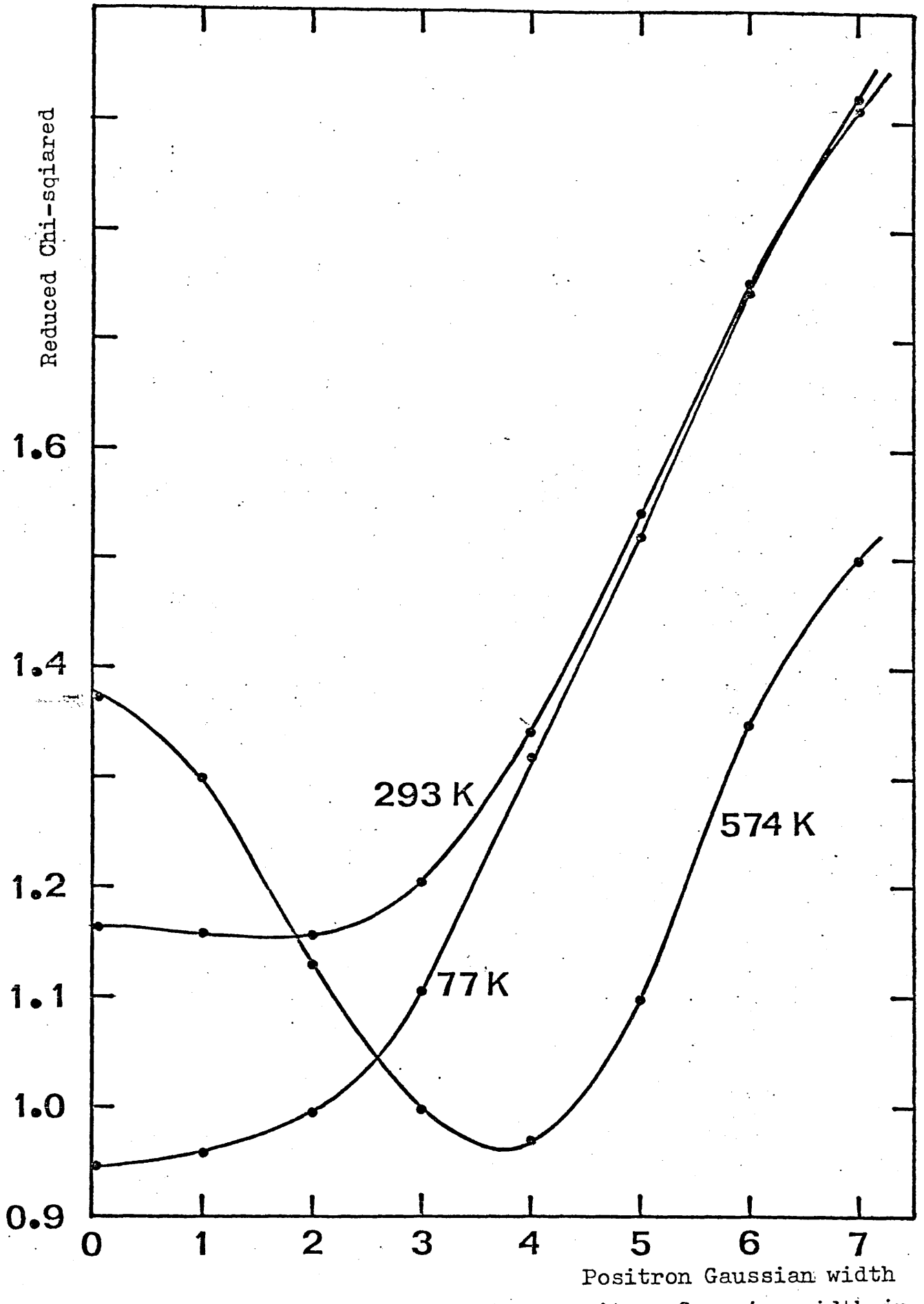

FIG. 3.6 The reduced chi-squared against positron Gaussian width in Single Crystal Cadmium.

The Gaussian plus inverted parabola model is applicable at best when dealing with perfectly annealed metal samples in which positrons are not trapped. Whenever positrons get trapped, at vacancies or dislocations in defective samples, the trapped positron will contribute significantly to the momentum of the annihilating pair. To include the effective zero point kinetic energy of the trapped positron, an effective response function is employed by folding the measured resolution function with a Gaussian distribution of width σ_{e^+}. The parabola-Gaussian model is then convoluted with the new response function and compared with the observed spectrum.

This is of course only a crude method of allowing for the positron contribution to the annihilating pair momenta but it gives an idea of the trapping strength at a defect. The choice of a more sophisticated and realistic positron function may make it possible to uncover specific features of the potential distribution at a defect in a metal. A similar approach had been used by Hautojarvi [147] in his study of positron trapping in dislocations in aluminimum and had also been used by Lichtenberger [93] and Jackman etal [109]

Fig (3.6) shows a plot of the reduced chi-square against the additional positron Gaussian width for a high temperature point in single crystal cadmium. It is seen to go through a minimum at roughly 3.6 (94 ev per channel). It has been noticed that aside from the improvement in the reduced chi-squared the electron Gaussian recovers some of its width at the expense of further narrowing of the parabola and an increase in the parabola percentage. The narrowing of the electron parabola seems to indicate that the local Fermi momentum and correspondingly the local conduction

electron density seen by the positron at the trapping site are smaller than in the regions of the perfect lattice.

3.8 General Remarks

3.8.1 System stability and the line shape parameters.

The problem of electronic stability in lifetime measurements is widely recognised whereas instrumental instabilities in annihilation photon energy spectrometers, although equally important, have received little attention until recently. While Campbell [148] discussed the appropriateness and sensitivity of different line shape parameters, Campbell and Schulte [149] outlined the methodology in observing and correcting for resolution degradation due to the system's instability in a case study in Ni and Al.

A system can exhibit long term or short term drifts and show dependence on all sorts of factors like the nitrogen level in the cryostat, counting rate, and most serious of all laboratory temperature. A general feature of a system suffering from one or all of these is the loss of centroid precision in addition to line broadening. It is necessary for a system that is to perform in a statistical manner that it should be operated under optimum temperature stability.

Kerr etal [150] described a correction technique for the F parameter by using the 478 Kev ^{7}Be gamma ray line as an energy resolution monitor.

Throughout the course of the experiments in this Thesis the 497 Kev ^{103}Ru gamma ray line was used as a simple stability monitor, but no attempt was made to use it for correction purposes since that would have necessitated a high counting rate for the 497 Kev line in order to achieve adequate statistics for the

correction to be effective. Such a requirement might have easily compounded the problem since the electronic system may respond differently to rate variation, had there been a need for rate correction, than to temperature variation.

An effective correction for temperature instability would have to account simultaneously for three factors. The first is the amount of the drift, the second is the direction of the drift, and the third is the rate of the drift. Simulation techniques might be invoked successfully [149] [150] in order to correct for the first two, but it is highly impracticable, if not impossible, to correct for the third one by simulation.

The ^{22}Na positron sources were supplied by the Radio Chemicals Centre as aqueous solutions of Carrier-free Sodium Chloride while ^{85}Sr and ^{103}Ru were irradiated at the Reactor Centre of London University. The intrinsic resolution at a total count rate of 5K cps was 1.15 Kev for the 514 Kev ^{85}Sr gamma ray line. Simultaneously with data collection the electronic stability was constantly monitored by the 497 Kev of ^{103}Ru and was found to be better than 0.5 channel in 8000.

3.8.2 e^+ zero point energy and partial trapping

If a programme employing the positron zero point energy approach could be used successfully across the whole temperature (or defect concentration) range under investigation, the information obtained might prove extremely valuable. It was found possible to analyse lines at both extremes of the trapping probability and the results appear to be satisfactory (appendix IV and V). Nevertheless the full impact of this approach could only be appreciated if the partial trapping case could be solved.

Strictly speaking one would need to perform a double deconvolution in two separate stages. In the first one the system's resolution would be unfolded and in the second one the positron zero point energy contribution. In a model dependent convolution approach the data would be compared to

$$[P_T(\text{parabola} + \text{Gaussian})_T * \sigma_\Theta + (1-P_T)(\text{parabola} + \text{Gaussian})_F] * \text{Resolution}$$

where * refers to convolution, P_T is the trapping probability, and T and F refer to trapped and free states respectively. If a third order degree polynomial is included to represent the background, such a minimization would require 14 free parameters.

Although this might appear a straight forward exercise in principle, it is nothing of the sort. From the computational point of view finding the genuine minimum, as apposed to local minima, in the multi dimensional space of 14 parameters is an exceedingly difficult task. The reduced chi-squared ought to be viewed as a function in the N-dimensional space of the fitting parameters. Since a complete search in this N-dimensional space is not always easy the next best thing is a study in the projected space of some of the fitting parameters. Nevertheless this can only be done if one had a fair idea of what the optimum value of some of these parameters ought to be, and in the case of partial trapping this approach might reduce the number of free parameters to nine, which are still a few too many.

The obvious advantages of the method, if applied successfully, are that it will provide reliable means of correlating the F parameter curve with the parabola

percentage in addition to showing how the profiles and the intensities of the various analytic functions behave as the trapping probability changes thus establishing a characterization of the defect involved in the trapping process. It will also provide the trapping probability as part of the minimization.

4. Positron Annihilation in Cadmium

4.1 Positron annihilation in polycrystalline cadmium

4.1.1 Sample Preparation

Two discs - each of 1.6 mm thickness and 20 mm diameter - of 5N purity polycrystalline Cadmium, supplied by Johnson and Matthey, were etched in dilute nitric acid. They were then annealed for 23 hours at 514°K under a vacuum of 10^{-6} torr. They were then slowly cooled to room temperature, etched again, and then approximately 0.09 m Ci of carrier-free $^{22}NaCl$ solution was evaporated directly onto the central region of the discs. The two discs, sandwiched together, were then wrapped in thin aluminium foil and mounted on the low temperature cryostat.

4.1.2 The F-curve

Figure (4.1) illustrates the temperature dependence of the F-parameter in annealed 5N cadmium from 4.2°K to 585°K. A count rate of 5K cps was used and the data reveal four regions in the temperature curve. The first region extends from 4.2°K to about 50°K and shows a small, but distinct, drop in the F-value as the temperature increases. The second region extends from 50°K to about 140°K and appears to be very nearly flat. The third region, from 140°K to roughly 340°K, shows a steep, possibly linear, increase with temperature. The largest rate of increase in F with temperature however is observed in the fourth region which extends from about 340°K to near the melting temperature. At the top end of this region the data, markedly less steep than the rest of the region, suggest the setting-in of a possible flattening effect. The data appears to be

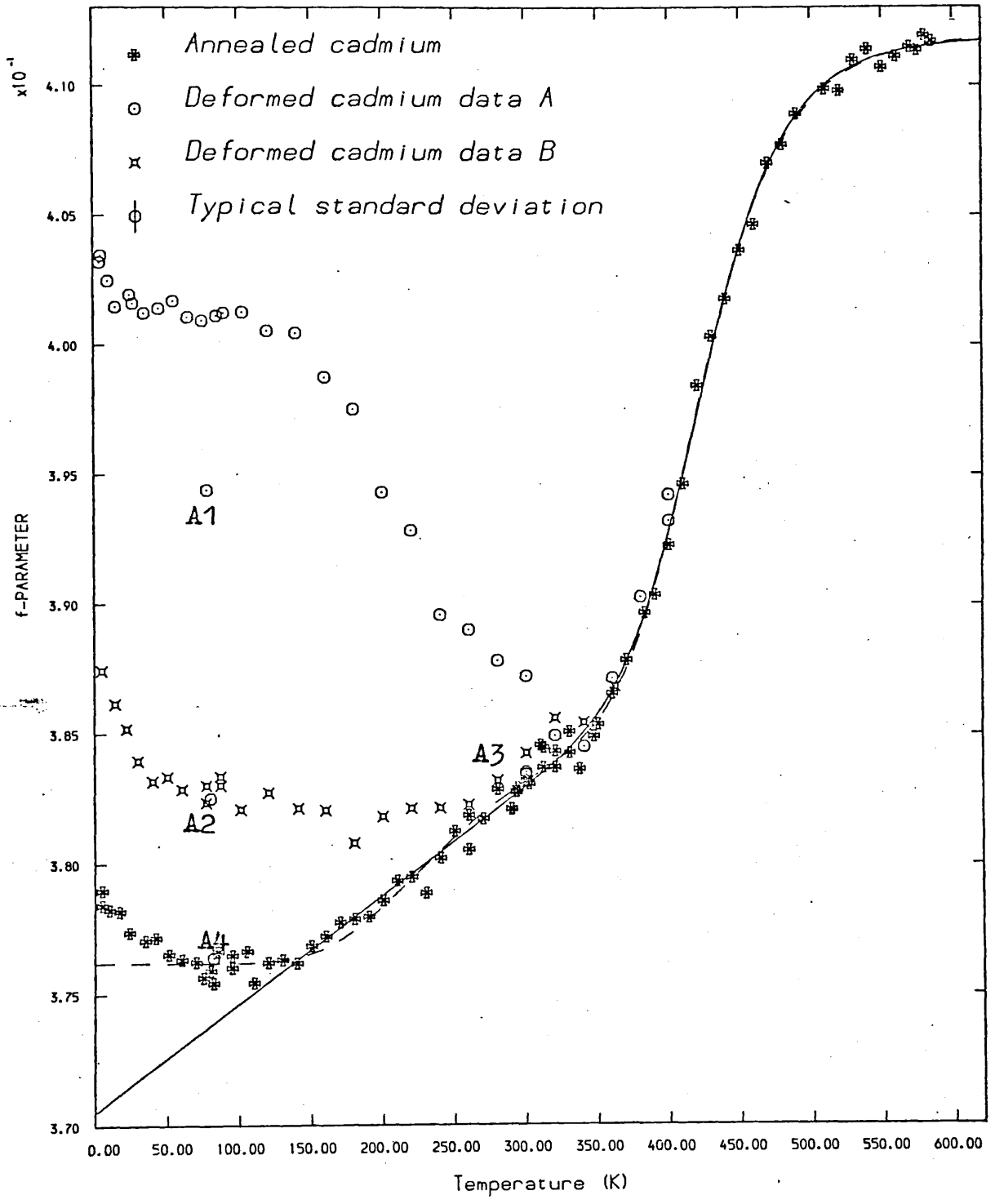

FIG. 4.1 The variation of the line-shape parameter F as a function of temperature for the annealed and the two deformed specimens of polycrystalline cadmium. The solid and the broken lines represent the linear rise and the self-trapping model fittings, respectively, outlined in the text.

in good agreement with Herlach etal [31] Doppler broadening and lifetime data and with Lichtenberger's [93] Doppler broadening data.

4.1.3 F-Parameter Analysis

The standard approach to the F-parameter anlysis has been outlined in (3.4). The results of this analysis for the different models are shown in table 4.1. one point that ought to be mentioned from the onset is that a single number, whether it be an E_v value or a chi-squared per degree of freedom, cannot be used in itself to vindicate a model from which it arises as a consequence. In that respect all models are considered equivalent until the behaviour of a model as a whole can be either confirmed and substantiated by another technique or verified by theoretical calculations. Whereas other techniques, like electrical resistivity measurements or specific heat measurements, might produce similar E_v values; they are plagued by their own problems and are in no position to check the subtleties of the trapping model when applied to positron behaviour in metals. It must also be kept in mind that comparing lifetime to either Doppler broadening or angular-correlation measurements is to compare two different physical measurements. Lifetime is a measure of the expectation value of the electron density of all momenta over the extent of the positron wave function (Bloch like for the defect-free annihilations). Both Doppler broadening and angular-correlation measurements, when analysed in terms of some line shape parameter or peak counting rate, are biased towards annihilations with electrons having narrowly restricted momenta. The results can sometimes show serious divergance as Lynn etal [130] showed in nickel.

TABLE 4.1
MODEL FITTINGS FOR POLYCRYSTALLINE CADMIUM

Model	E_v ev	F_f	F_{1v}	A_{1v} x10^{-5}	B x10^{5}	α x10^{+6}	F_{st}	ε ev	B x10^{-5}	χ^2/ν
a)Monovacancies plus linear rise above 140°K	0.56 ±.02	0.3705	0.4118	32.90	11.1					1.40
b)Monovacancies plus linear rise above 140°K	0.565 ±.02	0.3704	0.4083	42.00	11.23	15.5				1.19
c)Monovacancies plus Self-trapping above 70°K	0.54 ±.02	0.3762	0.4120	21.14			0.3886	0.123	76.14	1.15
d)Monovacancies plus linear rise plus divacancies above 140°K	0.60 ±.02	0.3703	0.4108	125.20	11.5					1.22
e)Monovacancies plus Self-Self-trapping plus divacancies above 70°K	0.56	0.3752	0.4112	52.52			0.3892	0.129	66.40	1.16

d) $F_{2v} = 0.4321$, $A_{2v} = 156.4 \times 10^8$, $E_{2v}{}^b = 0.100$ ev (e) $F_{2v} = 0.4163$, $A_{2v} = 213.6 \times 10^8$, $E_{2v}{}^b = 0.064$ ev

The controversy over an acceptable vacancy formation energy for cadmium is one that will take some time to settle. Differential dilatometry [119] [120] gives 0.41 ev, while quenching experiments [121] give 0.42 ev. Seeger [28] quotes a value of 0.39 ev from angular correlation measurements and 0.41 ev from lifetime measurements. Singh and West [63] reported a value of 0.47 ev while West [122] reported a value of 0.52 ev using a linear rise fit on Doppler broadening data. When he included a temperature dependance in F_V the value became 0.57 ev. Mackenzie etal [123], using the threshold temperature correlation technique on Doppler broadening data, decided on a value of 0.45 ev. It should be added however that Michin etal [124] predicted a theoretical value of 0.59 ev.

Any analysis attempting to fit with a two-state trapping model, data which is actually associated with three states, would be expected to result in high E_V values. Large E_V values do imply either a much larger positron trapping rate than in other comparable metals or a much larger formation entropy [28] [125]. This seems to be the case for this sample, since the A_{1V} values are abnormally high.

If one considers model (a) and assumes the lifetime of free positron in cadmium to be 190 p second [31] and the entropy of formation to be 1K,(where K is the Boltzmanns constant) the result is a specific trapping rate of positrons in vacancies in cadmium of about $6.3 \times 10^{15} s^{-1}$; which is an order of magnitude higher than what seems to be average acceptable values of trapping rates in metals [110]. In order to get this to be more in line with current acceptable values one would have either to postulate a vacancy formation entropy of about 3.5 K or a positron lifetime in the

free lattice of about 2400 p second. Both alternatives are out of the question. The results presented by Lichtenberger [93], when he used the same type of model, suffer from the same criticism. The results of the minimization shown by model (c) afford a slight improvement over (a) and (b) but it is still not sufficient enough to counter balance the strong effect of the formation energy exponential factor. While inclusion of divacancy parameters would, in general, be expected to result in a lower A_{1v} and E_v values; the reverse seems to be happening in this case. Therefore by no means can any of these minimizations be considered satisfactory. The apparent improvement of the chi-squared per degree of freedom might simply be due to the inclusion of more free parameters in the fittings. It should be stressed that there is nothing whatsoever wrong with the data. When one uses $5 \times 10^{14} s^{-1}$ as specific trapping rate and 190 p sec as lifetime of free positrons in cadmium, one obtains a vacancy concentration c_v of about 5.6×10^{-4} at the melting temperature similar to the one found by Feder and Nowick [119].

A series of factors that are bound to have complicated the issue must be mentioned however. The F-parameter itself is definition-dependent i.e. as the F-definition is changed, the minimization parameters change, A_{1v} in particular. There is also a case to be made for including a temperature dependence in the annihilation rate for free positrons, which occurs as part of A_{1v}, since, afterall, F_f has been allowed one and it is seen in the case of cadmium to be quite strong. Possible temperature dependances in the specific trapping rate, entropy of formation, and formation energy have all been set to zero, a fact which could not have helped determining the real A_{1v} if they genuinely existed.

4.1.4 Convolution

In an attempt to understand the origin of the temperature dependence of the annihilation line in cadmium the data has been analysed using a convolution technique. Section (3.6) describes the details of this procedure. A model consisting of the superposition of a Gaussian and an inverted parabola was used to represent the momentum distribution of annihilating positron-electron pair. The model was then convoluted with the experimentally measured resolution function and compared with each of the measured annihilation spectra. A least-square optimization procedure produced the best fit of the model to data based on the reduced chi-squared parameter. The results for the parabola width and Gaussian width are displayed in Fig (4.2), while (4.3) shows the variation of the parabola percentage, obtained as a result of the minimization, with temperature.

Correlation between the F-parameter curve and the parabola percentage is to be expected since both reflect the increase in the probability of a positron annihilating with conduction electrons. Jackman etal [109] find a value of 41% for the parabola percentage at 77°K while Stott and West [49] quote a value 40% below the onset of vacancies. These are in good agreement with Fig (4.3) which shows the parabolic percentage rising from about 38% at 100°K to about 40% at 350°K ; thereafter we see a steep rise, due to vacancies, to 45% near the melting temperature.

The narrowing of the Gaussian width which begins in the prevacancy region and continues, even to a higher

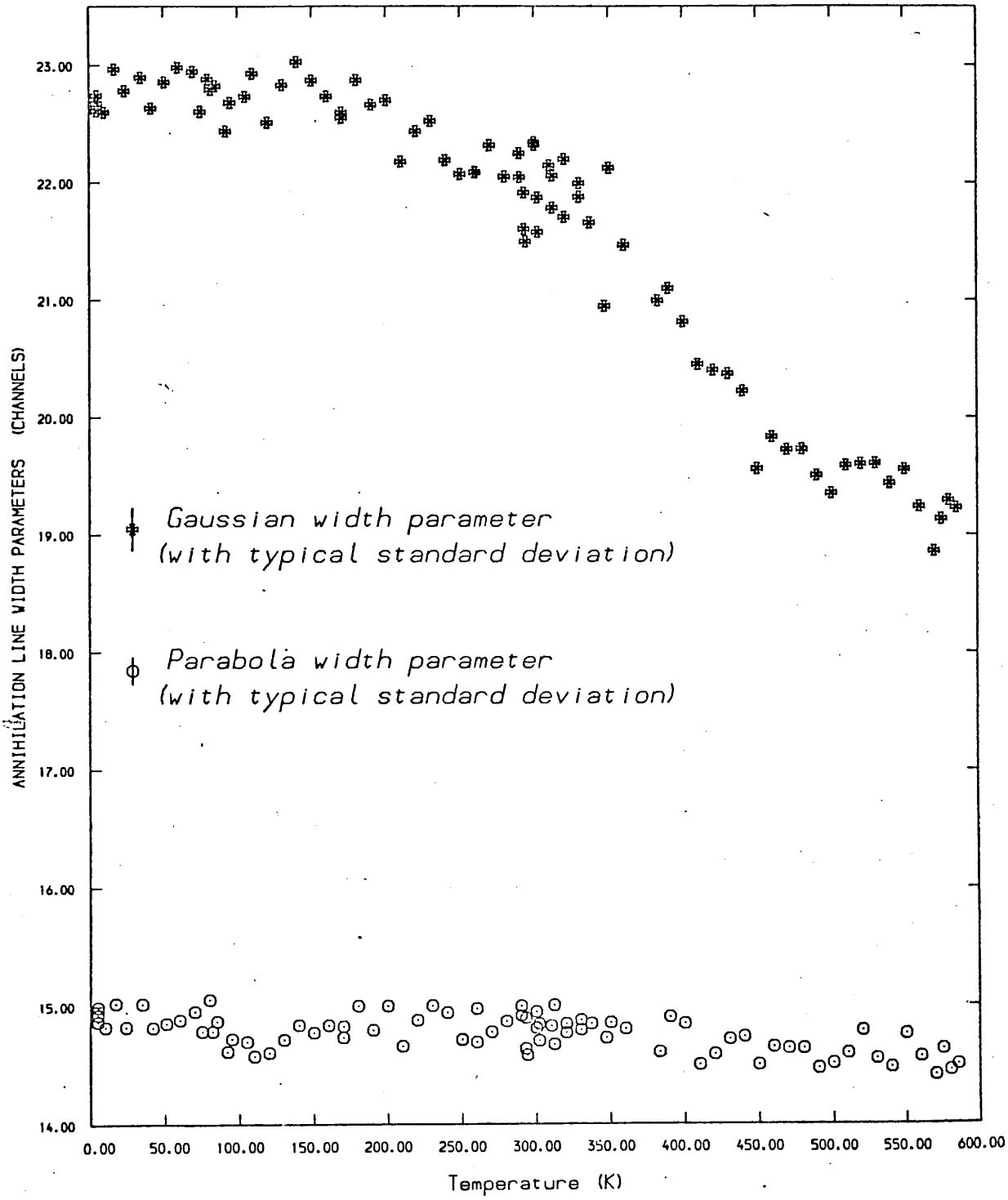

FIG. 4.2 The variation of the width parameters of the Gaussian and the parabolic components of individual lines for polycrystalline annealed cadmium as a function of temperature.

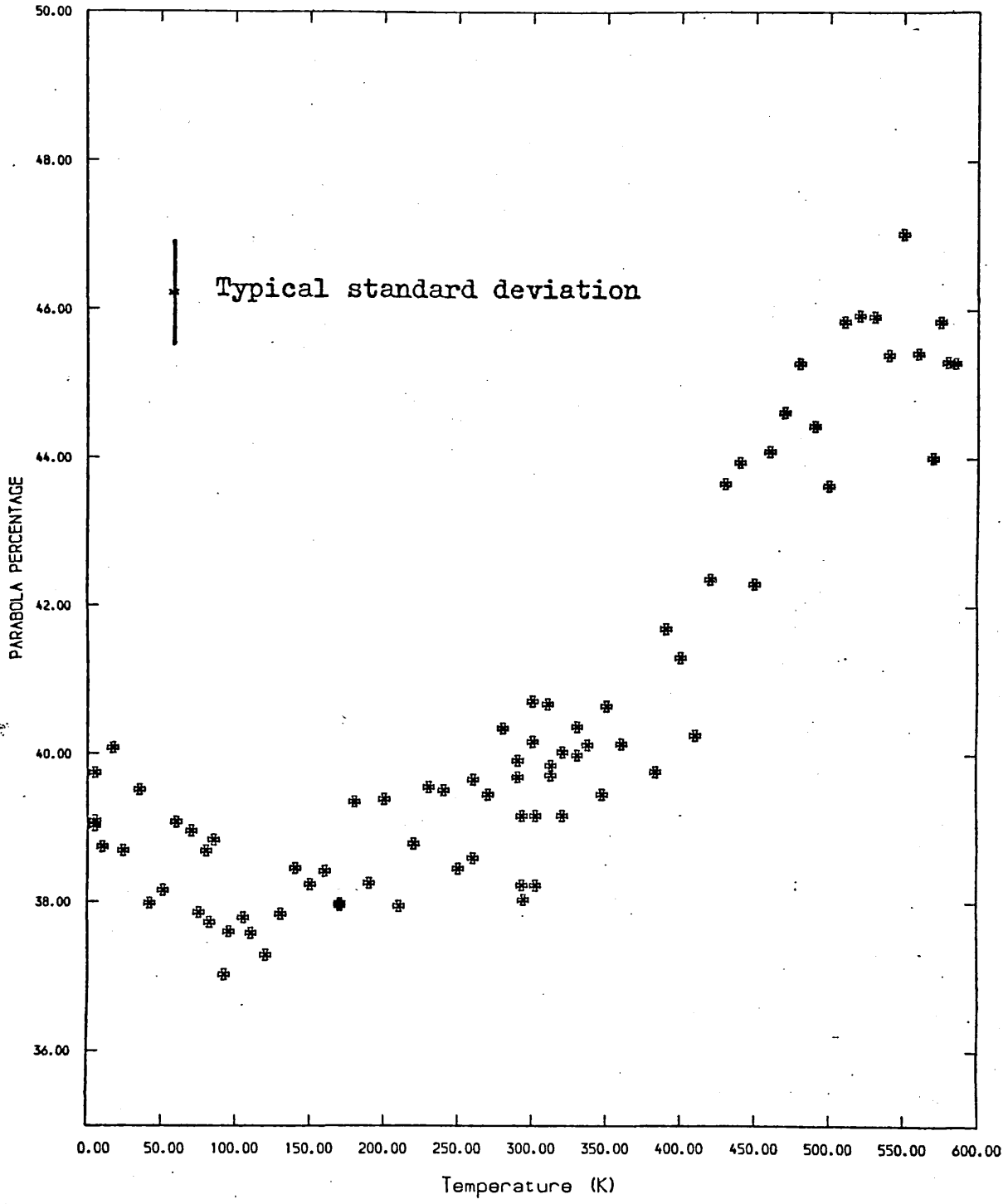

FIG. 4.3 The temperature dependence of the proportion of the annihilations contributing to the parabolic component of the line shape for polycrystalline annealed cadmium.

degree, in the vacancy region obviously contributes to the increase in the F-value thus making a quantitative correlation between the F-parameter and the parabola percentage difficult. A slight variation in the parabola width can be seen in Fig (4.2). This is probably due to a contraction of the Fermi surface. The average parabola width at low temperatures of 14.82 channels corresponds with an electron energy of 7.59 ev. This is in reasonable agreement with 7.47 ev, the accepted Fermi energy in cadmium according to Ashcroft and Mermin [131], and Kittel [132].

4.2 Positron annihilation in single crystal cadmium

4.2.1 Sample preparation

Two 1.5 mm thick and 10 mm diameter discs of single crystal cadmium were spark cut from a 6N pure rod supplied by Metals Research Ltd. They were first etched in dilute nitric acid and then they were electropolished in 45% concentration orthophosphoric acid using a carbon rod as the cathode. 0.1 m Ci of carrier-free $^{22}NaCl$ solution was then evaporated onto the central region of the discs. Sandwiched together, they were wrapped in a thin aluminium foil and mounted in the low temperature cryostat. The sample was then cooled down slowly to liquid nitrogen temperature.

4.2.2 The F-Curve

Figure (4.4) shows the F-Parameter plotted over the full temperature range. There are two new features that emerge from this when compared with the F-parameter curve for polycrystalline cadmium. The

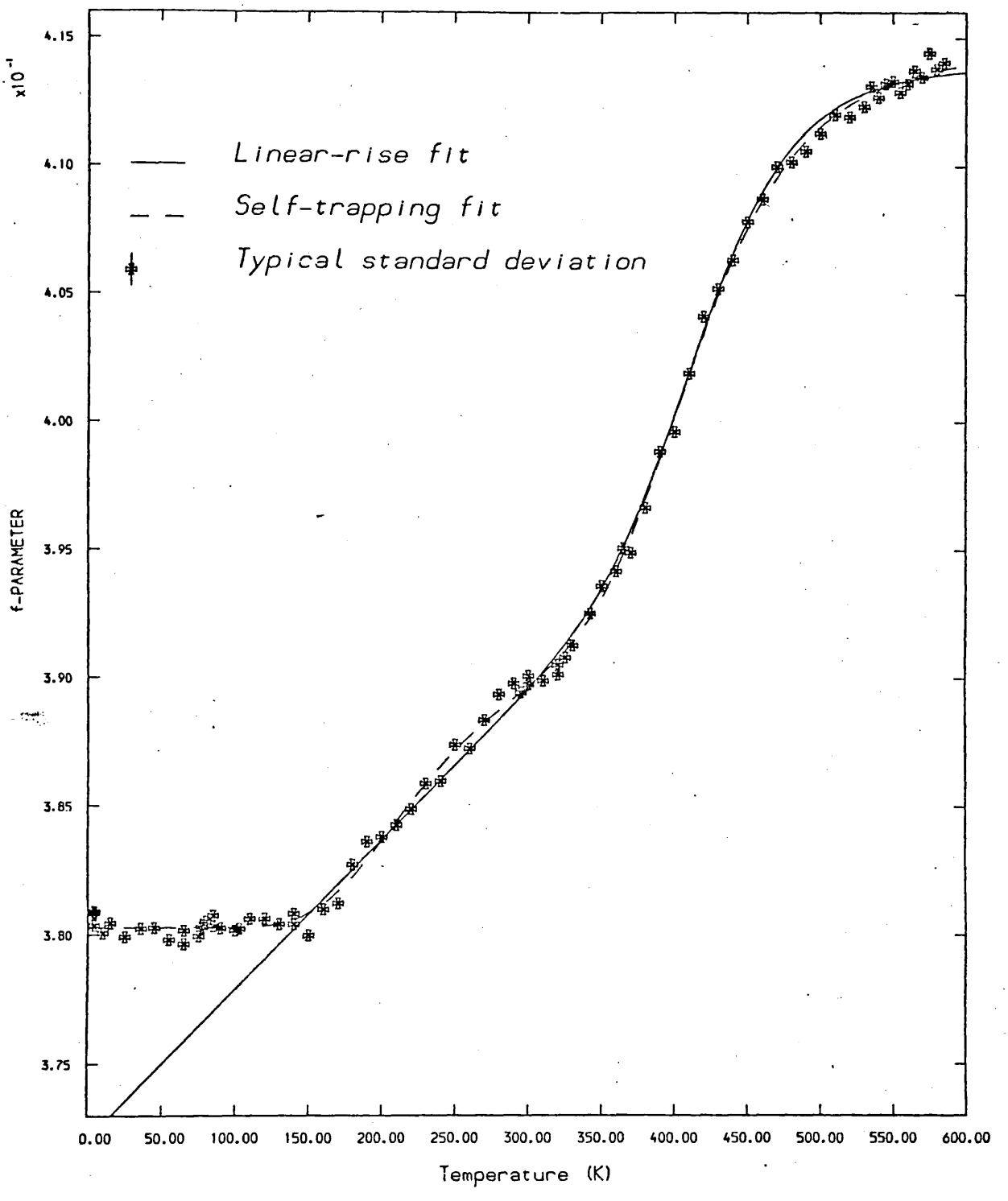

FIG. 4.4 The variation of F-parameter with temperature for single crystal cadmium.

first one is the absence of the low temperature (below 50°K) rise that we observe in polycrystalline cadmium. In single crystal cadmium the F-parameter is flat between 4.2°K and 140°K. The second one is that the temperature region 140°K to 330°K (prevacancy region) has a steeper slope than its counter part in polycrystalline cadmium (15.6×10^{-5} K^{-1} opposed to 11.2×10^{-5} K^{-1}). There is also a definite plateau between 280°K and 310°K. This region has been repeated several times to confirm this and Figure(4.5) shows the plateau for another run with all points taken in the low temperature cryostat.

4.2.3 F-parameter analysis

The results of the minimization using the linear rise model and the self-trapping model are shown in table (4.2). As would be expected the presence of a plateau at the top end of the prevacancy region would tend to improve the fit for the self-trapping model. The monovacancy formation energy obtained, 0.40 + 0.02 ev, is in good agreement with that obtained from differential, dilatometry, 0.41 ev [120], and quenching experiments, 0.42 ev [121].

If one assumes the free positron lifetime to be 190 ps [31] and that the entropy exponential factor is 3.0 [119], the result would be a specific trapping rate of 1.1×10^{14} S^{-1} to be compared with 2.5×10^{14} S^{-1} the value quoted by Hood and Mckee [110]. The value obtained from the linear rise fit is slightly higher (4.0×10^{14} S^{-1}) but it would be difficult to justify this model which is based on the idea that the prevacancy rise is a positron response to the thermal expansion of the lattice. Although the electron

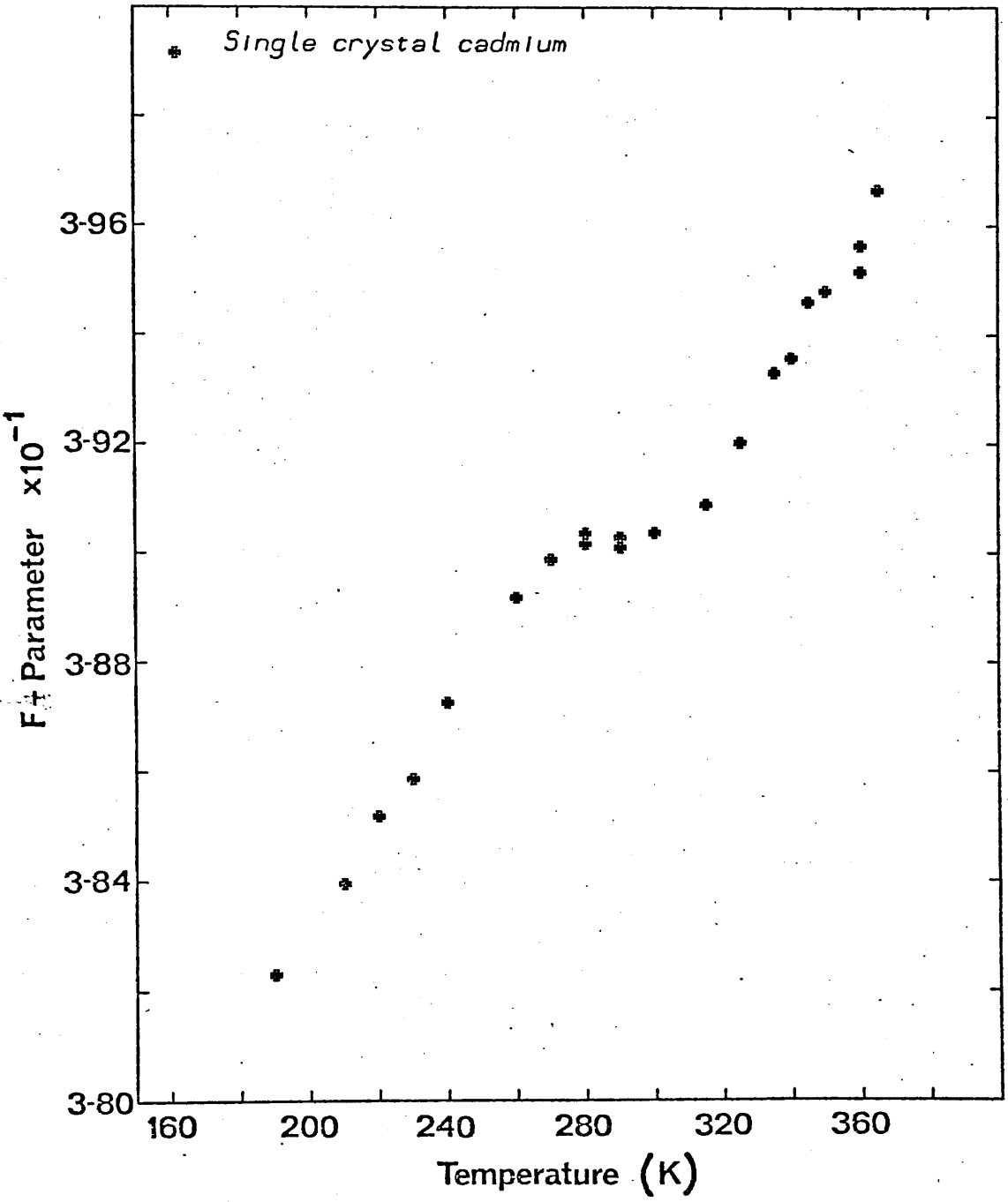

FIG.4.5 The F-parameter against temperature in Single Crystal cadmium with all points in the low temperature cryostat

TABLE 4.2
MODEL FITTINGS FOR SINGLE CRYSTAL CADMIUM

Model	E_v ev	F_f	F_{lv}	A_{lv} $\times 10^{-4}$	β $\times 10^5$	α $\times 10^5$	F_{st}	ϵ ev	B $\times 10^{-5}$	χ^2/ν
a)Monovacancies plus linear rise above 140°K	0.46 $\pm$0.02	0.3721	0.4139	22.85	15.6					1.44
b)Monovacancies plus linear rise above 140°K	0.48 $\pm$0.02	0.3724	0.4059	47.49	15.23	3.49				1.26
c)Monovacancies plus Self trapping 4.2K to 585°K	0.40 $\pm$0.02	0.3803	0.4147	6.3			-0.3932	0.13 $\pm$ 0.003	17.87	1.16

density must continue to increase as the lattice contracts below 140°K, the F-parameter remains flat between 4.2°K and 140°K. Between 140°K and 280°K the slope of the F-parameter is about five times the linear thermal expansion coefficient. Tam etal [128] calculated the effect of phonon-coupling and lattice expansion in cadmium and their conclusion was that the calculated combined effect is smaller by a factor of about 2 than that observed experimentally.

If the data is fitted with an expression for independent trapping at two types of thermally created defect, one obtains a chi-squared per degree of freedom of 1.17 with vcacancy formation energies of E_{1d} = 0.11 ev and E_{2d} = 0.50 ev. This would, however, be difficult to interpret physically.

4.2.4 Convolution

Figure (4.6) shows the parabolic component percentage plotted against temperature . At temperatures below 150°K it appears to be flat, the same as F in Fig (4.4). Thereafter it rises steadily, almost linearly, up to the highest temperatures. The percentage increase in the parabolic component between 150°K and 300°K is about 4%, similar to the percentage increase found by Gould etal [135] for the height of the angular correlation curve. When compared with Fig (4.3) for annealed polycrystalline cadmium, Fig (4.6) shows a slightly higher parabolic fraction (41% vs 38% at 100°K). This fraction rises more sharply in the prevacancy region than its counterpart in annealed cadmium; a fact which correlates with the high slope shown by the F-parameter in Fig (4.4). Because of the

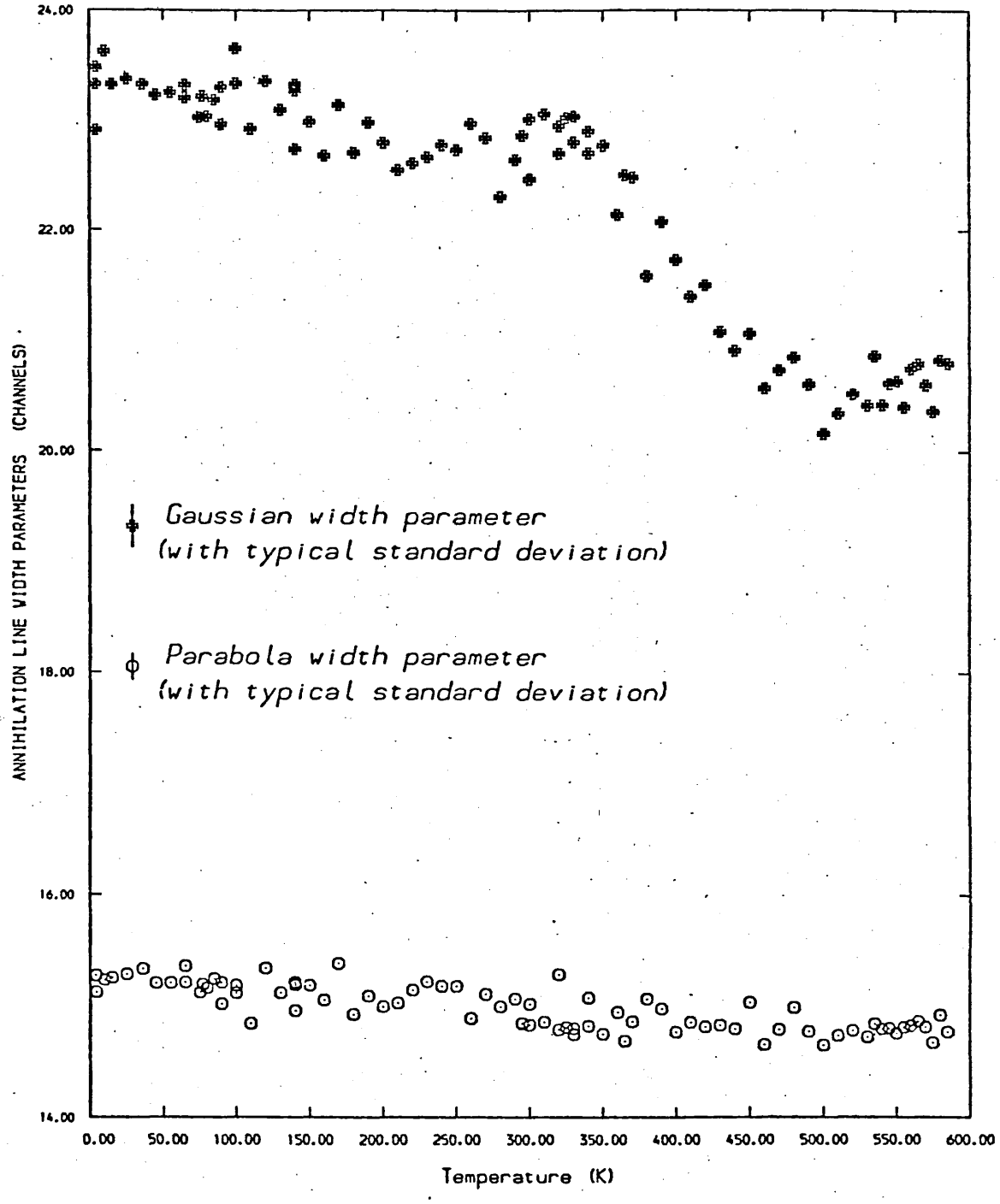

FIG.4.7 The temperature dependance of the width parameters of the Gaussian and parabolic components of individual lines for Single Crystal cadmium

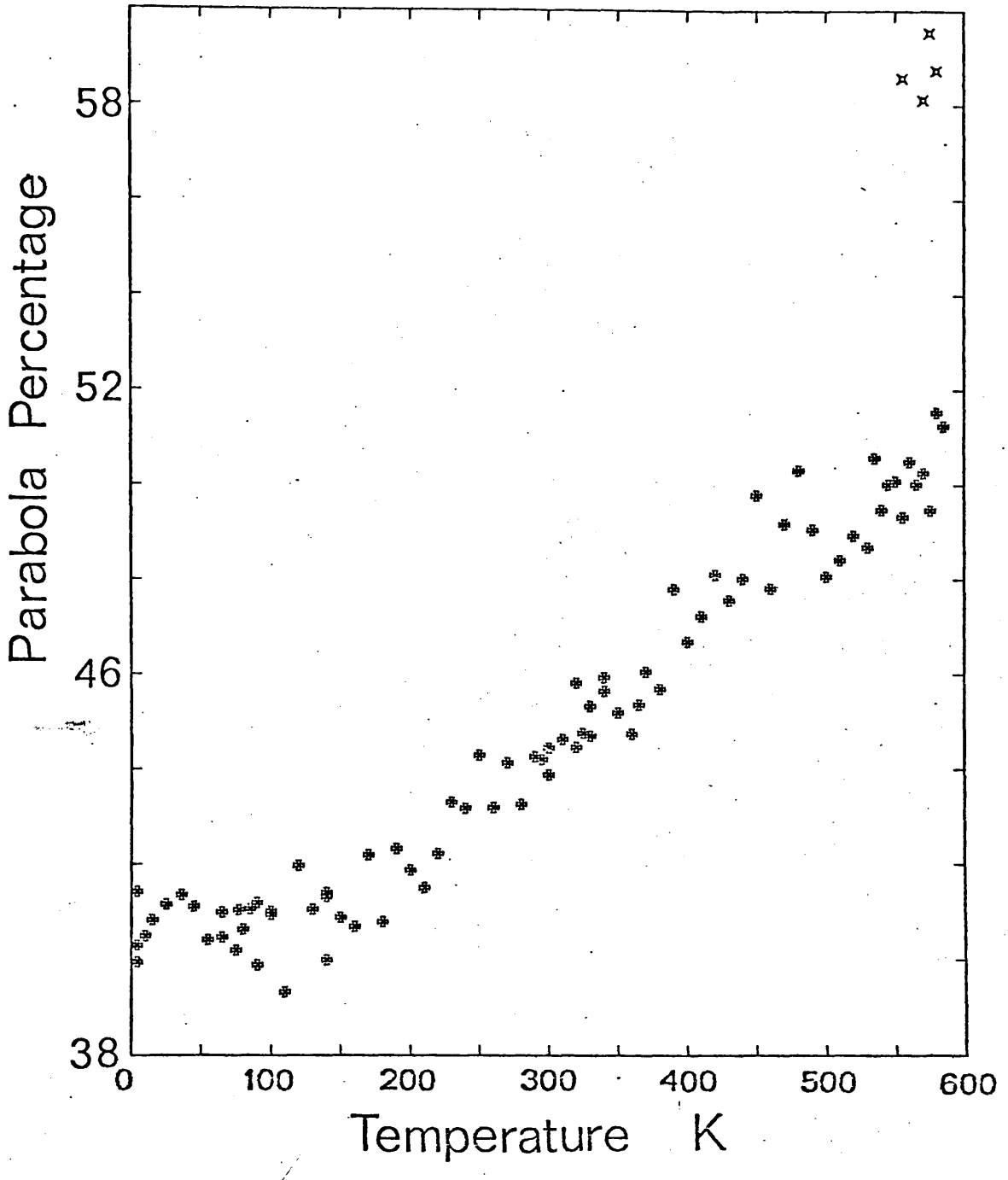

FIG.4.6 The variation of the parabolic percentage with temperature in Single Crystal cadmium

6?

scatter of the points in Fig (4.6) it is not possible however to ascertain whether there is a plateau corresponding to the one found in the F-parameter, Fig (4.5).

The changes shown in Fig (4.7) by the parabola and Gaussian width parameters are comparable to those for annealed cadmium, Fig (4.2). In Fig (4.7) the parabola width gently declines with increasing temperature, presumably due to the contraction of the Fermi Surface. The Gaussian width shows a similar decline with increasing temperature, that temporarily ceases between 250°K and 350°K, only to recommence thereafter in the vacancy region. The parabola width has an average value of 14.8 channels (94 ev per channel) at room temperature. This corresponds with an electron energy of 7.57 ev, in reasonable agreement with 7.47 ev, the accepted Fermi energy of cadmium [131] [132].

4.3 Deformed Cadmium

4.3.1 Introduction

Ideally, one should investigate a sample containing only dislocations which are of one kind, which do not have other imperfections associated with the dislocation line, and which are well separated from each other. The determination of the positron annihilation characteristics of such a system would thereby constitute the basic measurement from which one could proceed to more complex structures.
Unfortunately such a simple dislocation structure would be exceedingly difficult, if not impossible, to obtain. In practice, the structure investigated will be complicated and will depend on several parameters such as the material, the degree of deformation, the grain size, and the deformation temperature.

4.3.2 Sample preparation

A polycrystalline cadmium sample was prepared in a similar fashion to the one prepared in (4.1.1) and then its thickness was reduced by 5% at 77°K to become deformed cadmium-A. Care was taken to ensure that the sample temperature did not rise above 115°K while being transferred to the low temperature cryostat.

The previously used annealed cadmium sample received 30% thickness reduction at room temperature to become deformed cadmium-B. The F vs T curves were obtained by first cooling the sample down to 4.2°K and then warming it up in steps of 10 degrees, while data collection time was two hours at each point at a counting rate of 5K cps. Figure (4.1) shows the F-parameter curves for the two deformed cadmium specimens.

4.3.3 Discussion of Deformed Cadmium

The region from 4.2°K to 35°K shows a gradual drop in the F-parameter characteristic of polycrystalline cadmium in this region [31] [126].

This is more pronounced in the case of deformed cadmium-B than either deformed cadium-A or annealed cadmium. Between 35°K and 150°K no apparent change occurs and the F-parameter is found to be more or less constant in deformed cadmium-A, while the flatness persists up to about 270°K in deformed cadmium-B above which the curve rises gently to meet and follow that of annealed cadmium. In deformed cadmium-A however, above 150°K the F-value begins to drop markedly till it meets the annealed curve at about 330°K, the slope above 250°K being less steep than that between 150°K and 250°K.

The general features of this F-curve are not exactly in the best agreement with Lichtenberger's data on plastically deformed cadmium [93] but that is to be expected for samples of different history which are not of the same stock and were possibly subjected to different treatments. Lichtenberger had been able to observe a well defined annealing stage between 138°K and 153°K, which he attributed to vacancy migration, but since his data did not extend below 100°K, the (4.2 - 35)°K region behaviour was not reported by him. Sharp etal [133] reported that in deformed cadmium, dislocation rearrangement takes place in the region (200-250)°K. It is possible to explain the data of deformed cadmium-A if we assume that the two stages are not completely resolved in this case but that they are merged together because of a slightly higher vancancy migration energy. Lichtenberger's data shows most of the annealing occuring between 200°K and 250°K with the conclusion that dislocation rearrangement is the primary annealing stage to be identified. Nevertheless it is difficult to explain why dislocation rearrangement, within such a limited temperature region, should produce as large a change in the F-value as the one observed; since dislocations are classified, in the first place, as shallow traps. It is more plausible to adopt the view that the whole effect is due to an involved mechanism characterized by positrons trapped in vacancies which are in turn trapped in dislocations. This would account for the possible merger of the two stages. One may envisage the dislocation constituting the trapping potential, and when a positron is first trapped, its wave function is delocalized along the axis of the dislocation line. If a vacancy is trapped by a dislocation, the periodicity is broken, the vacancy then trap the positron resulting in a vacancy-like characteristic F-parameter. This

possibility seems attractive for another reason. When convolution results of line shape analysis (with zero-point motion of positrons included) of high temperature data, in annealed cadmium (almost saturation trapping) are compared with those obtained from low temperature deformed cadmium-A (below 120 K); the two appear surprisingly similar. The positron Gaussian width required for the best minimum in deformed cadmium-A is 3.4 with electron parabola width of 12.8 and electron Gaussian width of 21.6. The respective parameters for annealed cadmium are 3.8, 12.4, 21.3. This suggests that the same defect enviroment is perhaps responsible for positron trapping in both cases. Dannefear etal [27] came to the same conclusion when investigating positron lifetime in deformed Ni, and so did Doyama and Cotterill [134].

When this is taken in conjunction with deformed cadmium-B data, it appears that two types of traps might be present; a shallow one with a characteristic F-value of about 0.384 and a deep one with F of about 0.401. Strong trapping, resulting in high F values, dominates at low temperatures as a result of vacancy trapping in dislocations. Once vacancy migration and dislocation rearrangement set in, positrons revert to shallow trapping (characterized by lower F values) in the rest of the defect network. Point (A_1) was taken immediately after 200°K and they have similar F values, while point (A_2) was taken after 320°K. This could be indicative of the possibility that saturation trapping prevails over the whole region and the F-curve reflects the nature of the trapping site; the shallower the trap, the lower is its characteristic F-value.

When one considers the apparent flatness of deformed cadmium-B curve, Fig (4.1), between 40°K and 270°K,

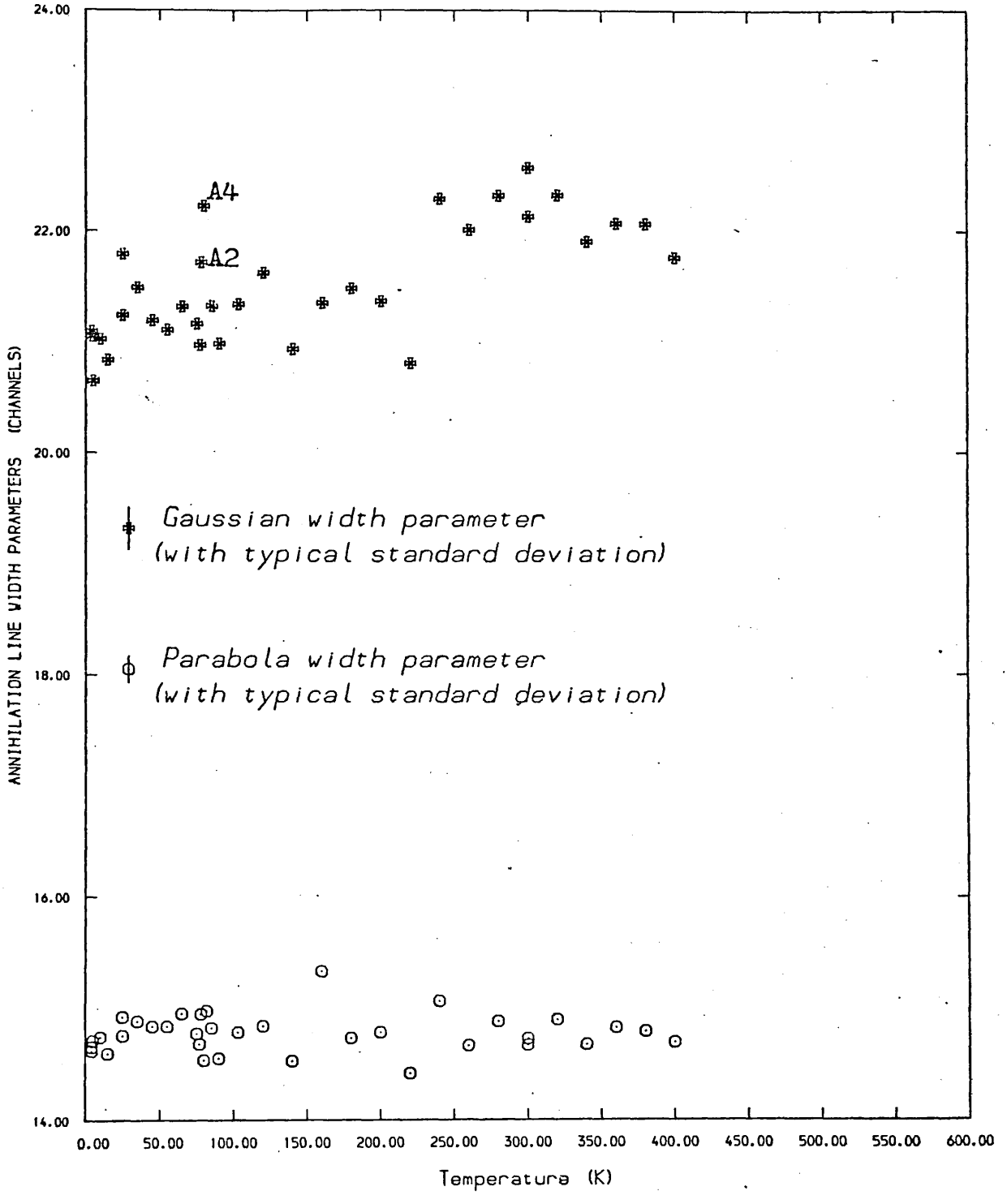

FIG. 4.8 The variation of the width parameters of the Gaussian and the parabolic components of individual lines for deformed cadmium-A as a function of temperature.

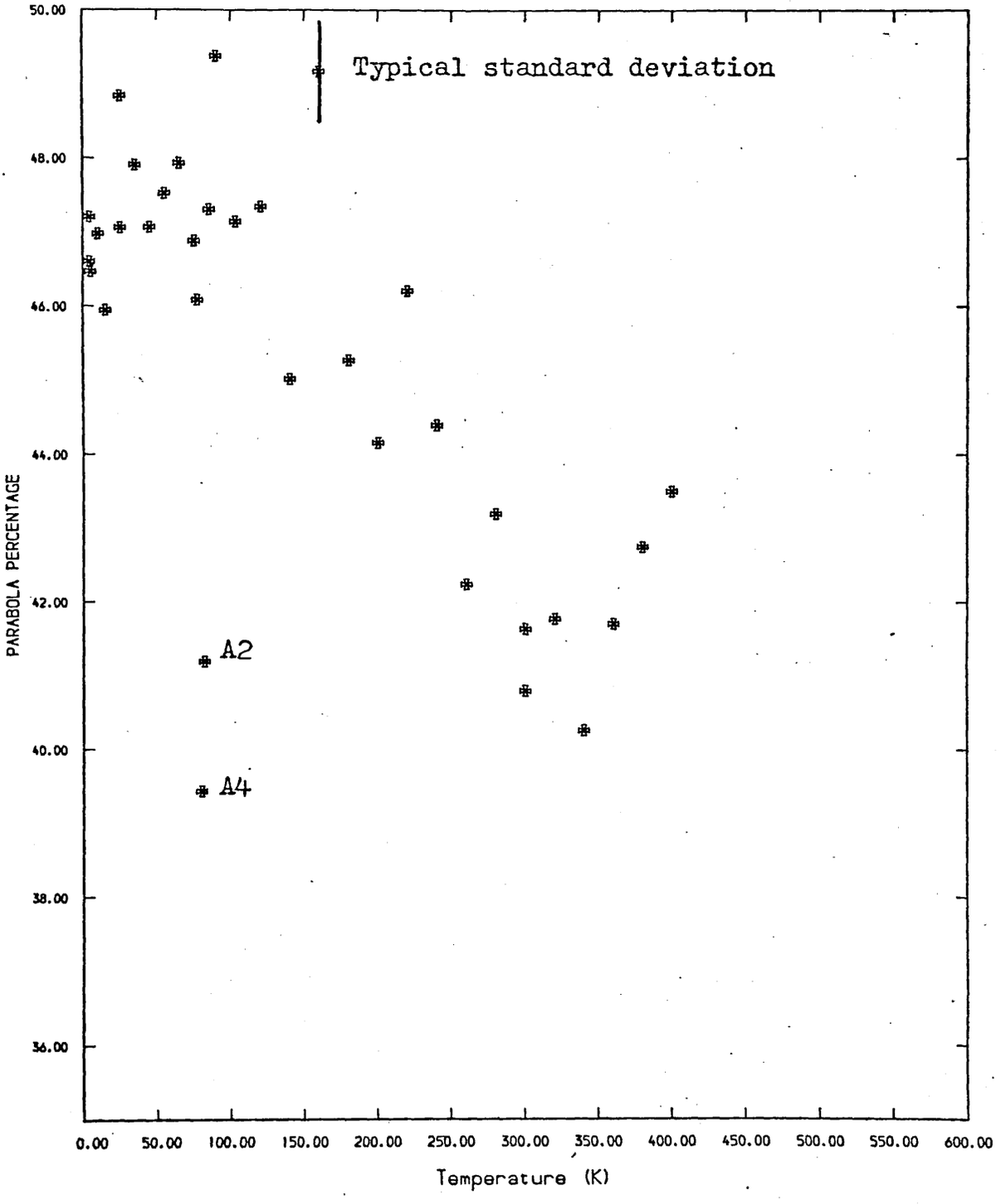

FIG. 4.9 The percentage of parabolic component in deformed cadmium-A .

one comes to the conclusion that; were this flatness really indicative of saturation trapping, then the F-value characteristic of this defect is highly insensitive to temperature. This type of assumption is used in the 7-parameter self-trapping minimization, where F_x (x = f, v, st) is treated as a constant. Nevertheless this is done under the implicit understanding that the minimization could, at a later stage, be refined by introducing a temperature dependence into these parameters whenever it is considered relevant [92]. This is not the case in deformed cadmium-B, which over the temperature range considered shows that, under the assumption of saturation trapping, one has a positron state which appears to be insensitive to temperature variations; in contradiction to models based on thermal expansion. It is of course possible that the F-parameter is not a sensitive enough parameter to respond to whatever weak temperature dependence that is in fact present. If it is not saturation trapping but only partial trapping, the same argument would still apply since the annealed cadmium curve shows a marked temperature dependence between 150°K and 280°K. Points (A_3) and (A_4) - Fig (4.1) - were taken immediately after a point at 400°K which illustrates complete annealing.

Fig (4.8) and (4.10) give the parabola and Gaussian width for data-A and data-B respectively. Defects that dominate at 77°K in data-A give a Gaussian width parameter of about 21.2 channels. A change occurs at about 250°K and a new, shallower defect type, exhibits a mean Gaussian width of 22.3. In deformed cadminum-B, since deformation took place at room temperature, defects of the first type disappeared before data accumulation began. The average Gaussian width of data-B is 22.3 up to 250°K.

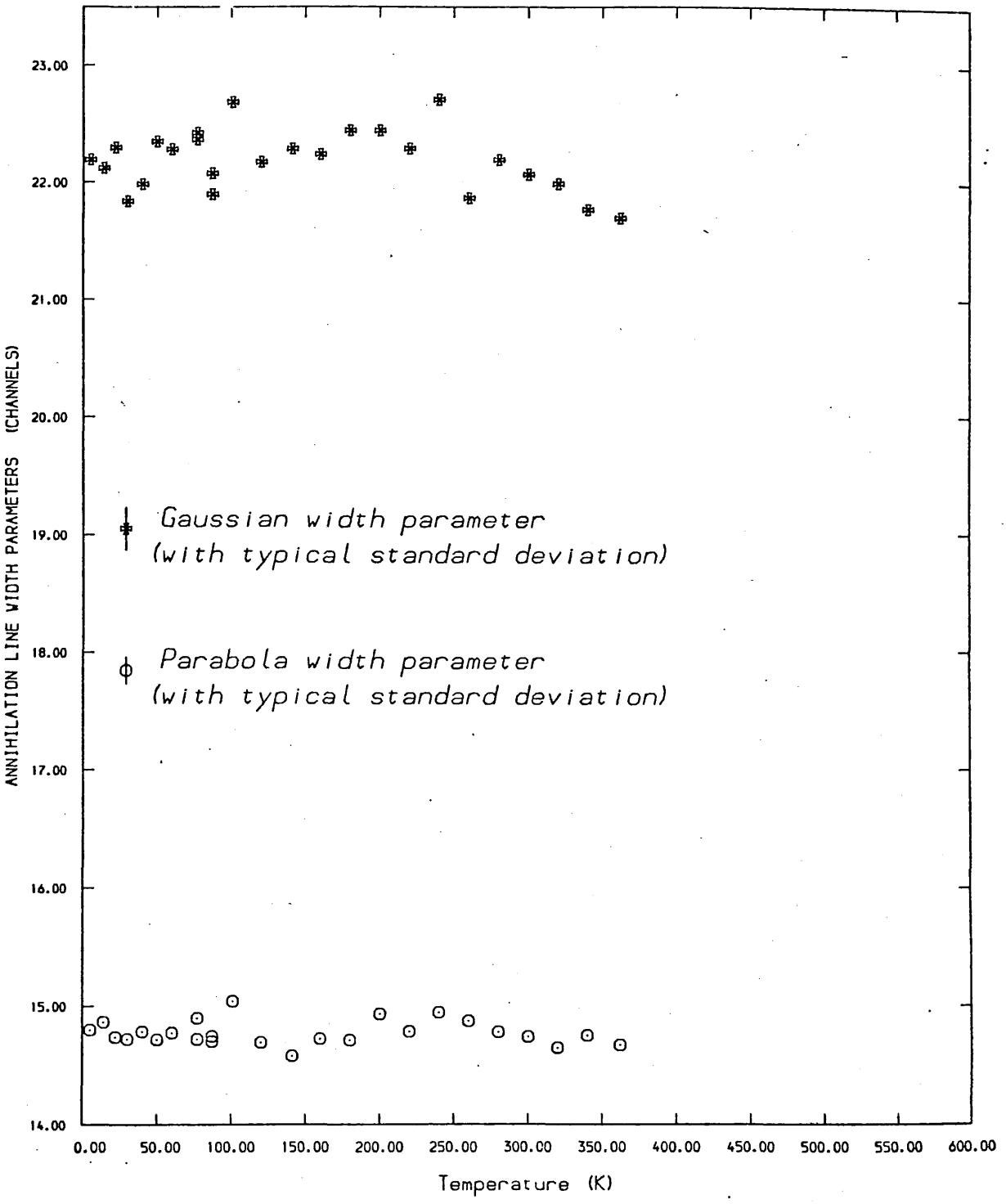

FIG. 4.10 The variation of the width parameters of the Gaussian and the parabolic components of individual lines for deformed cadmium-B as a function of temperature.

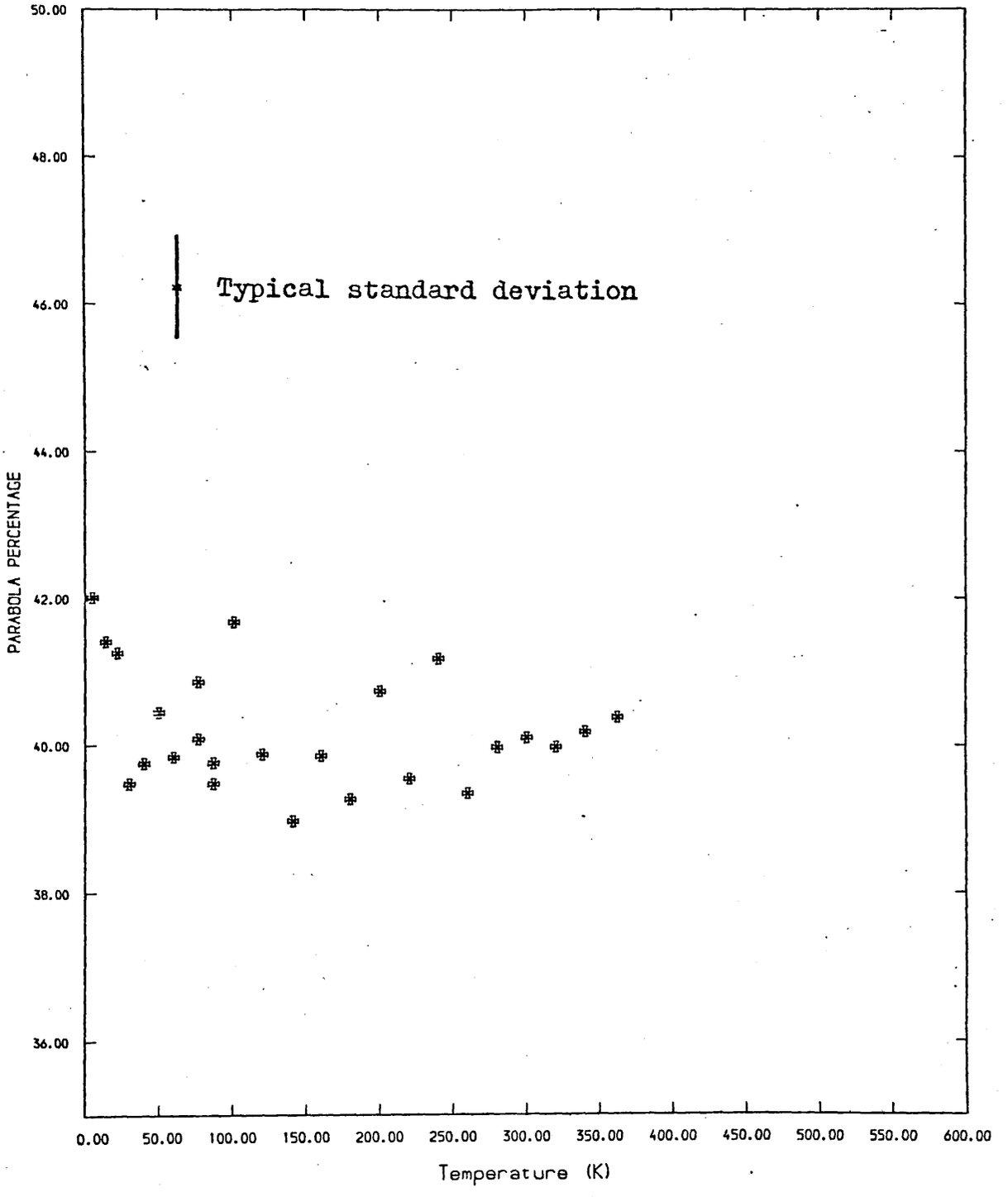

FIG. 4.11 The percentage of parabolic component in deformed cadmium-B .

Fig (4.9) shows the parabolic component percentage in deformed cadmium-A as a function of temperature. It is approximately 47.5% at 50°K and it steadily drops to about 40% at 300°K, after which it begins to rise due to annihilation in thermally created vacancies.

Fig (4.11) shows the parabolic component percentage for data-B. Over the range (50-300)°K it decreases by less than 1%. The annealed and the two deformed samples agree at about 300K.

The results of the convolution analysis (with positron zero-point motion included) for annealed and deformed polycrystalline cadmium is in appendix v.

4.4 The low-temperature effect

The anomalous behaviour exhibited by positron annihilation characteristics in polycrystalline cadmium at temperatures below 50°K is a genuine effect. It has been reported by other groups, Herlach etal [31] and Kupca etal [126], although there seems to be a dispute about its origin. Herlach etal [31] suggest that during the slowing-down process positrons travelling in crystallographic directions can preferentially leave the sample and annihilate in the helium gas or on the specimen surface. Kupca etal [126] interpret their lifetime measurements in terms of a temperature dependent trapping rate. Whatever the origin of this effect might be, it is not unique to cadmium. It has been reported in Zn [96] and Au [31] polycrystalline samples as well. Two facts might help shed light on its nature. The first is that it is absent in single crystal cadmium and secondly the magnitude of the effect seems to increase with deformation followed by annealing below recrystallization temperatures [126].

Deformed cadmium-B is a good example of the second point.

A possible explanation of this behaviour could be detrapping from remnant defects of which no sample is free, however carefully annealed and handled it is. Considering the magnitude of the effect, these defects would have to be shallow traps. Grain boundaries seem a likely candidate. Nevertheless there is nothing to rule out the possibility of a temperature dependent trapping rate as being the mechanism responsible for this effect. Kupca etal [126] claim that in their lifetime analysis of cadmium data they extracted a value of 230 ps for the trapped positron lifetime at these low temperatures. This lifetime is similar to that of positrons in deep traps, namely vacancies. Kupca etal prefer an explanation that involves indirect trapping into deep traps via shallow traps, grain boundaries, from which thermal detrapping can occur.

Positron annihilation in Indium

5.1 Positron Annihilation in polycrystalline indium

5.1.1 Sample Preparation

Two 99.9999% pure ingots of polycrystalline indium, supplied by Koch-Light, were made into discs of 22 mm diameter and 1.25 mm thickness. They were etched in dilute nitric acid and then carrier-free $^{22}NaCl$ solution was evaporated directly onto the central region of their surfaces, total activity being 0.09 mCi approximately. They were then made into a sandwich configuration and annealed under a vacuum of 10^{-5} torr for 8 hours at 398K and 13 hours at 373K. The sample was then cooled down slowly to room temperature first prior to cooling it further to 77K. The total counting rate was adjusted to be 5K cps. Each run of two hours accumlated about 900000 counts under the 511 Kev Line. The whole experiment, from 4.2°K to near the melting point, was done in the low temperature cryostat.

5.1.2 F-Parameter analysis

The F-parameter vs T for polycrystalline indium is shown in Fig (5.1). The F-parameter maintains a constant value to about 120°K, and then it begins to steadily rise with temperature. The slope between 120°K and 320°K, prevacancy region, is fairly shallow when compared with that above 320°K, where vacancy trapping is expected to dominate. The top of the F curve near the melting temperature does not show much curvature to allow speculation about saturation trapping.

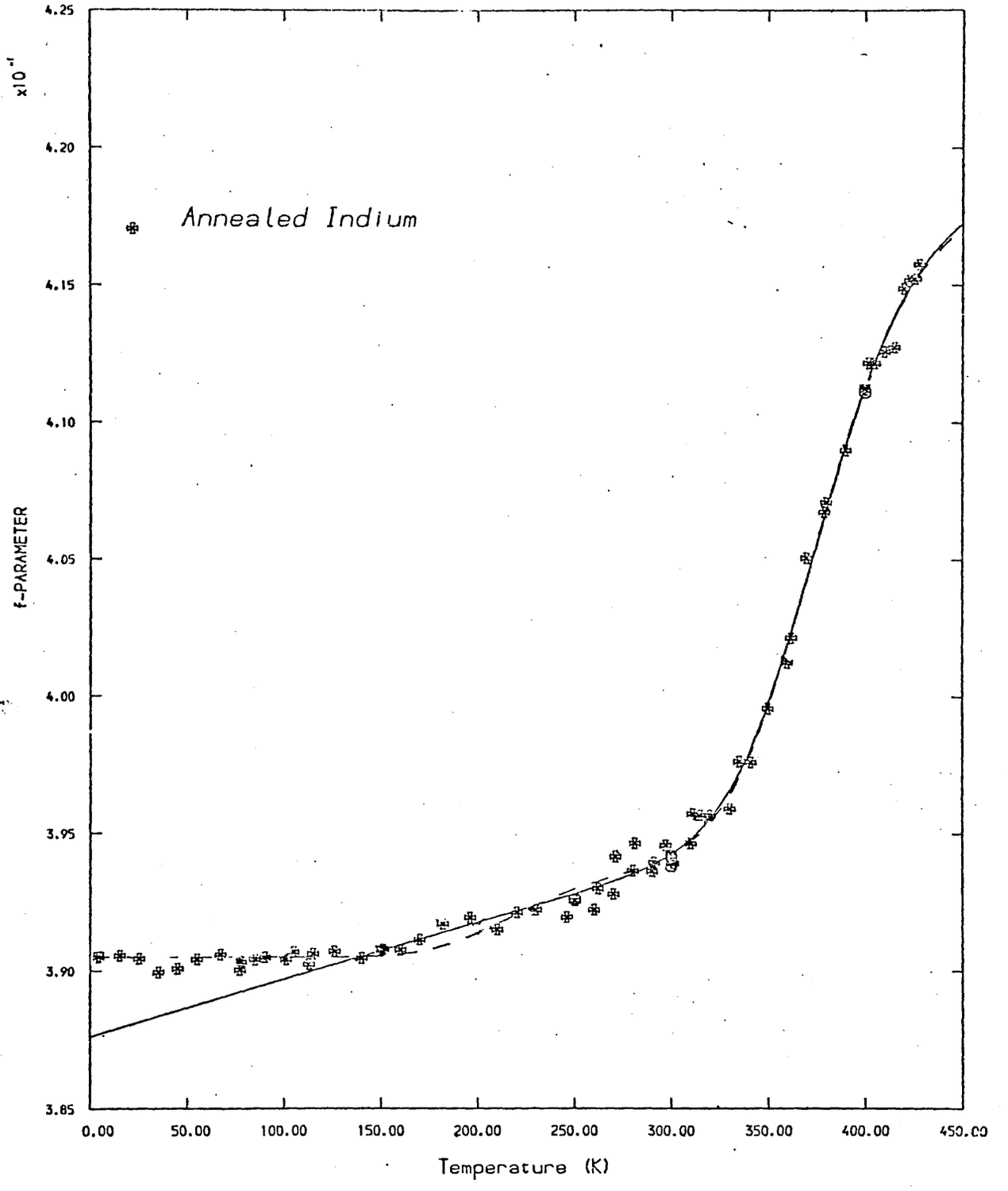

FIG. 5.1 For 6N annealed specimen of indium, the change in F-parameter as a function of temperature. The solid and the broken lines correspond to the cases where F_f is taken linearly to rise with temperature, and to fit Seeger's self-trapping model, respectively.

The first thing to be noted is that for indium there are no data available from other techniques. This problem is further supplemented by the fact that in indium positron measurements are not internally consistent. Angular correlation measurements as performed by McKee etal [10] gave for E_v a value of (0.55 $\pm$ 0.02) ev. This disagreed with the value of (0.45 $\pm$ 0.03) ev as obtained from centroid shift positron lifetime measurements [28]. Triftshauser [137] investigated the positron trapping in solid and liquid indium and obtained a value of (0.48 $\pm$ 0.01) ev for E_v by fitting the two-state trapping model after correction for thermal expansion. It should be mentioned however that the data used in [137] were normalized peak counting rate from angular correlation curves that extended from room temperature to the melting point. Singh etal [125] obtained a value of (0.39 $\pm$ 0.04) ev for E_v from a combination of the measurements of meanlife and line shape parameter as a function of temperature. Mackenzie etal [123] obtained a value of 0.41 ev from threshold temperature correlation. Using the self-trapping model to fit Doppler broadening data between 74K and 430K, Segers etal [92] obtained (0.48 $\pm$ 0.03) ev for E_v.

The minimized parameters resulting from using different models to fit the polycrystalline indium data are shown in table (5.1). The discussion of these will be deferred until those for single crystal indium, which are similar, are presented in (5.2). Nevertheless it is worth remarking that, although the E_v values in table (5.1) are in good agreement with those [92] [137] quoted in the previous paragraph, and with 0.48 ev as quoted by Schulte and Campbell [138], such a value would imply an astonishingly low vacancy

TABLE (5.1)
MODEL FITTINGS FOR POLYCRYSTALLINE INDIUM

Model	E_v ev	F_f	F_{1v}	A_{1v} $\times 10^{-5}$	B $\times 10^{+6}$	F_{st}	ϵ ev	B $\times 10^{-6}$	χ^2/ν
a)Monovacancies plus linear rise above	0.49 $\pm$ 0.02	0.3876	0.4194	30.10	5.3				1.15
b)Monovacancies plus Self-trapping above 4.2°K	0.49 $\pm$ 0.02	0.3905	0.4194	29.46		0.3943	0.18	39.57	1.27
c)Monovacancies plus Self-trapping plus divacancies above 4.2	0.49	0.3905	0.4114	45.3		0.3949	0.19	14.82	1.26

Additional parameters: c) $F_{2v} = 0.4231$, $A_{2v} = 23.33 \times 10^8$, $E_{2v}{}^b = 0.18$

concentration at the melting temperature compared with other metals. Such a low concentration might explain the lack of saturation trapping, usually evidenced by the flattening of the F-curve, at high temperatures. Model (a) and (b) table (5.1) give 84.3% and 83.7% respectively for the percentage of positrons trapped in vacancies at 429°K. The requirement for interpreting this data in a way that would result in a higher vacancy concentration at the melting temperature is that the extrapolated prevacancy effect should prove non-linear at high temperatures.

Stott and West [49] compared the effect of the lattice vibrations in indium between 100°K and 300°K to that of thermal expansion (volume + lattice) and found the former to be about three times greater than the latter. They concluded that although this does not rule out more complex positron-phonon coupling effects like self-trapping, qualitatively one would expect non-linearities at higher, as well as lower, temperatures. Below some characteristic temperature, which will depend on the details of the actual phonon spectral function, the temperature dependence should be weaker. This proves to be true since below 120°K the F-parameter appears flat.

5.1.3 Convolution

Each 511 kev line is fitted to a model composed of the superposition of a Gaussian and an inverted parabola having a common centre. Fig (5.2) shows the variation of the parabolic component percentage with temperature. It rises from 57.5% to 64% as the temperature is increased from 4.2°K to the melting point. The low temperature parabolic percentage is in good agreement

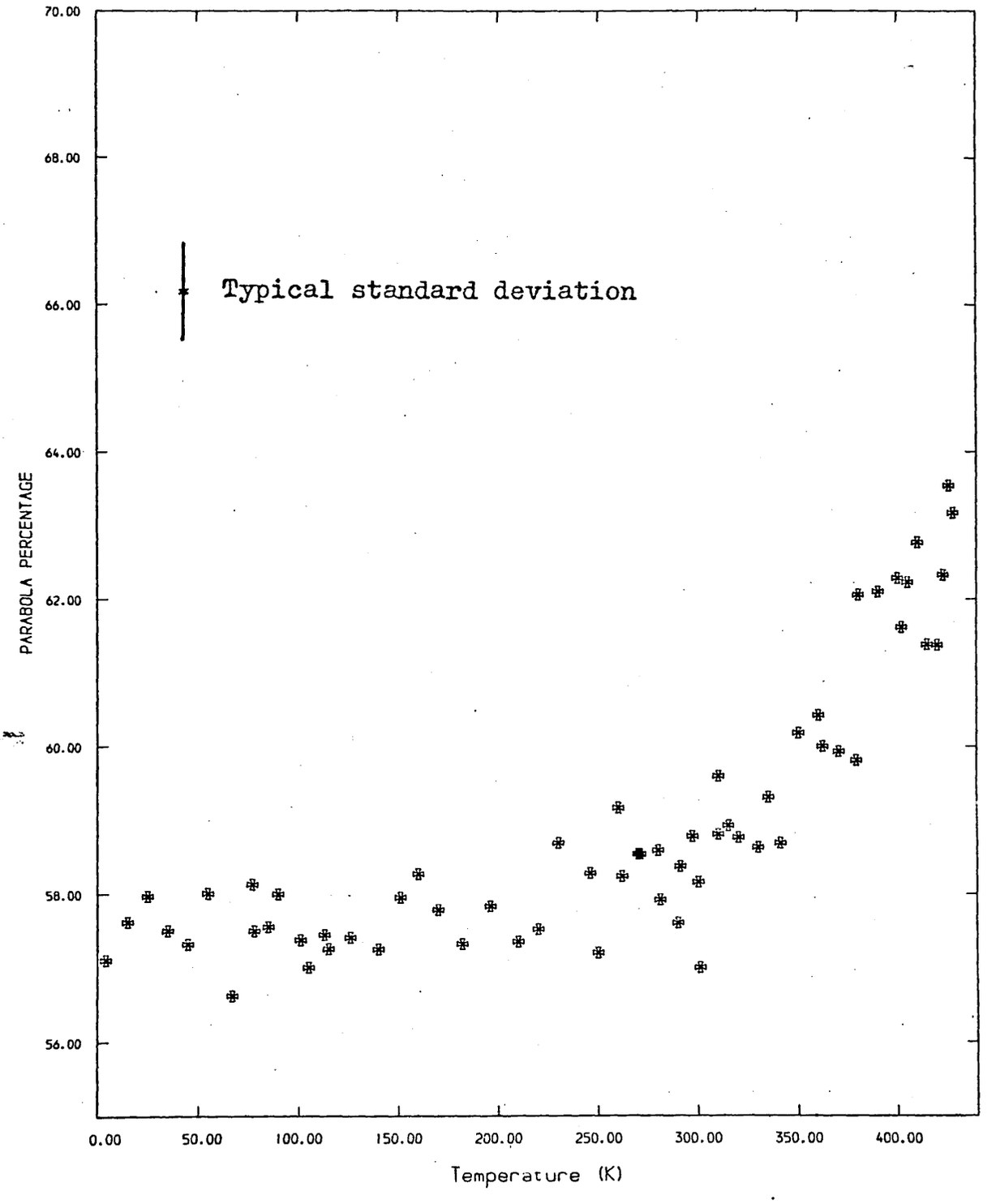

FIG. 5.2 For 6N annealed indium, the parabola percentage as a function of temperature.

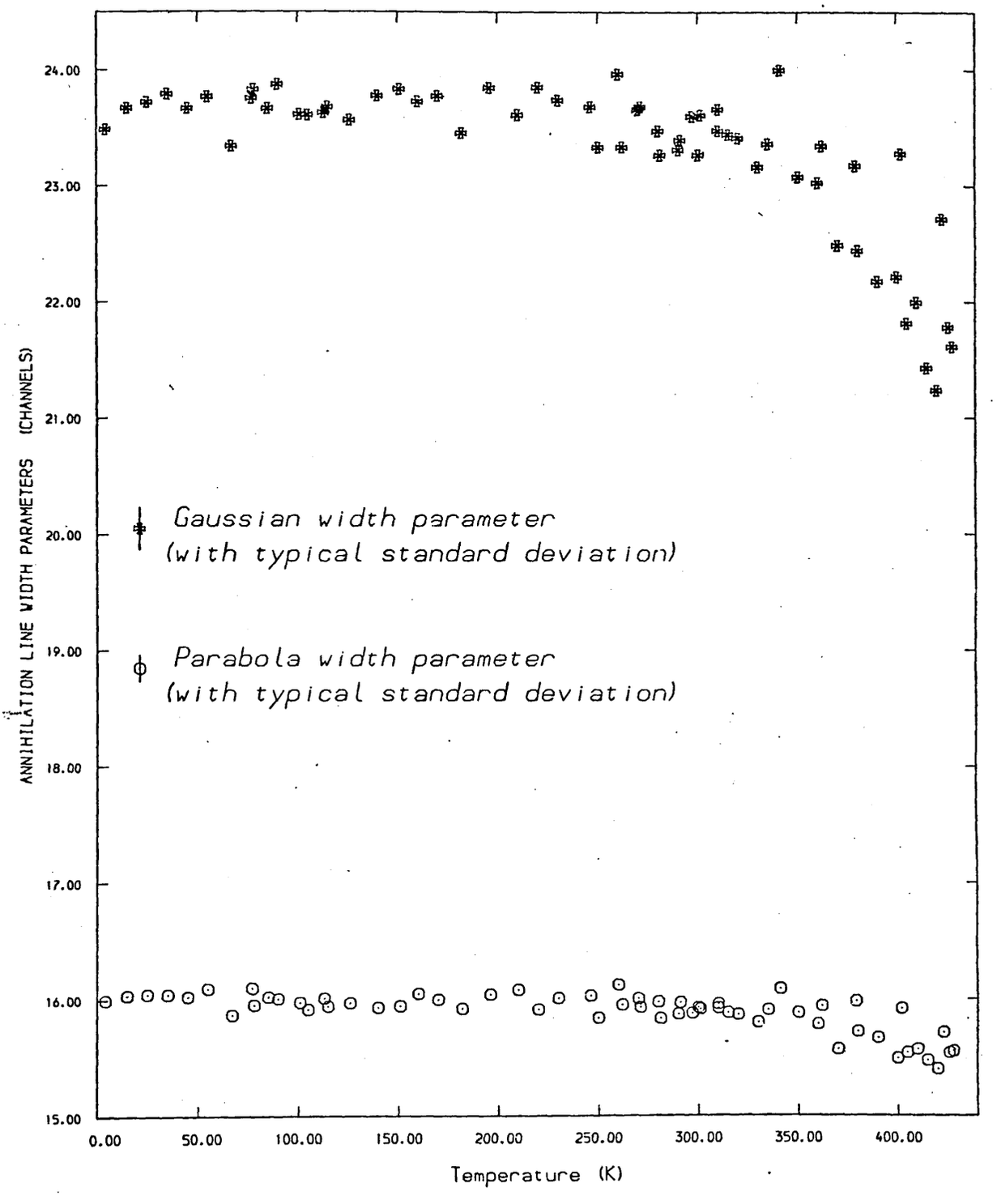

FIG. 5.3 Temperature dependence of the annihilation line width parameters for 6N annealed indium.

with the 57% quoted by West [56] from Kusmiss (Ph.D thesis, unpublished), the 57% found by Jackman etal [109], and 59% as quoted by Manninen etal [136].

The parabola and Gaussian width parameters are shown in Fig (5.3). The parabola width has an average value of 16 channels which corresponds to a Fermi energy of (8.85 $\pm$ 0.095) ev in good agreement with the accepted 8.6 ev Fermi energy for indium [131] [132]. The quoted error on the Fermi energy is the error on the energy calibration (94.0 $\pm$ 0.5 ev per channel). The standard deviation on the width parameter itself is much more smaller, about $\pm$ 0.05 channels.

5.2 Positron annihilation in single crystal indium

5.2.1 Sample preparation

Two discs, each 2.3 mm in thickness, were sparkcut from a 9mm long and 16mm diameter single crystal indium rod of 99.9999% purity supplied by Metals Research. The discs were subsequently etched in dilute nitric acid (60%) and electropolished. The electrolyte was one part concentrated nitric acid + two parts methyl alchol (total volume was 300 ml). Graphite/lead was used as the electrocathode. Finally 0.1 ml (approximately 0.095 m Ci) of carrier-free $^{22}NaCl$ solution was evaporated onto the central region of the surface of the two discs and they were put together in sandwich configuration and wrapped in two layers of thin aluminium foil. The sample was then inserted in the low temperature cryostat and cooled down slowly (less than a degree per minute) to 77°K overnight.

5.2.2 F-Parameter analysis

With an experimental set up that is similar to the one in section (5.1) for polycrystalline indium, the F vs temperature curve was obtained for single crystal indium and is shown in Fig (5.4). The results of the minimization using the linear rise model and self-trapping model are in table (5.2).

Dickman etal [140] measured the vacancy formation volume in indium and found it to be (39 $\pm$ 1)% of the atomic volume. This is indicative of considerable relaxation of the neighbouring ions into the vacancy, thus resulting in partial screening of the effective charge and reduction of the trapping potential at the vacancy; a prescription for detrapping at high temperatures. On the other hand, with indium being trivalent, one would expect a deeper trapping potential in indium compared with monovalent metals like Ag and Au and divalent metals like CD and Zn. The deciding factor in this argument is the direction in which a vacancy relaxes as the temperature increases. Theoretically as well as experimentally that is still a point of debate [30] [32] [141]. Herlach etal [31] in their CD data found that they get an improved fit with inward relaxation, while Gilder and Lazarus [30] [139] claim huge outward relaxation in the same metal. There are no available data on indium on this point except that Segers etal [92] remarked that in their Doppler broadened indium data an improvement of fit could be obtained by taking F_v as a linearly decreasing function of temperature. In table (5.2) models (b) and (c) show the minimization for such a temperature dependence in the linear rise model. The results are apparently inconclusive, probably due to the fact that within the

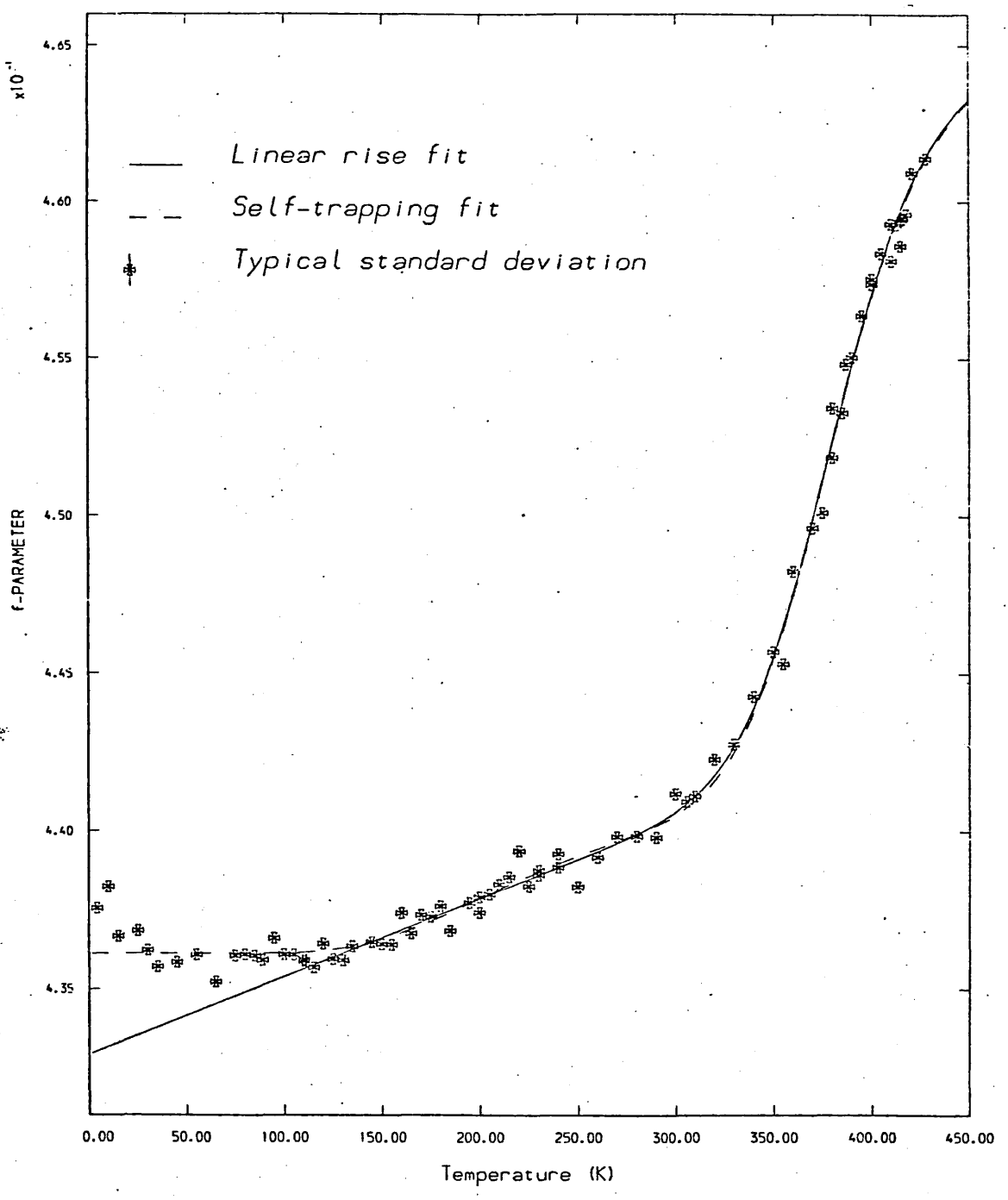

FIG.5.4 The variation of the F-parameter with temperature in Single Crystal indium

TABLE 5.2
MODEL FITTINGS FOR SINGLE CYSTAL INDIUM

Model	E_v ev	F_f	F_{lv}	A_{lv} $\times 10^{-5}$	β $\times 10^{+5}$	α $\times 10^{+6}$	F_{st}	ϵ ev	B $\times 10^{-5}$	χ^2/ν
a)Monovacancies plus linear rise above 125°K	0.52 $\pm$.02	0.43291	0.46537	54.4	5.71					1.006
b)Monovacancies plus linear rise above 125°K	0.51 $\pm$.02	0.43269	0.46733	51.0	5.96	-8.6				1.039
c)Monovacancies plus linear rise above 125°K	0.52 $\pm$.02	0.43288	0.46345	51.8	5.75	+9.6				1.029
d)Monovacancies plus Self-trapping	0.49 $\pm$.02	0.43612	0.46555	34.6			0.44335	0.102	3.39	1.060

scope of this model the data is not sensitive enough in the high temperature region to differentiate between the two alternatives. As indicated by the reduced chi-squared, the best fit is obtained when this point is ignored, and the temperature dependence of F_v is set to zero.

When both tables, (5.1) and (5.2), are considered; they seem to point to a value of (0.50 $\pm$ 0.02) ev for E_v. This is in reasonable agreement with that found by Seegers etal [92], Triftshauser [137], and Schulte and Campbell [138] using the trapping threshold temperature correlation. It should however be remarked that the threshold temperature correlation approach i.e. $E_{1v} = (-0.098 \pm 0.057) + (15.2 \pm 0.7)\ T_t \times 10^{-4}$ with T_t = (335 $\pm$ 10)K in the case of indium [138] exhibits the same weakness, may be to a lesser degree, that the linear rise model suffers from. An altered temperature dependence of F_f and/or the free positrons annihilation rate through the vacancy regime would radically change the correlation. Detrapping and divacancy effects would similarly do the same. Therefore despite the apparent agreement of this value with (0.81 $\pm$ 0.015) ev for the activation energy of self-diffusion [142] [143], a lower value would appear to have been more appropriate. A value like 0.55 ev obtained by McKee etal [10] is certainly incompatible with that of self-diffussion.

A value of 0.49 ev for E_v - model (a) table (5.1), model (d) table (5.2) - implies a vacancy concentration of 1.75×10^{-6} Exp (S/K) at 429 K and, unless the entropy factor is markedly higher than average, indium seems to melt prematurely. At the same time the product of the specific trapping rate and exp (S/K) is about $(1.7 \pm 0.3) \times 10^{16}\ S^{-1}$ (the annihilation rate of

free positrons is assumed to be 5.56×10^9 S^{-1} [92]). This does not fit at all with the correlation proposed by Hood and McKee [110]. Seeger [28] concedes that indium results in general seem to point to a higher than average trapping rate and that even if one accepts $S_{1v} = 0.8K$ and $E_v = 0.45$ ev as possible upper and lower limits for these two quantities, they would indicate $C_{1v}(T_m) = 10^{-5}$ i.e. more than an order of magnitude less than has been found in those metals in which $C_{1v}(T_m)$ has been determined directly.

A model assuming annihilation in two types of thermally activated defects in addition to free annihilation was used to fit the single crystal indium data. The result was $E_{1d} = 0.09$ ev and $E_{2d} = 0.48$ ev with a reduced chi-squared of 0.818. It is clear that the data prefer a three-state model to a two-state one, although it would be difficult in this case to assign physical significance to this model.

An unresolved divacancy contribution cannot be ruled out, since this would bring the desired effect of simultaneously lowering both the value of E_v, thus increasing the vacancy concentration at the melting temperature, and A_{1v}, thus reducing the abnormally high trapping rate. On the other hand it is difficult to imagine an appreciable divacancy concentration capable of positron trapping when the apparent monovacancy concentration deduced from $E_v = 0.49$ ev is so low. Either this value is in error by a large margin or we are already looking at divacancy effects, under the assumption that the trapping potential in a monovacancy in indium is not strong enough to trap positrons effectively. Both alternatives seem highly improbable since with an activation energy of self-diffusion of 0.81 ev E_{1v} would be expected to be in the range

(0.4 - 0.5)ev while E_{2v} would be much higher; unless of course there is a high divacancy binding energy.

According to McKee and McMullen [144] both lifetime and momentum measurements changes in several metals indicate the presence, above room temperature, of contributions in addition to static lattice expansion. As has been remarked in section (5.1.2) Stott and West [49] predict large contribution from lattice vibrations between 100K and 300K which they expect to show non-linearity at both extremes of the temperature scale. In the absence of a quantitative model describing this non-linear behaviour at high temperatures (a crucial criterion in determining the extrapolated contribution to be subtracted in order to arrive at a true estimate of E_v) the value of (0.49 $\pm$ 0.02) ev found here should be appropriately viewed as an upper limit for the mono vacancy formation energy in indium. So should all similar values, with which it is in reasonable agreement, found by other groups [92] [137] [138] because the same criticism applies equally to them. Unless, for some reason, in indium serious non-linearities affect positron trapping at high temperature, the vacancy concentration at the melting point appears remarkably below average compared with other metals ($< 10^{-5}$) yet at the same time it is associated with a higher than average specific trapping rate.

Triftshauser [137] shows momentum parameter curves for Al and In which are flat above their melting points, and argues that under the assumption of saturation trapping thermal expansion has no influence on the annihilation characteristics of trapped positrons. One wonders about the plausibility of using the reversed form of this argument to infer a possible, and

as yet unaccounted for, saturation trapping in these metals at low temperatures since the F curves can be shown to be unquestionably flat below the onset of the prevacancy effect. It might prove after all that the model recently proposed by Smedskjaer etal [127] [145] is correct. They claim that trapping in dislocations, of which no metal is free however annealed it is, plays a more important role, particularly at low temperature, than has been hitherto assumed.

5.2.3 Convolution

A model for the electron-momentum distribution composed of the superposition of an inverted parabola and Gaussian was convoluted with the resolution function and Fig (5.5) shows the result of the minimized parabola and Gaussian width parameters against temperature. The parabola width parameter has an average value of 15.9 channels (94 ev per channel) at room temperature which compares well with that for the polycrystalline sample and implies a Fermi energy of 8.74 ev in reasonable agreement with 8.63 ev the accepted Fermi energy for indium [131] [132]. At high temperatures however where vacancy trapping dominates the parabola width parameter shows a gradual drop.

The Gaussian width parameter starts from about 23.7 channels at the low temperature, but shows a steep decrease in the vacancy region (above 320)$^{\circ}$K). Near the melting temperature it is about 20.5 channels. The percentage of the parabolic component is shown in Fig (5.6) and it rises from about 57.5% at low temperatures to 61.8% near the melting temperature.

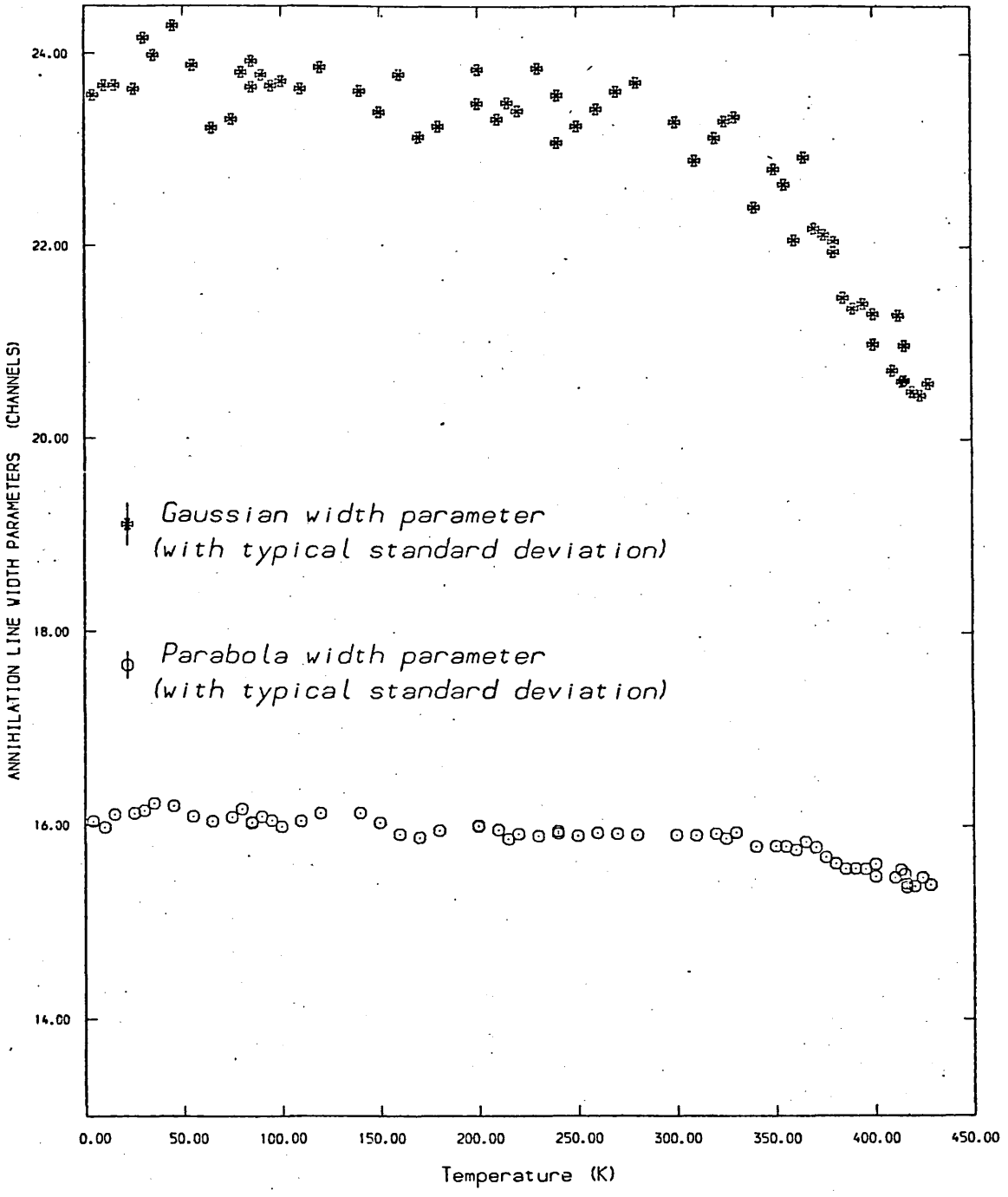

FIG.5.5 The temperature dependance of the width parameters of the Gaussian and parabolic components of individual lines for Single Crystal indium

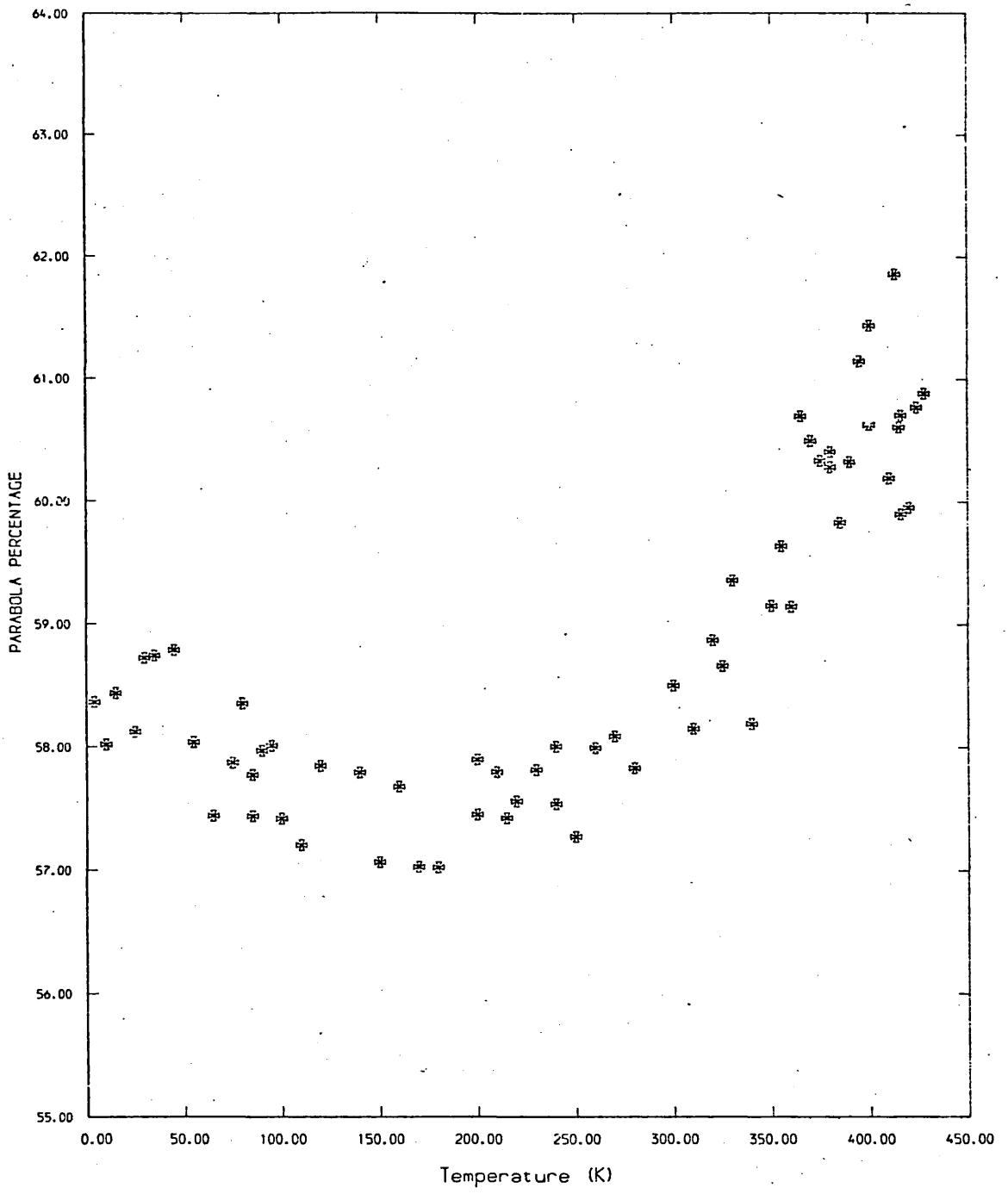

FIG.5.6 The temperature dependance of the parabolic percentage in Single Crystal indium

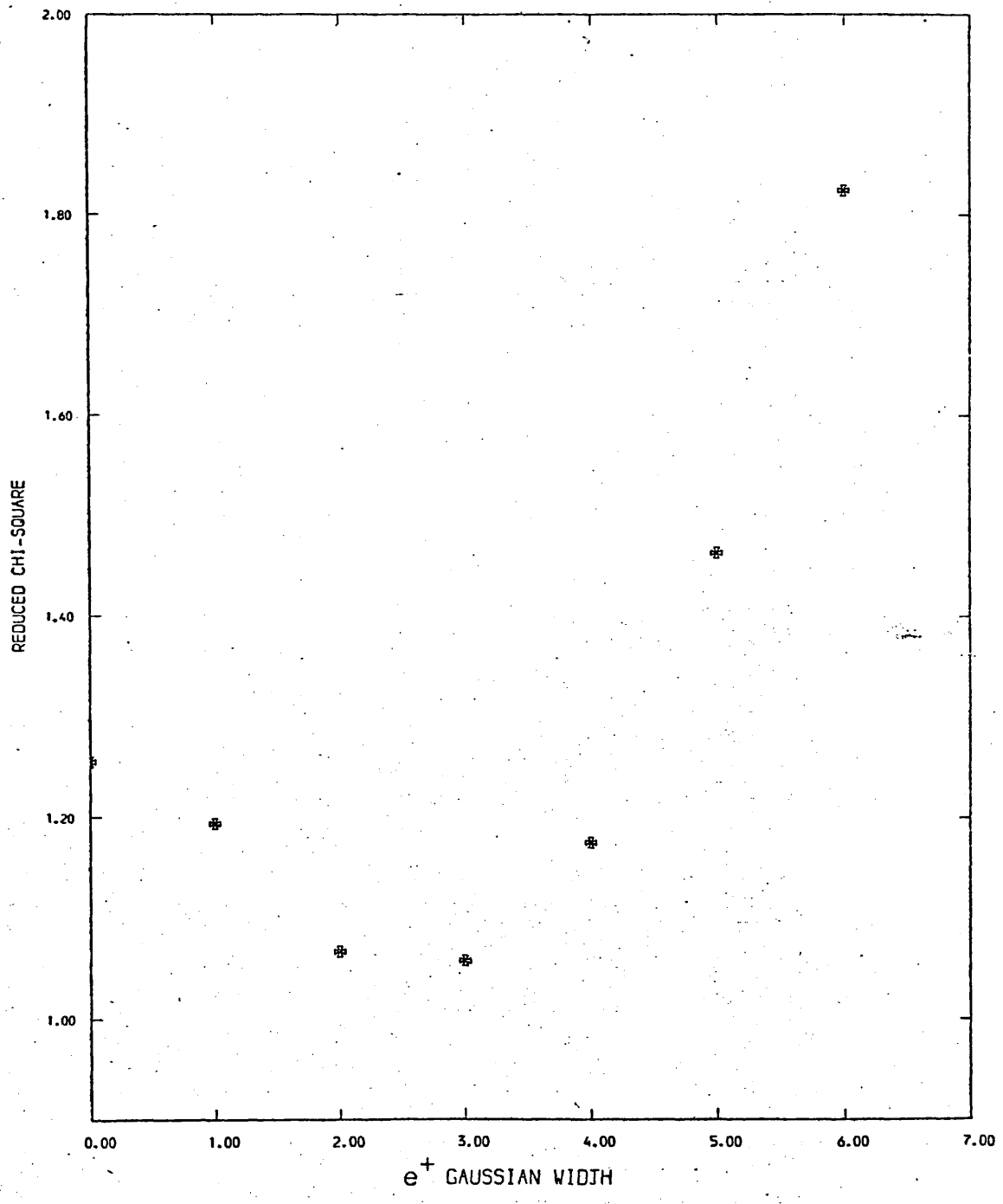

FIG.5.7 The variation of the reduced Chi-squared with the positron Gaussian width in Single Crystal indium at 420 K

It was, however, noticed that in the vacancy region the minimization (reflected in the reduced chi-squared) got progressively worse with increasing temperature. Assuming that the trapped positron contributes significantly to the momentum of the annihilating pair, an attempt was made to include the effective zero-point motion of the trapped positron by convoluting the measured resolution function with a Gaussian distribution of certain assumed width which was then observed. Fig (5.7) shows the result of such a procedure for a line taken at 416°K. The minimum in the reduced chi-squared occurs at a positron Gaussian width of about .28 Kev. In this minimization the electron Gaussian width parameter recovered from 20.5 channels to 22.0 channels. While the parabola width dropped to 14.8 channels indicative of a local Fermi energy of 7.58 ev; the parabolic percentage went up 65.8%.

6. Positron Annihilation in Tin

6.1 Sample Preparation

Two 15 mm x 15 mm x 1 mm pieces of 99.999% pure tin, supplied by Metals Research, were etched in nitric acid + alcohol and 0.1 ml -approximately 0.1 mCi - of carrier free $^{22}NaCl$ solution was then evaporated directly onto the central region of the surfaces. The estimated diameter of the active area was 2 mm. The two pieces were then put together in sandwich configuration and wrapped in two layers of thin aluminium foil.
The sample was then mounted in the high temperature cryostat and annealed at 450 K for 15 hours under a vacuum of 3×10^{-6} millibar. It was then cooled down slowly to room temperature in about 8 hours and transferred to the low temperature cryostat. Under a vacuum of 4×10^{-6} millibar it was cooled down slowly to 77 K and then data accumulation started.

6.2 The F- Curve

The F parameter vs temperature curve is shown in Fig (6.1). It appears flat to about 200°K and then it begins to rise slowly, almost linearly, until it reaches (400 ± 10)° K above which the F- parameter shows a steeper slope that continues to 500°K. There is no indication of any saturation effect at the top end of this temperature range.
Kusmiss etal [151] in an early work remarked that upon melting the angular correlation curve in tin showed a change as apposed to metals like cadmium, lead, and indium that showed a large change prior to melting, but none upon melting.

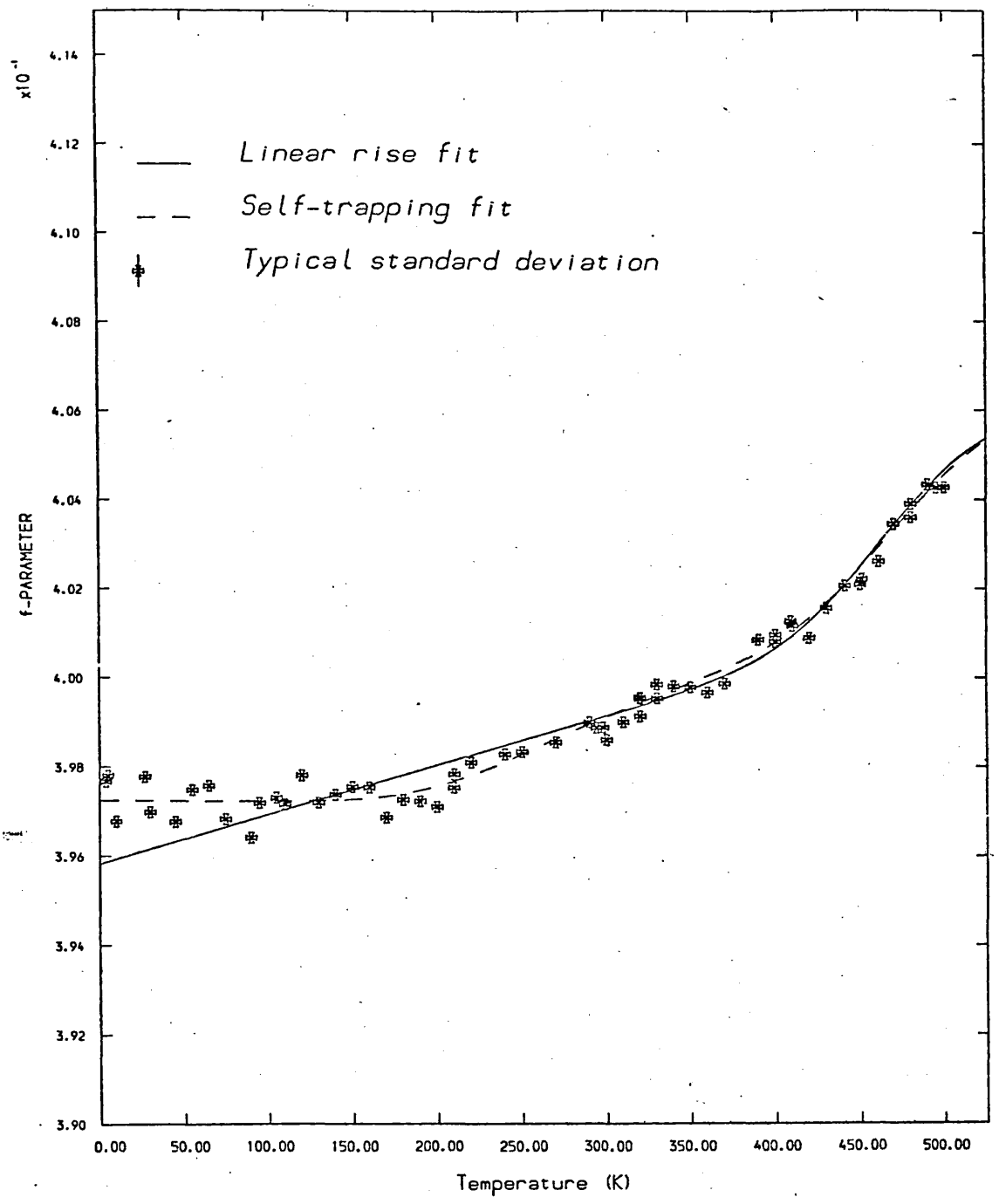

FIG.6.1 The variation of the F-parameter with temperature in Tin

The data compare favourably with that of Lichtenbergers [93] and Dedoussis etal [152]. Although it is difficult to compare quantitatively data that employ different definitions of different line shape parameters, the overall change in Lichtenbergers W parameter 93 is about 0.0060, that in Dedoussis etal [152] F- parameter is about 0.0063, while the data in Fig.(6.1) show an overall change of about 0.0067.
Evidence seems to converge that although line shape changes in tin as a function of temperature appear small, nevertheless they are quite distinguishable and it is not possible to attribute them to electronic instabilities. During the course of this experiment the systems stability was constantly monitored by the 497 Kev gamma ray line of ^{103}Ru and was found satisfactory.

6.3 F- parameter analysis and discussion

As it happens tin is one of those metals that have not yet had their fair share of attention as far as the positron technique is concerned. The angular correlations for tin have been measured by Mogensen and Trumpy (153) and further analysed by Kontrym-Sznajd (154).
The result of the minimization for the data in Fig (6.1) using the linear rise model is as follows

(a) $E_v = (0.56 \pm 0.01)$ev, $A_{1v} = (8.00 \pm 0.64)\times10^5$

$F_f = (0.39582 \pm 0.00044)$, $F_{1v} = (0.40647 \pm 0.00063)$

$\beta = (28.0 \pm 3.6)\times10^{-6}$

with a reduced chi-squared of 0.907 and where the temperature dependence of F_v has been set equal to zero.
The result of the minimization using the self-trapping model is as follows:

(b) $E_v = (0.52 \pm 0.02)$ev, $A_{1v} = (2.64 \pm 0.95)\times10^5$

$F_f = (0.39723 \pm 0.00007)$, $F_{1v} = (0.40691 \pm 0.00073)$

$F_{st} = (0.40243 \pm 0.00056)$, $B = (7.25 \pm 1.17)\times10^5$

$\epsilon = (0.142 \pm 0.005)$ev

with a reduced chi-squared of 0.763.

The proportion of trapped positrons at T = 500 K is 67% for case (a) and 63% for case (b).

The E_v value obtained from (a) compares well with the 0.56ev obtained from threshold temperature correlation by Mackenzie etal (123) and Schulte and Campbell (138). Dedoussis etal (152) obtained a value of (0.50 ± 0.01)ev from lifetime measurements and a value of (0.51 ± 0.05)ev from Doppler broadening measurements. Lichtenberger (93) estimated E_v to be 0.53ev using the threshold temperature correlation. These values are in reasonable agreement with the energy of self-diffusion of (1.11ev parallel to the C-axis, 1.09ev perpendicular to the C-axis) in tin as quoted by Peterson (72) from Coston etal (155).

If one assumes that the lifetime of free positrons in tin is 215ps (152), then A_{1v} gives for the product of the trapping rate and the entropy exponential factor a value of (a) 3.7×10^{15} s^{-1}, (b) 1.2×10^{15} s^{-1} from the two models. This is to be compared with 1×10^{15} s^{-1} obtained by Dedoussis etal (152).

Seeger (28) quotes that the radius of the Sn^{+4} ion (0.71 Å) is small compared with the half interatomic distances (1.51 A° &1.40 A°). Compared to lead where a Pb^{+4} ion has a radius of 0.84 A° and half an interatomic distance of 1.75 A°, tin and lead are both considered narrow core metals.

With both metals being tetravalent one expects the high valence to favour the formation of a positron bound State.

Nevertheless the monovacancy trapping effect is not apparently evident in tin as it is in lead.

A qualitative explanation for the weak trapping effect in tin has been suggested by Seeger (28). While the monovacancy formation volume in lead is 0.4, tin has a monovacancy formation volume which is much smaller, about 0.25. i.e. similar to those found in alkali metals that show no trapping effect. Strong vacancy relaxation implies that for a monovacancy in tin if the neighbouring ion cores relax inwards, they substantially reduce the charge to be screened by the conduction electrons thus resulting in a shallow trapping potential and a small positron-vacancy binding energy; an effect which counteracts the formation of a positron bound State. Seeger (28) quotes from Hodges (4) values of 5.2ev and 1.4ev for the trapping potential and the binding energy respectively of a positron in a vacancy in tin. However, these values have no immediate relevance since they are calculated in the "rigid" vacancy model and relaxation effects were not allowed for.

Tin is anomalous in that at the melting point its tracer self-diffusion coefficient is about three orders of magnitude smaller than that for most metals (155). Therefore if the monovacancy mobility near the melting point is the same as that for other metals and if one takes E_v as 0.56ev then C_v at 505 K is about exp(S/K) x 2.3×10^{-6} i.e. the melting point vacancy concentration in tin is about two orders of magnitude smaller than in most metals. When judged by its vacancy concentration in thermal equilibrium, Seeger (28) classified tin as a metal that "melts too early".

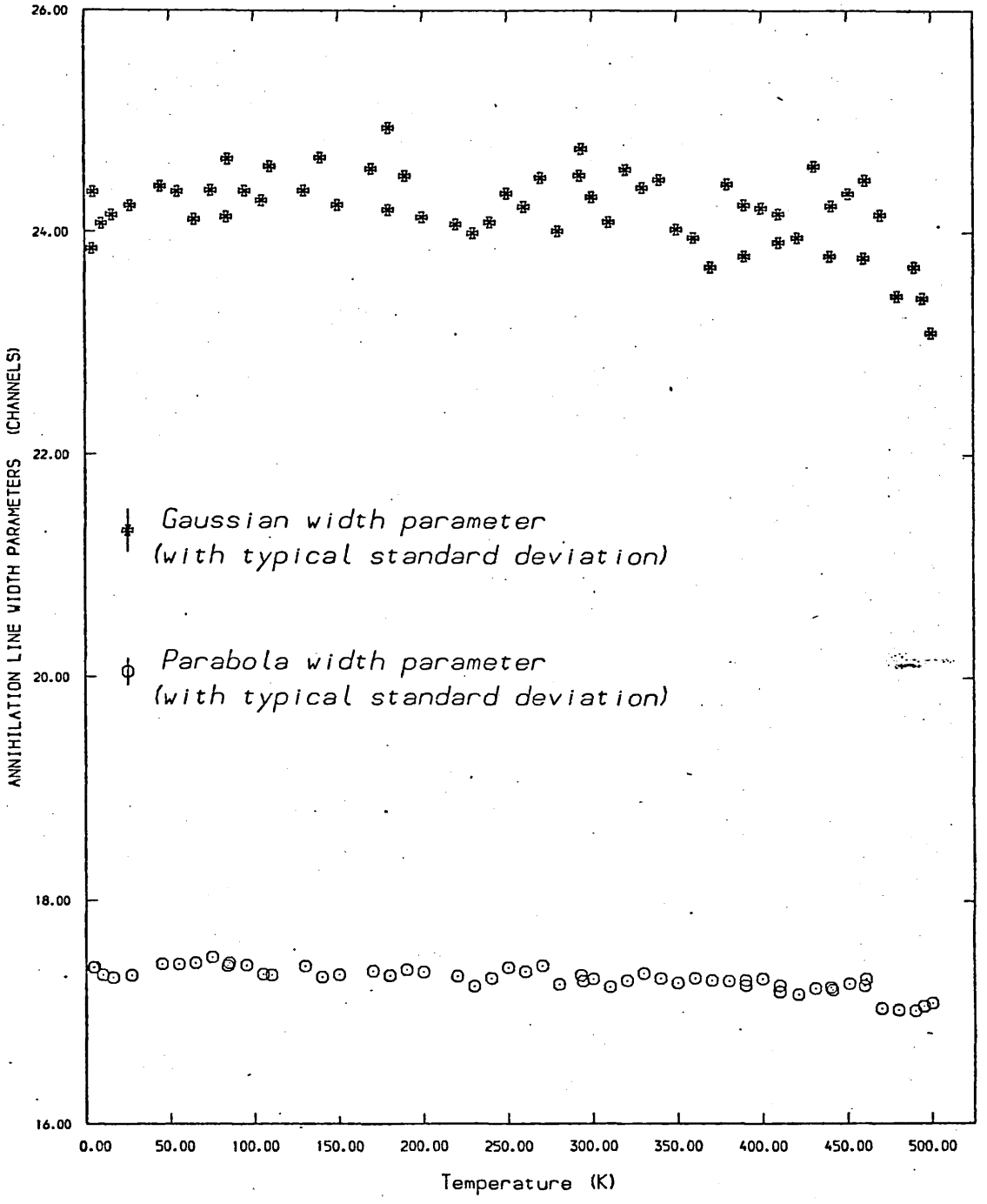

FIG.6.2 The temperature dependance of the width parameters of the Gaussian and parabolic components of individual lines for Tin

6.4 Convolution

The model dependent convolution technique outlined in section (3.6) was used in analysing the tin data. Fig(6.2) shows the variation of the parabola and Gaussian width parameters with temperature. A parabola width of 17.3 channels at room temperature gives a Fermi energy of 10.35ev which is in reasonable agreement with 10.2ev the accepted Fermi energy for tin (131) (132).
Fig(6.3) shows the variation of the parabolic percentage with temperature. It is almost a constant within the dispersion of the data except near the melting point where it rises slightly. An average value of 68% is in good agreement with that quoted by Jackman etal (109) and Manninen etal (136). There is no appreciable worsening of the reduced chi-squared at high temperatures and the result of the inclusion of an extra Gaussian function in the systems resolution is shown in Fig(6.4). The required extra Gaussian for the best minimization is seen to be very narrow, nothing as significant as that found in Cadmium and Indium. This is again consistent with the result found by Jackman etal (109). For a positron Gaussian width of 0.3 channels even at 500°K there is no significant change in the parabola and Gaussian width parameters or in the parabolic percentage.

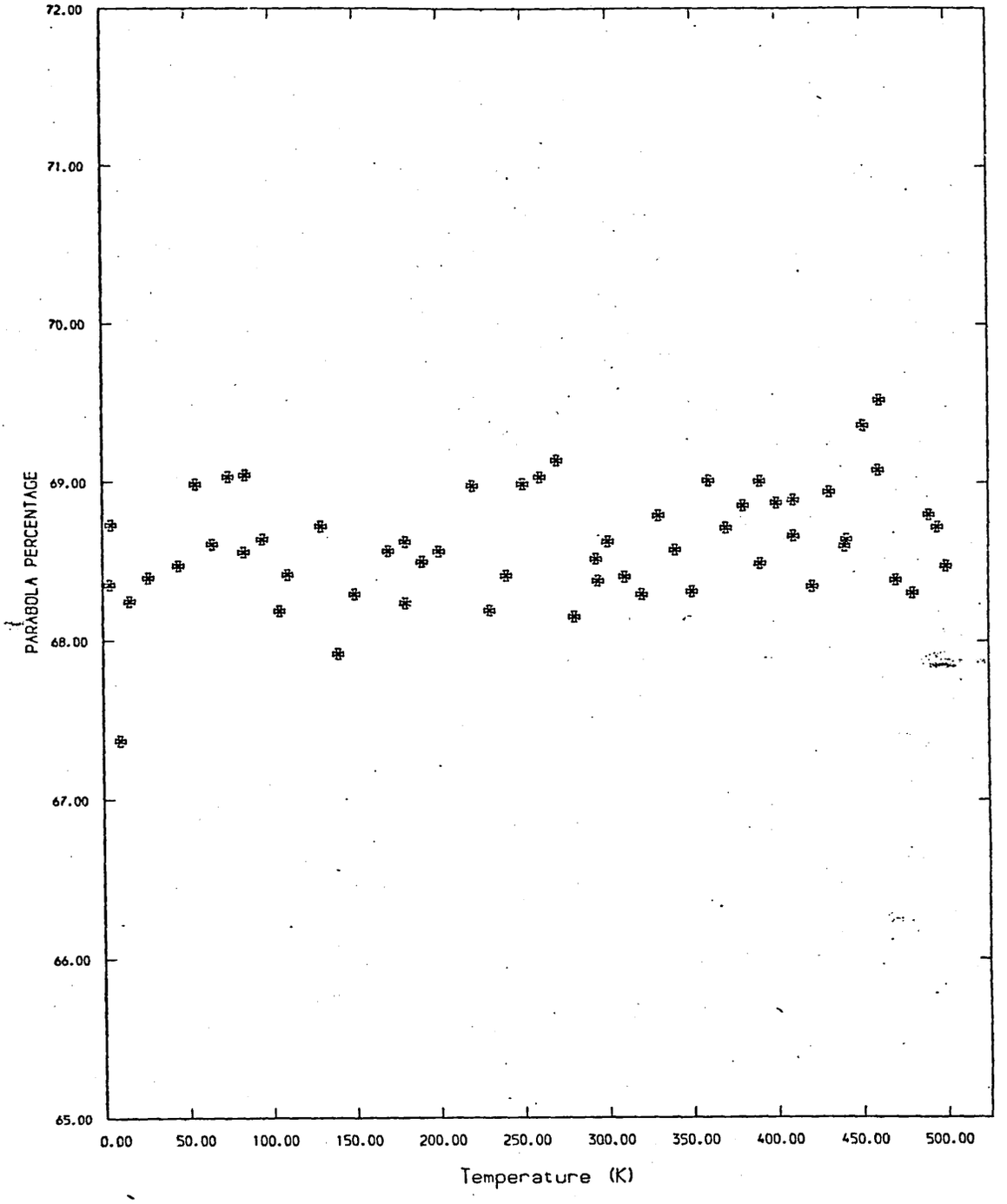

FIG.6.3 The temperature dependance of the parabolic percentage in Tin

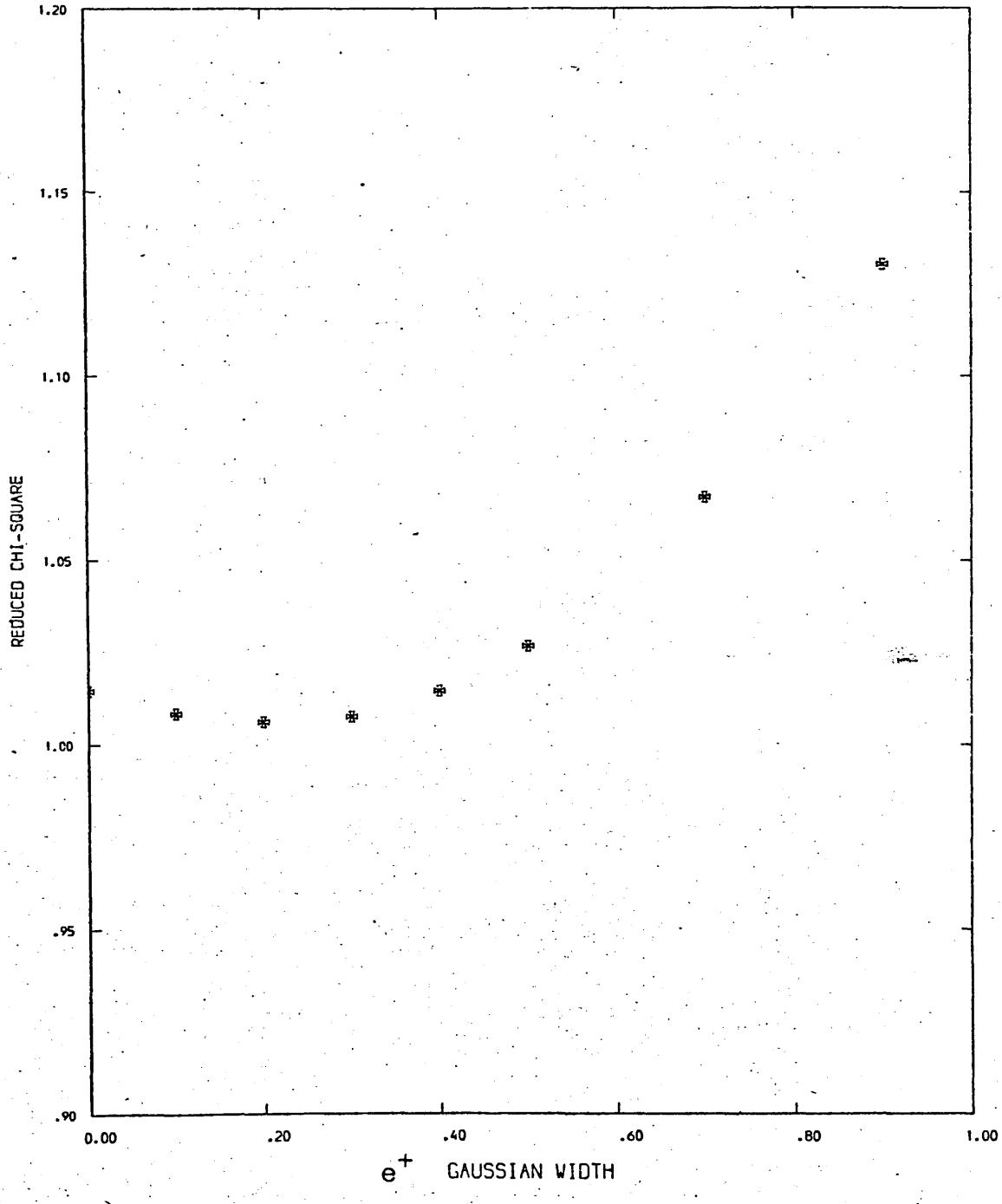

FIG 6.4 The variation of the reduced Chi-squared with the positron Gaussian width in Tin at 500 K

7. Positron Annihilation in Aluminium.

7.1 Sample Preparation

Two 11mm x 16mm pieces of 99.999% pure aluminium each of 3.5mm thickness were produced by slicing an aluminium ingot. They were etched in a solution of equal volumes of concentrated hydrochloric acid and nitric acid. They were then rendered as flat as possible and the thickness of each piece reduced to 2mm and then etched again. 0.1ml of carrier-free $^{22}NaCl$ solution (0.94 mCi per ml) was then evaporated centrally onto the surface of the two pieces. The active area diameter was less than 3mm. The two pieces were then made into a sandwich configuration and wrapped by two layers of thin aluminium foil. The sample was mounted in the high temperature cryostat and annealed under a vacuum of 10^{-6} torr for 12 hours at 750°K. Over the next 12 hours it was then gradually cooled down to room temperature. Finally the sample was transferred to the low temperature cryostat and cooled down slowly to 77°K, the count rate was adjusted to 5 K Cps, and data accumulation started.

7.2 The F- Curve

The F- parameter vs temperature curve for aluminium is shown in Fig.(7.1). It appears flat up to (200 $\pm$ 10)K above which it starts rising with a somewhat shallow slope. Above (500 $\pm$ 20)K the slope becomes much steeper due to the onset of trapping in monovacancies. Although points above 800K tend to show a saturation effect, it is worth mentioning that when the sample was taken out after the high temperature run there was some contamination in the high temperature furnace.

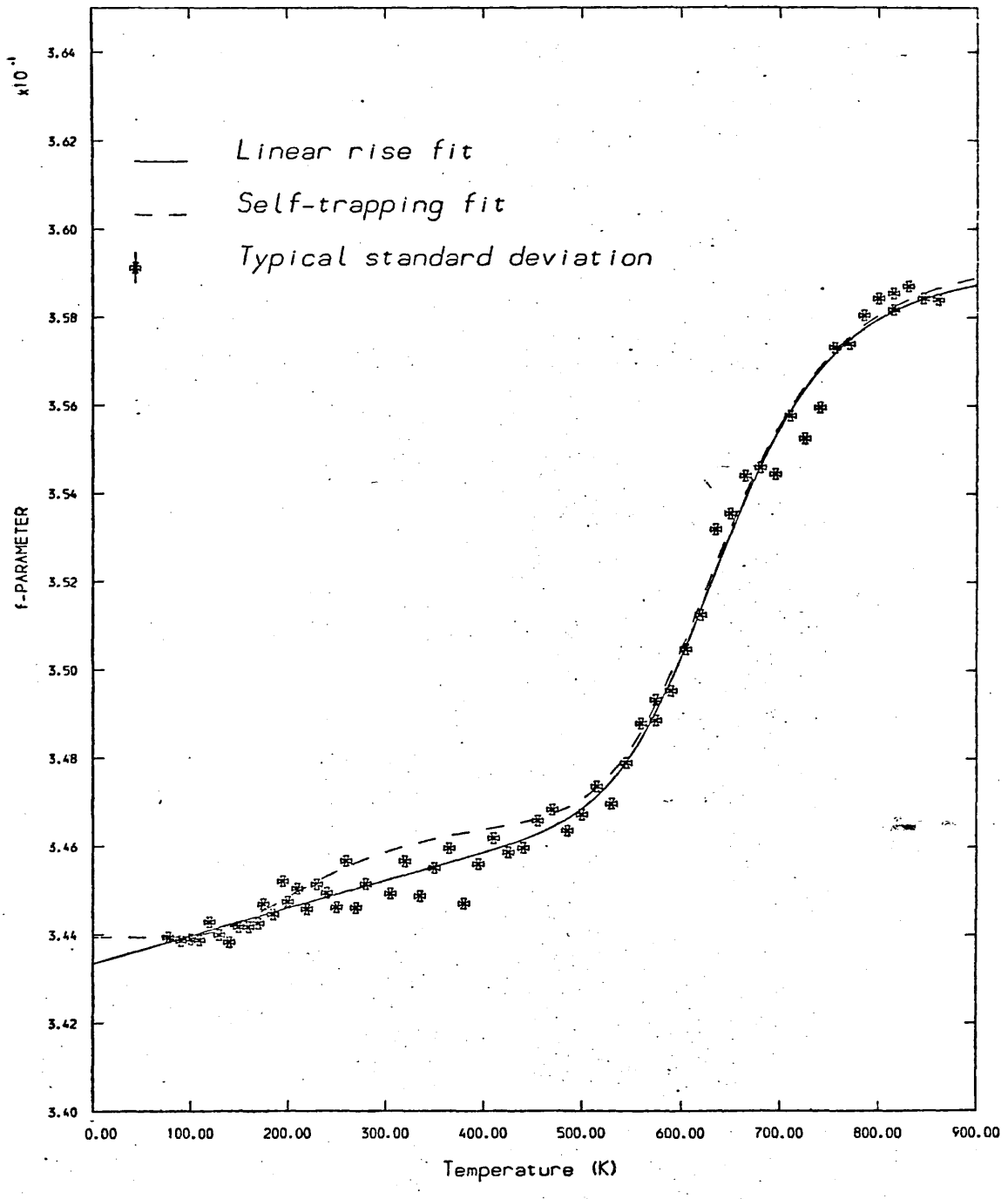

FIG.7.1 The variation of the F-parameter with temperature in Aluminium

7.3 F- Parameter Analysis and Discussion

Of the group of trivalent metals aluminium has been studied most extensively (Berko and Plaskett(80), Stroud and Ehrenreich(156), Okada etal(157), and Mader etal(158)). Lynn (159) studied the Doppler broadened data in aluminium with a system of two Ge(Li) detectors in coincidence. A peak-to-background ratio greater than 10^5 enabled them to observe the $(1S)^2$ core contribution. A considerable amount of experimental data on C_v and E_v in aluminium is available, Siegel(73).

The least-square minimization for the data in Fig (7.1) using the linear rise model above 185K is as follows:

(a) $E_v = (0.68 \pm 0.02)$ev, $A_{1v} = (1.74 \pm 0.8)\times10^5$

$F_f = 0.34325 \pm 0.00023$, $F_{1v} = 0.35893 \pm 0.00018$

$\beta = (19.0 \pm 1.9)\times10^{-6}$

with a reduced chi-squared of 1.008. According to this minimization the proportion of trapped positrons at 900K is 96%.

The self-trapping model gives

(b) $E_v = (0.58 \pm 0.02)$ev, $A_{1v} = (3.01 \pm 0.54)\times10^4$

$F_f = 0.34412 \pm 0.00013$, $F_{1v} = 0.35967 \pm 0.00015$

$F_{st} = 0.34877 \pm 0.00093$, $B = (9.22 \pm 3.25)\times10^4$

Epsilo $= (0.102 \pm 0.01)$ev

with a reduced chi-squared of 0.839.

The allowance of a linear temperature dependance in Fv has become a fashionable aspect of the application of the simple two State trapping model in recent work (29). A positive linear dependance in Fv usually

results in a higher than average E_v values, while a negative one results in lower E_v values with the constant A_{iv} having to compensate for this effect in both cases. The improvement in the reduced chi-squared, though apparent, might not be physically significant since it is done at the expense of E_v and A_{iv}. Experience seems to suggest that the end result of this approach is more likely to be nothing more than a computational artefact. The temperature dependance of F_{iv} in (a) and (b) has therefore been set to zero.

Arponen etal (160) judged the possibility of detrapping in aluminium to be negligible. They estimated the positron-vacancy binding energy to be 2.6ev, while Brandt(45) calculated it to be 6ev, Manninen etal (136) 1.75ev, Mori(161) 0.8ev, and Hodges(4) obtained 2.0ev and 3.8ev with and without electron-electron correlation respectively.

The results for aluminium are numerous and generally they are in reasonable agreement with respect to both E and A_{iv}. Mackee etal(10) found 0.66ev and 1.2×10^{15} S^{-1} for E_v and v exp(S/K) respectively using angular correlation data, while Hall etal(162) found 0.64ev and 0.8×10^{15} S^{-1} from lifetime measurements. Triftshauser(137) obtained 0.66ev and 0.6×10^{15} S^{-1} by applying the two state trapping model to the peak counting rate in the angular correlation curves, while Kim etal(163) obtained 0.67ev and 1.7×10^{15} S^{-1}. Dlubeck etal(164) found 0.68ev and 1.9×10^{15} S^{-1}, while Fluss etal(165) extracted 0.66ev and 0.8×10^{15} S^{-1} from their lifetime measurements. These are to be compared with 0.68ev and 1.048×10^{15} S^{-1} found from the model fitting in (a). Hood and Schultz(29) work

on Doppler broadened data in aluminium explored the parameter and range dependence of the minimization.

Stott(32) quoted Popovic etal(166) calculation for the temperature dependence of the vacancy formation energy and volume in aluminium using the pseudo potentials. Both are shown in this treatment to decrease by about 30% over the 900K temperature range.

When the lifetime of free positrons in aluminium is assumed to be 166 ps (144)(167), and $S_{iv} = 0.6K$ (28)(168) where K is the Boltzmann constant; then a trapping rate of $5.75 \times 10^{14}\ s^{-1}$ and $C_v(Tm) = 4.26 \times 10^{-4}$ can be estimated from (a). These are to be compared with $4.3 \times 10^{14}\ s^{-1}$ and 9×10^{-4} quoted by Hood and McKee(110).

Quenching experiments have generally yielded somewhat higher values of E_v; 0.69ev (169), 0.70 ev (170), 0.76ev (167). Siegel(73) deduced a total equilibrium vacancy concentration at the melting temperature of 9.4×10^{-4}, about 42% of which is in divacancies with $E_{iv} = 0.66ev$, $S_{iv} = o.7K$, $E^b_{2v} = 0.28ev$ and $S^b_{2v} = -1.2K$. In view of the ongoing discourse concerning the divacancy contribution to the total vacancy concentration at high temperatures in aluminium (28)(72)(73), divacancy parameters were included in the linear rise model above 700K. The result of the minimization was

(c) $E_v = 0.66ev$, $A_{iv} = 1.74 \times 10^5$

$F_f = 0.34324$, $F_{iv} = 0.35769$

$\beta = 18.1 \times 10^{-6}$, $F_{2v} = 0.36387$

$A_{2v} = 1.33 \times 10^8$, $E^b_{2v} = 0.08ev$

with a reduced chi-squared of 1.060. According to this

minimization at 930K 63.5% of the positrons are trapped in mono vacancies, 34.8% are trapped in divacancies, and 1.8% are still free.

Finally it is worth remarking that, as Hood etal(29) has demonstrated, although both the F and W parameter curves in aluminium show in general an overall S-shaped temperature dependence, their respective profiles are quite distinct in detail. When this is coupled with the observation that both parameters are definition-dependent and that the best-fit minimization is range dependent; it suggests that although the simple trapping model description at this stage appears adequate, it might conceivably prove incomplete. The simple trapping model can provide reasonable E_v values but not sufficient description of the temperature dependence of all the parameters involved in deriving these values.

7.4 Convolution

The model of a Gaussian and an inverted parabola was used to fit individual 511 Kev annihilation lines. At low temperatures the Gaussian has an average width of 25 channels while the parabola has a width of 18.8 channels which gives a Fermi energy of 12.2ev, Fig(7.2) This is to be compared with 11.63ev, the accepted Fermi energy for aluminium (131)(132). Shizuma (116) found 11.89ev and 12.33ev for the same quantity.

The parabolic percentage, Fig(7.3), at the low temperatures has an average value of about 82%. Jackman etal (109) found the parabolic percentage in aluminium at 300K to be 83.2%, while Shizuma (116) using a model-independent deconvolution technique found it to be 79.7%. Manninen etal(136) and Stott and West (49) both quoted a value of 83%.

The minimization above 500K (the vacancy threshold) provides an example in which the inadequacy of the model-dependent convolution technique is exposed, and the correlation between the F- parameter and the parabolic percentage extracted in this fashion breaks down. While the F- parameter continues to rise above 500K, the parabolic percentage declines with temperature at the expense of severe narrowing of the Gaussian width. Shizuma (116) anticipated the occurance of such a breakdown and cautioned against the application of this technique to a line profile if the intensity of one of the two functions to be used dominates. Jackman etal (109) found the same when they used a model dependent convolution programme on their deformed aluminium data and extracted a parabolic percentage of 79.1% as opposed to 83.2% for annealed aluminium.

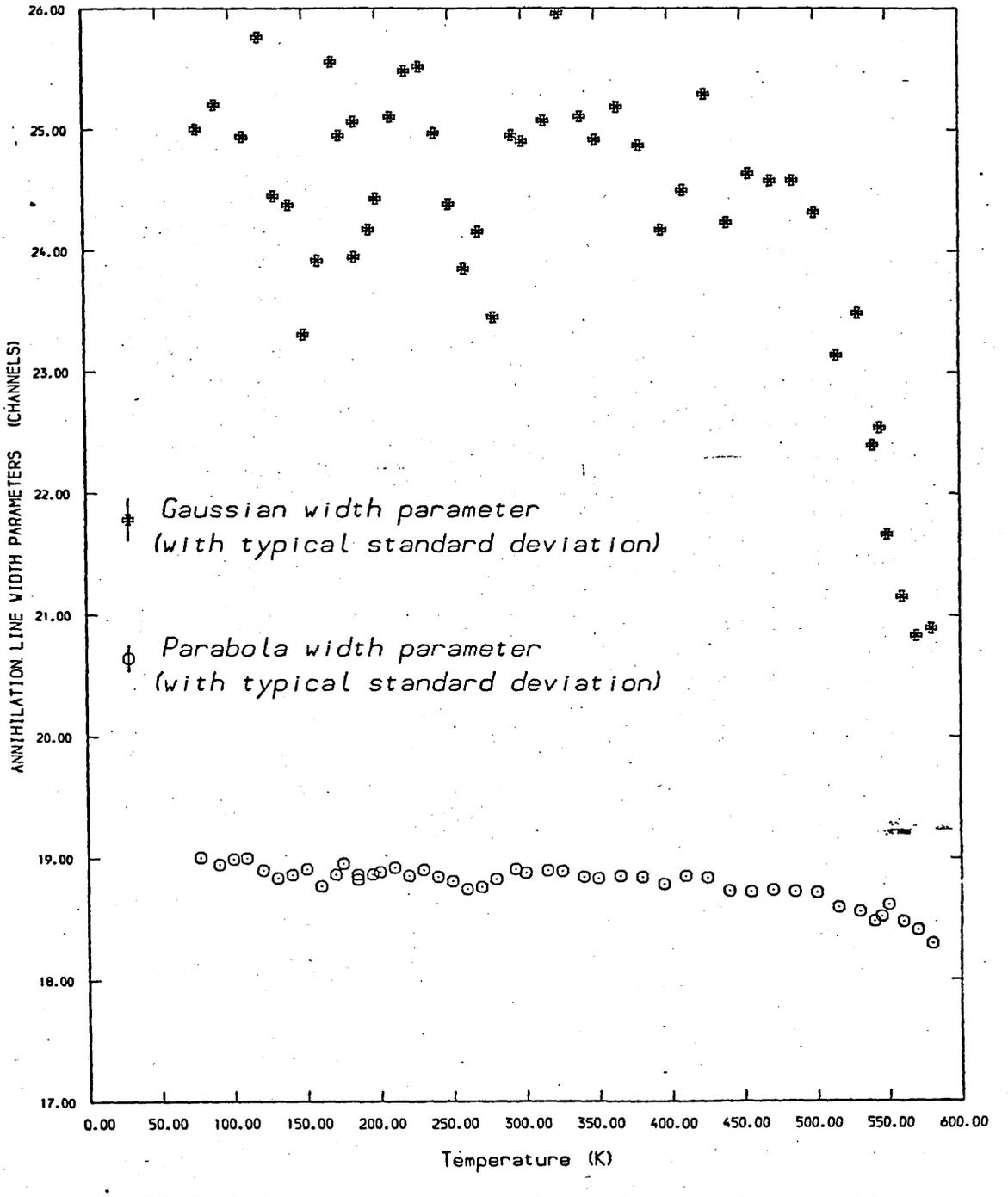

FIG.7.2 The temperature dependance of the width parameters of the Gaussian and parabolic components of individual lines in Aluminium

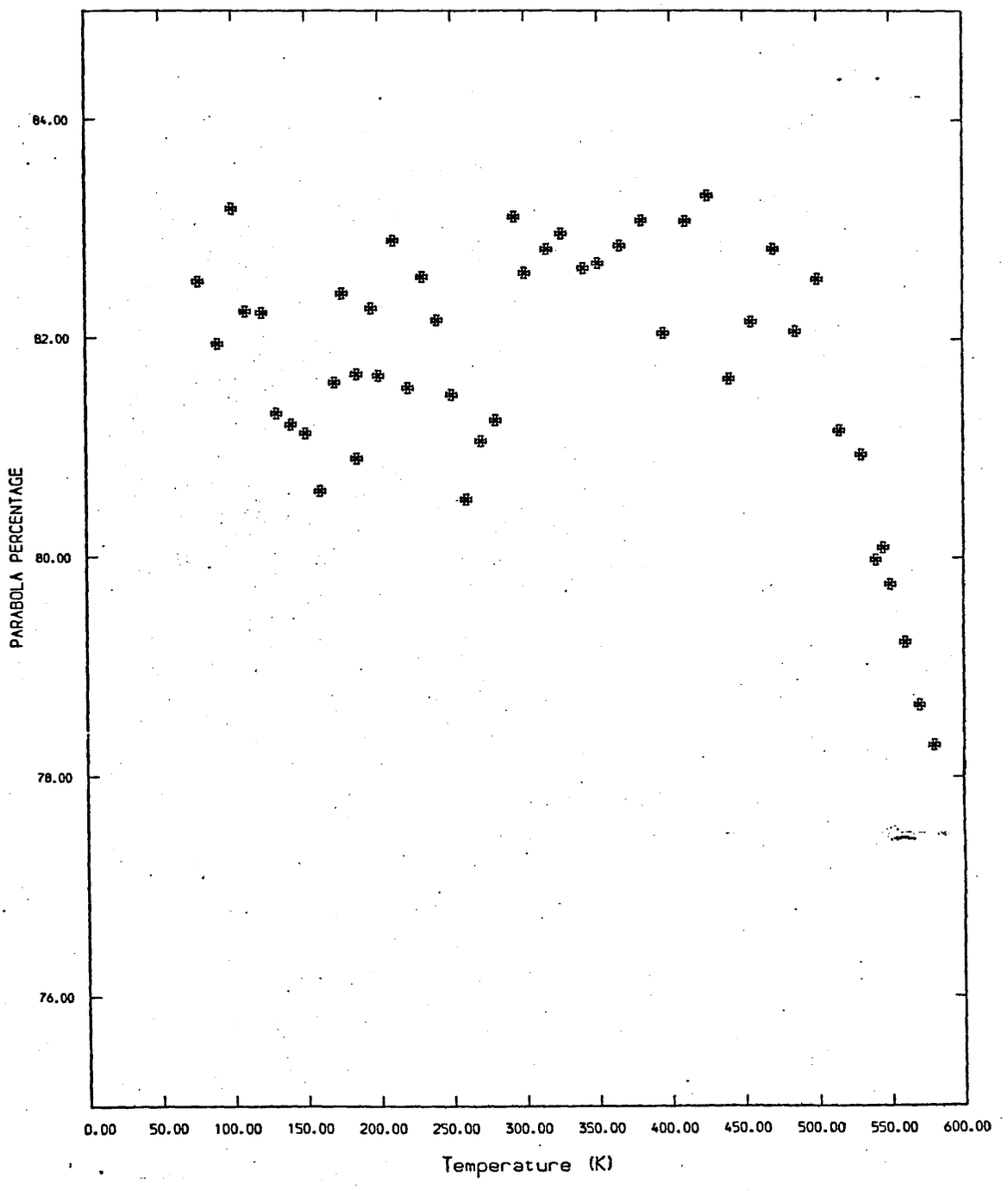

FIG.7.3 The temperature dependance of the parabolic percentage in Aluminium

It seems that the departure of the local electronic distribution at the vacancy and the relaxation of neighbouring ion cores with temperature can no longer be approximated satisfactorily by a perfect Gaussian and parabola. This departure manifests itself in a Gaussian whose width narrows rapidly from 25 channels to about 19 channels to resemble that of the parabola and thus the minimization ceases to have any physical significance aside from the numerical one reflected in the reduced chi-squared.

8. SUMMARY AND CONCLUDING REMARKS.

Throughout the course of these experiments the the Deoppler broadening technique has been used exclusively. It is generally accepted that the positron-defect interaction has opened up new possibilities for investigating the electronic structure of defects as well as their concentration. Monitoring the positron behaviour in the metals studied between 4.2 K and their melting temperatures provided reasonable estimates of their vacancy formation energies and related parameters i.e. concentrations, trapping rates, in addition to the information obtained about positron-electron interactions below the vacancy threshold.

The sensitivity of the positron as an effective probe has been demonstrated in its ability to reveal different annihilation characteristics in single crystal samples as opposed to polycrystalline samples of the same metal. The anomalous low termperature effect found in Cadmium is a genuine one; and if properly understood might hopefully clarify certain aspects of positron annihilation at low, as well as moderate, temperatures in annealed metals. It seems reasonable at this stage to interpret it as a trapping effect,which opens up the exciting possibility of positron trapping in one form or another at moderate temperatures in annealed metals in general. However, additional experimental evidence is required to positively identify the nature of this phenomenon.

The capability of the technique when applied to annealing studies cannot be over stressed. The positron is a highly effective probe that can provide information about annealing stages, and if a quantitative model can be formulated, a unique characterization of the different types of defects involved. If the positron zero point energy approach is exploited within the convolution technique, the possibility of binding energy studies might prove a promising field of research.

There is not yet sufficient information on which generalization regarding the high-temperature features of positron annihilation in metals can be based. Different annihilation parameters seem to exhibit varying degrees of temperature dependence in metals near their melting temperatures. Nevertheless, despite the possible complex origin of the high temperature features of positron data, a fairly general and useful description of the onset of vacancy effects on the annihilation parameters can be made in terms of the systematics of positron-vacancy interaction and the trapping model.

In view of the wealth of the available data, and the sometimes apparent divergence of different schools of thought in interpreting it, some criticism ought to be levelled against the model which is most frequently used in analysing it, the simple trapping model. The major assumption about the linear temperature dependence for free positrons persisting to the melting temperature, reflecting thermal expansion, usually overestimates Ev and is in need of revision. A second widely applied assumption

is the use of a constant annihilation rate for the free positron, whereas the very existence of the prevacancy effect reflected in a temperature dependent F_f, seems to contradict that.

Recent work in this laboratory has shown that the prevacancy effect in single crystal cadmium has a directional dependence. In light of such exciting and provocative material previous estimates of vacancy concentrations and formation energies in metals would need to be viewed with caution. A more complex theoretical description might be needed and the calculation might prove less straightforward than has been hitherto assumed. Nevertheless, because of the many inherently interesting applications of the positron technique, and its ability to provide information that might prove valuable in solving difficult problems in fields like radiation damage, one can only look forward to further developments in this relatively new and fast growing field of research.

NB Bibliography bound in after published papers

APPENDICES

Positron Annihilation in Indium, Zinc, Cadmium, and Gold in the Temperature Range Down to 4 K

P. Rice-Evans, I. Chaglar, and F. El Khangi
Department of Physics, Bedford College, University of London, Regent's Park, London NW1 4NS, Great Britain
(Received 11 August 1977; revised manuscript received 30 January 1978)

Doppler-broadening measurements have been made on the 511-keV photons resulting from positron annihilation in annealed and plastically deformed samples of indium, zinc, cadmium, and gold. Over the temperature range 4–400 K, distinctive features are observed in each case. Studies with a single crystal of cadmium associate the features with defects at grain boundaries.

Uncertainty surrounds the behavior of positrons in metals at low temperatures. At higher temperatures the trapping model, in which vacancies are assumed to trap positrons, has enjoyed some success; Arrhenius plots and values of vacancy formation energies (E_v) have been reported (for review, see Seeger[1] and West[2]). At intermediate temperatures below the vacancy region, measurements show that the annihilation parameters (for example F, defined in Rice-Evans, Hlaing, and Rees[3]) are a function of temperature; and the original interpretation based on thermal expansions has been challenged by the observation in cadmium of two distinct subvacancy regions,[4] and by models based on phonon-assisted dilatations[4] and self-trapping metastable states.[5] At the Helsingor positron conference, August 1976, a Doppler-broadening study on 99.9999+% pure (6N) annealed indium[6] gave strong support to Seeger's self-trapping model, but controversy reigned. However, subsequently we have failed to find evidence for self-trapping in 5N indium.[7]

As liquid helium temperatures are approached new effects have appeared; in annealed cadmium and gold an unexpected rise in F has been seen at the lowest temperatures,[8] but not in copper.[9,10] In addition, although it has long been known that defects in plastically deformed metals trap positrons,[11] it is only recently that investigations of these phenomena at low temperatures have shown interesting features.

In this Letter we present new Doppler-broadening measurements for a range of temperatures down to 4.2 K. A germanium detector with a resolving power of 1.15 keV at 514 keV has been employed to determine the shape of the 511-keV annihilation γ line. We have used a conventional F parameter[3] defined by the ratio of the number of counts in a chosen central region of the line divided by the counts in the whole line. With this definition, F is linearly related to the number of positrons annihilating with the conduction electrons and hence contributing the narrow paraboiic component of the line. Each point in the figures corresponds to a line containing 900 000 counts. Simultaneous measurement of a control ^{103}Ru 497-keV γ ray has been instituted to assess any electronic drift and to allow appropriate correction where necessary. A G parameter, similar in conception to F, was applied to the 497-keV line, and runs corresponding to any significantly low values (rare) were rejected.

The samples were held in a cryostat (<400 K) and a furnace (>300 K), in a vacuum better than 10^{-5} Torr. The temperatures were controlled automatically, and in the cryostat a Au/0.03%-Fe–Chromel thermocouple was used.

Four polycrystalline metals have been studied: indium, zinc, cadmium, and gold. Carrier-free ^{22}NaCl positron sources were evaporated onto the central regions (<5 mm diameter) of two etched specimen disks (diameter >10 mm) which were then pressed in a sandwich configuration. For the annealed samples, the respective purities, disk thicknesses, manufacturers, and annealing conditions were In, 6N, 1.25-mm, Koch-Light, 8 h at 398 K plus 13 h at 373 K, 10^{-5} Torr; Zn, 5N, 1.0 mm, Johnson-Matthey, 8 h at 633 K, 10^{-5} Torr; Cd, 1.6 mm, 99.9996%, Johnson-Matthey, 23 h at 514 K, 10^{-6} Torr; Au, 0.75 mm, 5N, Koch-Light, 21 h at 1000 K, 10^{-6} Torr.

Defects were introduced into the metals by plas-

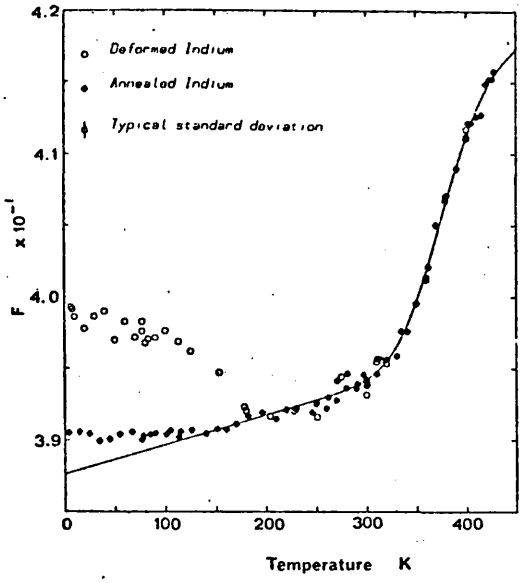

FIG. 1. Temperature dependence of the line-shape parameter F in annealed and deformed indium.

tic deformation, i.e., compression at room temperature, except for indium and one cadmium sample which were compressed at 77 K and not allowed to warm up. The thickness reductions and final disk thicknesses were In, 40%, 1.5 mm; Zn, 30%, 0.7 mm; Cd, 30%, 1.6 mm; Au, 25%, 0.75 mm.

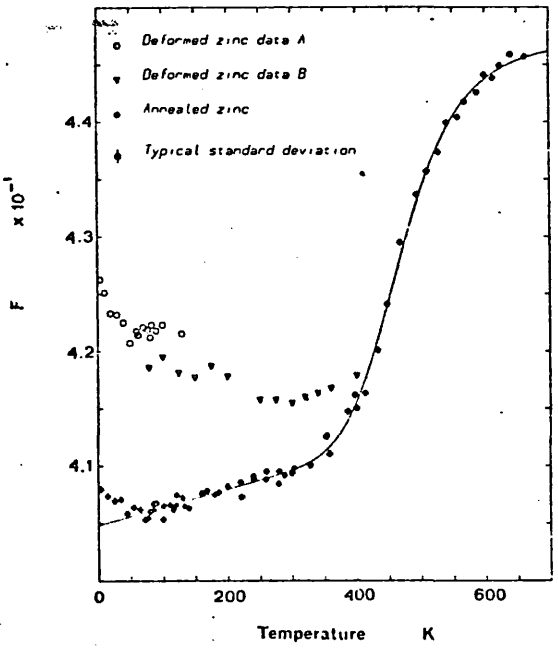

FIG. 2. Temperature dependence of the line-shape parameter F in annealed and deformed zinc. After the acquisition of data A, the deformed sample was allowed to warm up to 293 K for 72 h prior to subsequent cooling and collection of data B—partial annealing is observed.

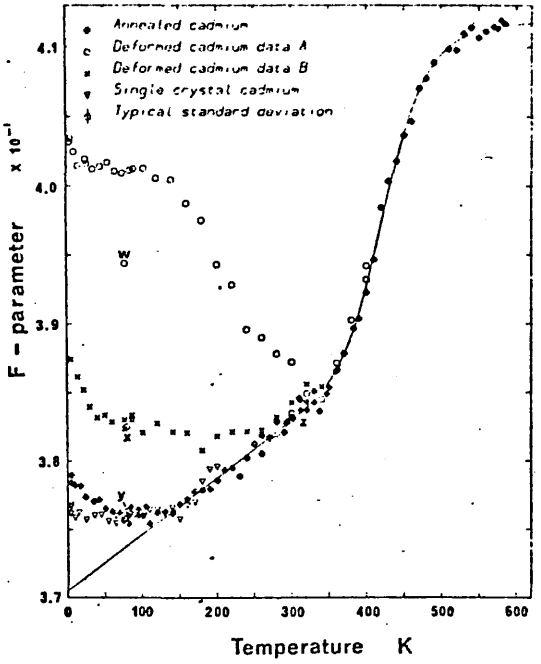

FIG. 3. Temperature dependence of the line-shape parameter F in annealed and deformed cadmium. For points (w,x) see text. Points (y,z) were after a final annealing. Cadmium single-crystal data are included.

In addition, a single-crystal (6N) specimen of cadmium has similarly been studied at low temperatures. Supplied by Metals Research Ltd., after spark cutting, etching, and electropolishing, the two sandwich elements each had a diameter of 10 mm and thickness of 1.1 mm.

Figures 1–4 show the line-narrowing parameter F plotted as a function of temperature for the four metals. Considering first the annealed samples, at the higher temperatures the rise in the

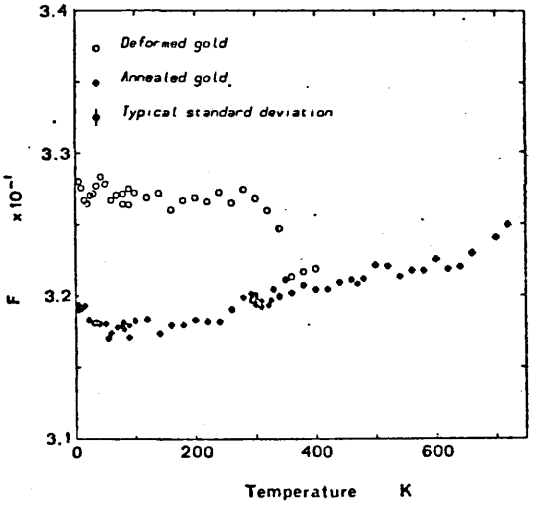

FIG. 4. Temperature dependence of the line-shape parameter F in annealed and deformed gold.

parameter F is associated with the creation of single vacancies (but not seen in Fig. 4). Below this region an approximately linear slope is observed for all samples. At still lower temperatures distinctive behavior is noticed, the most dramatic being in cadmium where the curve flattens at 130 K and rises again below 70 K. A similar but smaller rise is seen in zinc below 40 K, and also in gold. On the other hand, in indium the graph appears flat over the range 4 to 120K —as was previously found in the case of copper.[9]

The precise measurements of Kubica and Stewart[12] indicate that positrons thermalize in metals, even at the lowest temperatures. Compared with the electrons the positron energies are therefore negligible. Of course, at these temperatures, the uncertainty principle implies that the positron wave function is spread over ten or more lattice sites.

Gold and copper are fcc crystals, cadmium and zinc hcp, and indium tetragonal. For annealed metals, an important question is whether the differences in the figures can be attributed to the crystal structure. From the following table one can say that although gold and copper appear similar, compared to zinc the cadmium slope β is anomalously high [where $F = F_0(1+\beta T)$].

	In	Zn	Cd	Au	Cu
Approximate linear thermal expansion coefficient (10^{-6} K^{-1})	28	28	30	14	17
Slope (β) of intermediate linear region (10^{-6} K^{-1})	54	39	112	28	32

For annealed copper[13] we have found F to be flat below about 270 K (N.B.: this is not in agreement with Smedskjaer *et al.*,[14] who, however, analyze second momenta σ^2), and we find a similar flat region for gold (Fig. 4) below 250 K. Unlike our copper data, at the lowest temperatures (< 40 K), in gold the line narrows; it also does so in zinc and to a marked degree in cadmium. It is tempting to associate this increase in F with the negative expansion coefficients (a axis) of anisotropic cadmium and zinc below about 25 K, but this is unsatisfactory quantitatively and is of no help in the case of gold. On the other hand the suggestion[8] that positrons escape from the sample by channelling[15] within the grains is unconvincing —e.g., in cadmium, the conventional maximum range of positrons is 200 μm ($R = 0.407E_{\max}^{1.38}$; here $E_{\max} = 0.545$ MeV,[16] which is unlikely to be increased to 1.5 mm, the sample thickness, by channelling.

Even in well-annealed samples, grain boundaries exist—e.g., in this zinc specimen, micrographs showed the grain diameters to range from 20 to 300 μm with an average of 60 μm. It is known that positrons may be trapped in such boundaries[17,18]; whether they will be here will depend on the average grain size, i.e., the area of boundary, and whether a significant proportion of positrons would encounter a boundary. It is conceivable that at the lowest temperatures in cadmium and zinc, because of forces arising from the anisotropic expansions of neighboring randomly oriented grains, additional defects will appear at the boundaries and hence might contribute to a larger F. However, this would not apply to gold. Alternatively, the shape of the potential well (trap) may be important. MacKenzie[19] has suggested that the increase in F at the lowest temperatures implies that positrons are captured in shallow grain-boundary traps, and that the negative slope (dF/dT) indicates thermal detrapping.

When the single-crystal data for cadmium are considered (Fig. 3). one sees that F is independent of temperature below 150 K. This demonstrates that the low-temperature effect seen in annealed cadmium must be associated with the trapping of positrons by defects in the grain boundaries. This conclusion would be in agreement with the case of annealed indium (Fig. 1); the flatness of the data would be a consequence of the large grain size, i.e., the relative absence of boundaries.

The curves for the deformed samples (Figs. 1–4) again show distinctive features at the lowest temperatures. In both cadmium specimens, and in zinc, a sharp increase in F is seen, whereas only a small negative slope occurs for indium, and apparently none in gold. (They are all reversible.) The cadmium specimen (A) and probably the indium were kept below their recrystallization temperatures and hence little annealing would be expected. On the other hand, the zinc and cadmium (B) were deformed at room temperature and hence many defects would have annealed out prior to insertion in the cryostat.

The data of cadmium (A) are especially informative. Apart from the unexplained rise in F below 25 K, one sees a flat F for 25–100 K implying a temperature-independent positron trapping rate. Above 100 K annealing commences, each point following the previous point by $2\frac{1}{2}$ hours. Point (W) was taken immediately after the point at 200 K; the fact that they both have the same F sug-

gests again a constant trapping rate for a smaller concentration of defects. Point (X) followed point (320 K); this is remarkable. Even though F(320 K) virtually equals the F(320 K, annealed) the large value of $F(X)$ at 77 K indicates that a high proportion (perhaps >70%) of positrons are still trapped in defects. This suggests two distinct types of trap, one with $F \sim 4.01$ and the other with F between 3.82 and 3.86. It is not possible to say whether in the annealing process one type of trap ($F = 4.01$) changes into the other, or whether they are both present after the deformation and that the $F = 4.01$ traps dominate.

The steep prevacancy slope (dF/dT) of annealed cadmium in the range 100–350 K is recognized as being extraordinary; its elucidation should be helped by the observation that at 320 K, positrons annihilating in the annealed metal yield the same line parameter F as those annihilating in defects.

In the case of cadmium (A), if 100% trapping be assumed, the sharp fall in F over the region 4–25 K might indicate either changes in the electron environment within a defect, or changes in the proportions trapped by different types of defect. An important question, for zinc and cadmium at least, is whether the low temperature rises in F have the same cause in both annealed and deformed specimens. In this event, one must beware: Because equations of the type $F = PF_1 + (1 - P)F_2$ are normally invoked,[3] similar magnitudes of change in F (e.g., zinc) imply quite different trapped proportions. If the origin lies in thermal detrapping[19] from, say, grain boundaries, which might indeed correspond to a larger F than, say, edge dislocations, it would be necessary to explain why traps containing a high concentration of conduction electrons, relative to core electrons, are so very shallow. Alternatively, if only partial (<100%) trapping is occurring, the variation in F might reflect a change in the trapping rate; then potential varriers[20] and the contributions to diffusion rates of positron scattering on electrons, phonons, and crystal imperfections[21] would have to be considered. Perhaps impurities or surface annihilations play a part. Further detailed work on many metals is required at these low temperatures.

We are pleased to thank Professor E. R. Dobbs and Dr. M. J. Lea for their interest and the gift of a cadmium crystal. We are indebted to the Science Research Council for financial support. One of us (F.El K.) would like to thank the Sudanese Energy Commission for sponsorship.

[1]A. Seeger, J. Phys. F 3, 248 (1973).
[2]R. N. West, Adv. Phys. 22, 263 (1973).
[3]P. Rice-Evans, T. Hlaing, and D. B. Rees, J. Phys. F 6, 1079 (1976).
[4]P. C. Lichtenberger, C. W. Schulte, and I. K. MacKenzie, Appl. Phys. 6, 305 (1975).
[5]A. Seeger, Appl. Phys. 7, 85 (1975).
[6]D. Segers, L. Dorikens-Vanpraet, and M. Dorikens, Appl. Phys. 13, 51 (1977).
[7]P. Rice-Evans, T. Hlaing, and I. Chaglar, Phys. Lett. 60A, 368 (1977).
[8]D. Herlach, H. Stoll, W. Trost, H. Metz, T. E. Jackman, K. Maier, H. E. Schaefer, and A. Seeger, Appl. Phys. 12, 59 (1977).
[9]P. Rice-Evans, T. Hlaing, and I. Chaglar, Phys. Rev. Lett. 37, 1415 (1976).
[10]S. Mantl and W. Triftshauser, in Proceedings of the Fourth International Conference on Positron Annihilation, Helsingor, Denmark, 1976 (unpublished), paper E22.
[11]S. Berko and J. C. Erskine, Phys. Rev. Lett. 19, 307 (1968).
[12]P. Kubica and A. T. Stewart, Phys. Rev. Lett. 34, 852 (1975).
[13]P. Rice-Evans and T. Hlaing, J. Phys. F 7, 821 (1977).
[14]L. C. Smedskjaer, M. J. Fluss, D. G. Legnini, M. K. Chason, and R. W. Siegel, J. Phys. F 7, 1715 (1977).
[15]D. S. Gemmell, Rev. Mod. Phys. 46, 129 (1974).
[16]E. Segrè, *Experimental Nuclear Physics* (Wiley, New York, 1953), Vol. I, p. 296.
[17]K. G. Lyn, R. Ure, and J. G. Byre, Acta Met. 22, 1075 (1974).
[18]H. P. Leighly, Appl. Phys. 12, 217 (1977).
[19]I. K. MacKenzie, Phys. Rev. B 16, 4705 (1977).
[20]W. Frank and A. Seeger, Appl. Phys. 3, 61 (1974).
[21]W. Brandt, Appl. Phys. 5, 1 (1974).

ON THE TRAPPING RATE OF POSITRONS IN DEFORMED LEAD OVER THE TEMPERATURE RANGE 4–100 K

P. RICE-EVANS, I. CHAGLAR and F. El KHANGI
Physics Department, Bedford College, University of London, London NW1, Great Britain

Received 28 November 1977

The trapping of positrons in annealed and plastically deformed samples of lead has been studied over the temperature range 4–100 K. The rate of trapping by defects has been found to be independent of temperature – a finding that supports the golden rule positron trapping model.

This letter demonstrates that the trapping rate of positrons in plastically deformed lead is essentially independent of temperature over the range 4–100 K. In the theoretical debate, the evidence favours the quantum mechanical trapping approach rather than the classical diffusion model.

It is well known that defects in metals, e.g. vacancies [1], dislocations [2] and voids [3], can trap positrons. In the absence of defects, positrons annihilate in the metal with low-momentum conduction electrons and with higher-momentum inner core electrons, in characteristic proportions. Trapping alters these proportions and this fact has been exploited experimentally to assess defect concentrations and defect parameters such as monovacancy formation energies, etc. [4–6]. In these studies positrons are assumed to thermalise before annihilation [7] and hence their low energies are considered insignificant.

In the trapping model, the rate σ at which thermalised positrons are trapped by a unit concentration of defects is compared with the annihilation rate of the positrons. The fraction of positrons trapped at annihilation is given by

$$P = \frac{\sigma C/\lambda}{1 + \sigma C/\lambda}$$

where C, the concentration rate, is considered constant, and $1/\lambda$ is the positron lifetime. To assess the temperature dependence and allow a comparison with theory one may write $\sigma = \sigma_0 T^x$.

Experimentally, the first studies of the temperature dependence of the trapping rate, by vacancies in gold [8], found none (i.e., $x = 0$); and in our laboratory, we have obtained no temperature dependence in plastically deformed copper over the range 77–273 K [9]. However, recently, in the lower temperature range 4–77 K, various dependencies have been observed in both annealed and deformed samples, e.g. in copper [10, 11], cadmium [12, 13], gold [12] and zinc [13]. It has proved difficult to distinguish any defect trapping rate temperature dependence from other possible effects arising out of the characteristics of the metals.

In the present experiment the shape of the 511 keV annihilation line has been studied with a high resolution (1.15 keV for the 514 keV ^{85}Sr line) germanium gamma ray detector. It is assumed that positrons quickly thermalise on entering the lead, and that the e^- momentum of the $e + e^-$ pair causes a Doppler broadening of the annihilation line. It is well known [5, 6] that the line narrows when positrons are trapped in defects, and this can be expressed with the linear parameter $F = PF_t + (1 - P)F_f$, where F is a parameter, in our case defined in ref. [14], calculated for each 511 keV peak containing 900 000 counts (each acquired in a two hour run).

The samples consisted of two lead discs, initially 3.0 mm thick and 10 mm diameter, derived from Johnson–Mathey 99.9995% pure rod, etched in dilute nitric acid, which sandwiched a carrier-free 90 μC ^{22}NaCl centrally and directly evaporated positron source. The samples were placed in a cryostat regulated to within 1 K by an Oxford Instrument controller in conjunction with a gold–iron thermocouple. To allow a full nucleation and growth of grains, the annealing consisted of maintaining the specimen at 520 K for 42 hours below 10^{-6} torr. In lead, most defects anneal out rapidly at room temperature. Hence the deformed samples were prepared by compression at 77 K, and during the transfer into the cryostat the momentary warm up did not exceed 120 K.

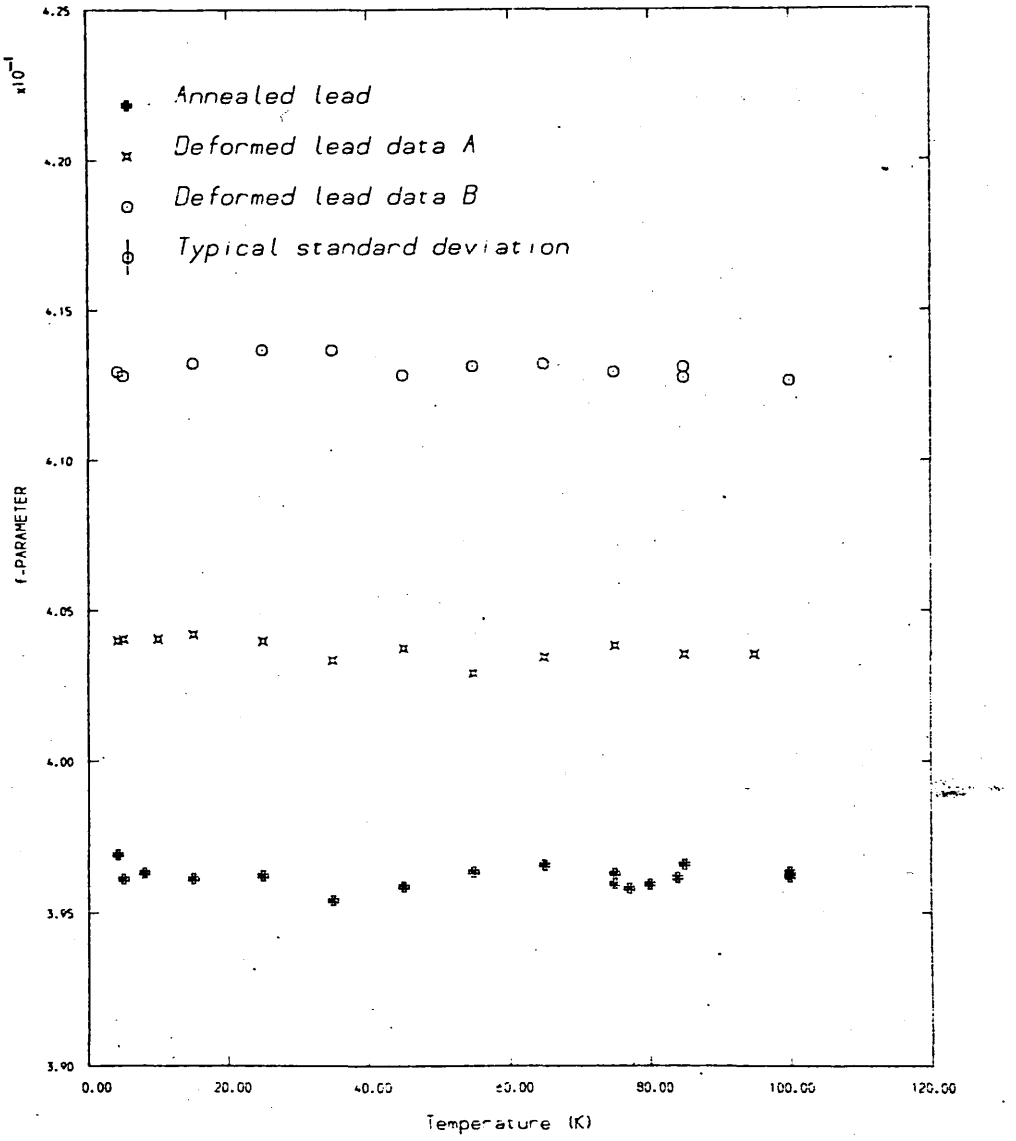

Fig. 1. The variation of the F parameter with temperature for annealed, lightly deformed (A), and strongly deformed (B) specimens of lead.

In fig. 1, the variation of the F parameter with temperature is shown for three specimens. The lower set of points concerns the annealed sample which was assumed to contain an insignificant number of defects with $F = F_f$ and $P = 0$. The upper set corresponds to a sample that had undergone a 15% compression (i.e. thickness reduction), and the intermediate set to a separate 5% compression. After another annealing the sample was later subjected to a 25% compression, and the value of F obtained from three points taken at 77 K was 0.4141 ± 0.0005. Hence the top set of points virtually corresponds to saturation trapping, i.e. $F = F_t$ and $P = 1$. The intermediate set of points on the 5% sample would not be flat if the positron trapping rate were temperature dependent. In fact one sees an approximately flat line yielding $x = -0.03 \pm 0.02$, i.e. no temperature dependence is observed.

Several theoretical models have been proposed. Classically, a $T^{1/2}$ dependence for the vacancy trapping rate was predicted by Connors and West [15] for free-

ly propagating positrons: a $T^{-1/2}$ rate was suggested by Seeger [16] governed by the diffusion of positrons arising from frequent scattering with acoustic phonons. This approach was extended by Frank and Seeger [17] who obtained the expression

$$\sigma = \frac{4\pi r_0}{\Omega}\left[\frac{1}{D_+} + \frac{1}{k_0 r_0 \Delta r_0}\right]^{-1},$$

where the positron diffusion coefficient D_+ would be temperature dependent. $k_0 r_0 \Delta r_0$ represents a capture rate. Brandt [18], who considered the effects of positron scattering on electrons, phonons and crystal imperfections, obtained a diffusion coefficient of the form:

$$(D_+)^{-1} = AT + BT^{1/2} + DT^{-d}.$$

An alternative quantum mechanical approach to trapping was initiated by Hodges [19] who found that the rate was independent of temperature. This result was supported by Bergersen and Taylor [20] for freely propagating positrons, and by McMullen and Hede [21] for strongly phonon-scattered positrons in the weak trapping limit. In recent months temperature independence has been reasserted by Bergersen and McMullen [22] for dislocations with the hypothesis that excess energies are absorbed by electron–hole pair formation; and by McMullen [23] on the basis of estimates of positron densities at the defects and their dependence on temperature and positron–phonon scattering.

From fig. 1, one may observe that lead appears to be free of the extraneous trapping effects observed in other polycrystalline metals at low temperatures [10–13]. This suggests deep traps dominate. Furthermore, the experiment finds an insignificant temperature dependence for the positron trapping rate in the range 4 K to 77 K. Although McMullen's calculations [23], relating trapping rates to densities of untrapped positrons, are limited to a hydrogenic trapped state in a monovacancy it appears likely that the golden rule positron trapping theory can be extended to account for other defects. On the basis of the present results, we shall not be surprised if the extension of the theory indicates a temperature independent trapping rate for dislocations.

It is a pleasure to thank Professor E.R. Dobbs for his interest and the Science Research Council for financial support. We are indebted to members of the computer staff, Dr. P. Pal, Mr. P. Taylor, Mr. J. Turner and Mr. C. Kirton for their advice and assistance. One of us (F. El K.) wishes to thank the Sudan Atomic Energy Commision for sponsorship.

References

[1] B.T.A. McKee, W. Triftshauser and A.T. Stewart, Phys. Rev. Lett. 28 (1972) 358.
[2] R.M.J. Cotterill, K. Petersen, G. Trumpy and J. Traff, J. Phys. F2 (1972) 459.
[3] O. Mogensen, K. Petersen, R.M.J. Cotterill and B. Hudson, Nature 239, p. 98.
[4] M.W. Thompson, Defects and radiation damage in metals (Cambridge Univ. Press, London, 1969).
[5] A. Seeger, J. Phys. F3 (1973) 248.
[6] R.N. West, Adv. Phys. 22 (1973) 263.
[7] P. Kubica and A.T. Stewart, Phys. Rev. Lett. 34 (1975) 852.
[8] B.T.A. McKee, H.C. Jamieson and A.T. Stewart, Phys. Rev. Lett. 31 (1973) 634.
[9] P. Rice-Evans and Tin Hlaing, J. Phys. F7 (1977) 821.
[10] P. Rice-Evans, Tin Hlaing and I. Chaglar, Phys. Rev. Lett. 37 (1976) 1415.
[11] S. Mantl and W. Triftshauser, Proc. 4th Intern. Conf. on Positron annihilation (Helsingor, 1976) Paper E22.
[12] D. Herlach et al., Appl. Phys. 12 (1977) 59.
[13] P. Rice-Evans, I. Chaglar and F. El Khangi, submitted for publication.
[14] P. Rice-Evans, Tin Hlaing and D.B. Rees, J. Phys. F6 (1976) 1079.
[15] D.C. Connors and R.N. West, Phys. Lett. 30A (1969) 24.
[16] A. Seeger, Phys. Lett. 40A (1972) 135.
[17] W. Frank and A. Seeger, Appl. Phys. 3 (1974) 61.
[18] W. Brandt, Appl. Phys. 5 (1974) 1.
[19] C.H. Hodges, Phys. Rev. Lett. 25 (1970) 284.
[20] B. Bergersen and D.W. Taylor, Can. J. Phys. 52 (1974) 1594.
[21] T. McMullen and B. Hede, J. Phys. F5 (1975) 669.
[22] B. Bergersen and T. McMullen, Solid State Commun. 24 (1977) 421.
[23] T. McMullen, J. Phys. F7 (1977) 2041.

PHILOSOPHICAL MAGAZINE A, 1978, VOL. 38, NO. 5, 543–558

Positron annihilation in lead

By P. RICE-EVANS, I. CHAGLAR and F. A. R. EL KHANGI
Department of Physics, Bedford College, University of London,
Regent's Park, London NW1 4NS, England

[Received 8 May 1978 and accepted 5 July 1978]

ABSTRACT

The Doppler-broadening of the radiation from positrons annihilating in lead has been measured over the temperature range 4·2–600 K. The creation of monovacancies at the higher temperatures has been studied. On the basis of several hypotheses, including positron self-trapping and divacancy production, values of the monovacancy formation enthalpy have been estimated. The trapping of positrons by defects introduced by compression of the lead at 77 K has been investigated : complete annealing occurs before 300 K.

§ 1. INTRODUCTION

When positrons from a radioactive source enter a metal they rapidly thermalize (Carbotte and Arora 1967, Kubica and Stewart 1975). They survive with a mean lifetime (τ_f) of about 200 ps before they annihilate with an electron. Broadly, two possibilities exist : the free positron can annihilate with a conduction electron or with a (higher momentum) core electron. The relative proportions may be defined by a ratio $R_f = N_{cond}/(N_{cond} + N_{core})$. An annealed metal at a particular temperature will have a characteristic value of R_f.

It is known that if defects are present in a lattice, for example, vacancies (McKee, Triftshäuser and Stewart 1972), voids (Mogensen, Petersen, Cotterill and Hudson 1972) dislocations (Cotterill, Petersen, Trumpy and Traff 1972) or grain boundaries (Lyn, Ure and Byrne 1974), they are liable to trap positrons. At defects, geometrical distortions exist and the local electron environment is affected. Positrons may then experience an attractive potential and become bound. Thus when trapped positrons annihilate, the proportion of conduction-electron annihilation (R_d) is likely to differ from R_f. The value of R_d will depend on the type of defect concerned.

In practice what happens is that a percentage of the incident positrons is trapped—depending on the concentration of defects (C), the positron diffusion, and the nature of the traps. It is often possible to determine R_d and R_f in positron annihilation experiments ; and then, in defected specimens, measurements of intermediate values of R will indicate in a linear fashion the fraction of positrons trapped. These values may be used to assess changing concentrations of defects.

In this experiment the characteristics of lead have been investigated. By observing the annihilations in annealed samples up to the melting point the thermal creation of vacancies has been measured and estimates of the

monovacancy formation energy (E_v) have been made. Also the declining concentration of defects, initially introduced into samples by plastic deformation, has been monitored during annealing.

§ 2. Experimental approach

The positron annihilation technique normally relies on one of three experimental approaches (for reviews, see Seeger 1973 b, West 1973). The first is lifetime spectrometry. If, for example, a ^{22}Na source be used, the emission of a positron is accompanied by the emission of a 1·28 MeV gamma-ray, and its subsequent annihilation is registered by the emergence of two 511 keV photons. A measurement of the delay interval with two scintillation counters yields information on local electron densities.

The second is the γ–γ angular-correlation method. The annihilation mass of the e^+e^- pair appears as two 511 keV photons emerging in opposite directions. Small deviations from 180° in the laboratory frame give indications of transverse momentum due to the energy of the annihilating electron—the thermal energy of the positron being negligible. Typically, two scintillation counters connected in coincidence are situated behind thin slits which sit on radial arms that can rotate about an axis through the specimen. The angular distributions are therefore localized electron-momentum distributions.

A third method, which has been adopted in the present experiment, is to study the shape of the 511 keV-annihilation-photon line with a high resolution detector (fig. 1). The momentum of the annihilating electron causes a Doppler-broadening of the lineshape. The photon energies are actually

$$E_\gamma = m_0c^2(1 \pm v/2c),$$

Fig. 1

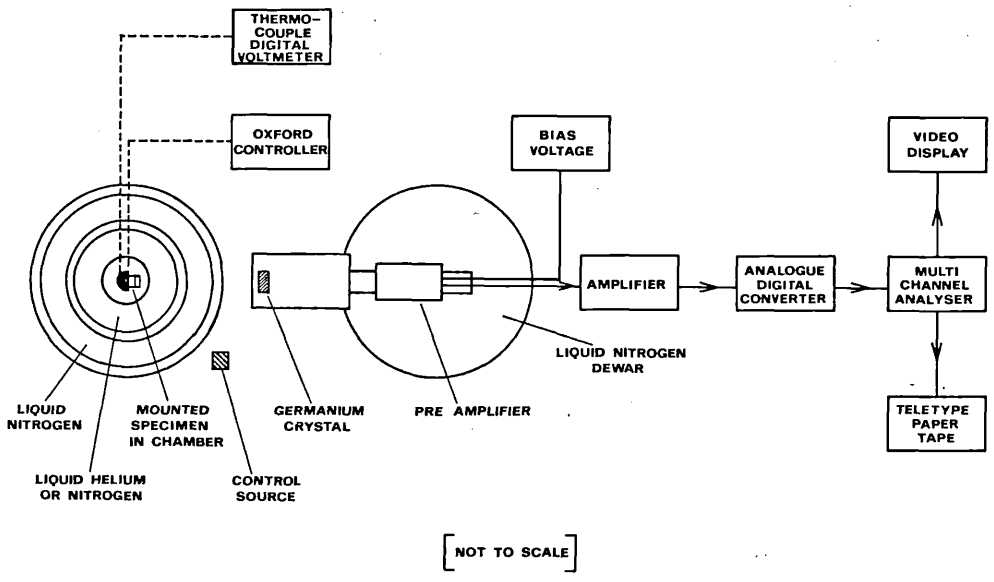

The liquid helium cryostat and gamma-ray detector.

where $v/2$ is the velocity component of the e^+e^- centre of mass in the direction of emission of the two photons. To illustrate the magnitude of the effect: a 6 eV Fermi electron can cause a photon shift of up to 1·3 keV. In fig. 2 one sees the response of a germanium detector to a monoenergetic 514 keV nuclear gamma-ray. The intrinsic linewidth of the measuring system at this energy, i.e. the full width at half maximum, is 1·15 keV. In addition, a typical annihilation 511 keV photon lineshape is plotted: the increased width is the result of the Doppler-broadening. Although this method does not offer the fine resolving power of the angular correlation technique, its higher efficiency partially compensates for this because it allows faster measurement with better statistics; the method is therefore suitable for defect studies.

Fig. 2

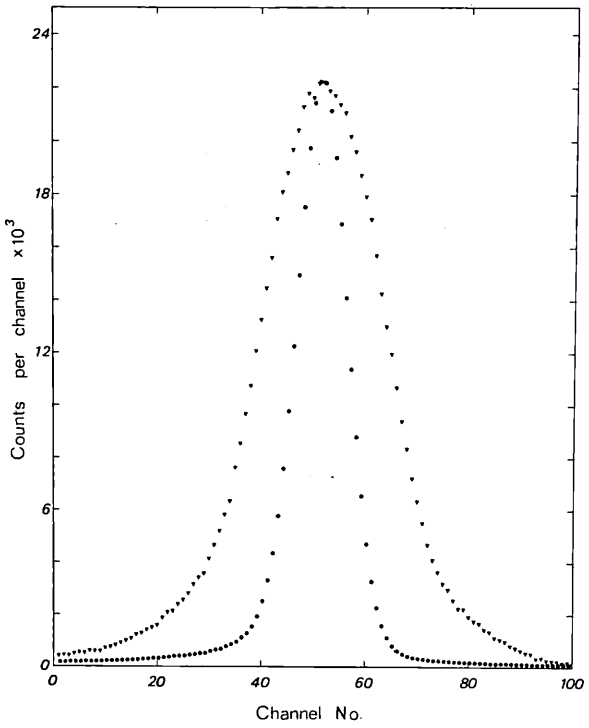

A comparison of lineshapes. The intrinsic response of the detector system to a monoenergetic 514 keV gamma-ray from strontium 85 is shown. The wider 511 keV annihilation line is a result of the Doppler-broadening of the radiation. (N.B. the peak positions have been adjusted to overlap.) ▼ = 511 keV annihilation line; ● = 514 keV Sr-85 line.

In the case of annihilations with conduction electrons it can be shown that the energy distribution of the photons is an inverted parabola centred at $E_\gamma = m_0c^2$, extending to $E_\gamma = m_0c^2(1 \pm v_F/2c)$ where v_F is the Fermi velocity. On the other hand, annihilations with core electrons result in photon distributions that appear to be reasonably described by a Gaussian curve. Because

the velocities of core electrons, on the average, exceed those of conduction electrons, the Gaussian curve is likely to be broader than the parabola.

Figure 3 shows how the line shape may be analysed in the two components. Sophisticated curve-fitting computer programmes are required to take account of the intrinsic resolution of the system, but reasonable minimized χ^2-fits are obtainable, and the areas of the Gaussian and parabolic components can be estimated within a few per cent.

Fig. 3

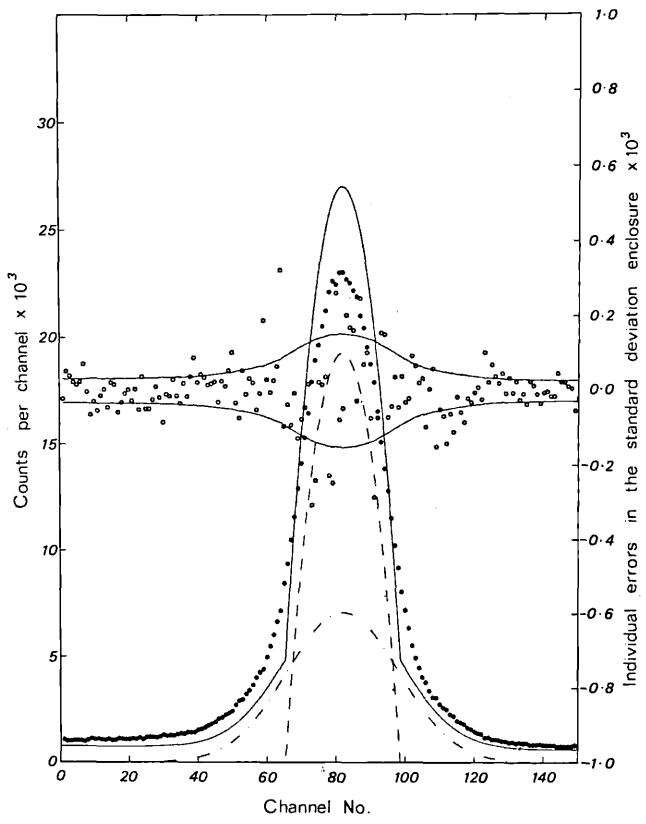

A typical experimental annihilation line. Curve-fitting programmes allow for the intrinsic lineshape, and analyse the data into two components of parabolic and Gaussian form.

In practice it is convenient to use a simple parameter F to indicate changes in the proportions of the components. F is defined as the number of counts in a central region of the line divided by the counts in the whole line. This parameter is therefore merely the height of the peak ; it has the advantage over, say, the linewidth (σ^2) because it is linearly related to R. Any narrowing (say) of the lineshape as a function of temperature would then be seen as an increase in F.

§ 3. Trapping model

In the trapping model (e.g. see Seeger 1973 a, b) the thermalized positron is assumed to diffuse through the metal until either it annihilates as a free particle, or it becomes trapped at a defect. If the number and lifetime of untrapped positrons are denoted by n_f and τ_f $(=1/\lambda_f)$; and if it is assumed that there are different types of traps with atomic concentrations C_j, positron trapping rates σ_j, with numbers n_j and lifetimes τ_j of trapped positrons $(j=1, 2, \ldots)$, then the rate equations are

$$\frac{dn_f}{dt} = -\lambda_f n_f - \sum_j \sigma_j C_j n_f + N, \tag{1}$$

and

$$\frac{dn_j}{dt} = -\lambda_j n_j + \sigma_j C_j n_f \tag{2}$$

where the detrapping of positrons is assumed to be negligible, and where N is the flux of incident positrons into the metal per unit time. In the steady state

$$\frac{dn_f}{dt} = 0$$

and

$$\frac{dn_j}{dt} = 0.$$

Hence we can calculate the fractions of annihilations that occur in the free and trapped states :

$$P_f = \lambda_f (n_f/N) = \frac{\lambda_f}{\lambda_f + \sum_j \sigma_j C_j}, \tag{3}$$

and

$$P_j = \lambda_j (n_j/N) = \frac{\sigma_j C_j}{\lambda_f + \sum_j \sigma_j C_j}. \tag{4}$$

In experiments where it is hoped to monitor the concentration of defects as a function of temperature it is important to consider whether the trapping rate σ per unit defect concentration varies with temperature. Frank and Seeger (1974) and Seeger (1975) have recognized that the transition into a bound state might be slow if the binding energy is large compared with the maximum phonon energies in the crystal, and after considering both the diffusive motion of the positron towards the trap and the overcoming of a barrier prior to trapping, they obtained for the trapping rate

$$\sigma = \frac{4\pi r_0}{\Omega_A}\left[\frac{1}{D_+} + \frac{1}{k_0 r_0 \Delta r_0}\right]^{-1}, \tag{5}$$

where Ω_A is the atomic volume, r_0 the capture radius, and $k_0 r_0 \Delta r_0$ the capture rate. The positron diffusion coefficient (D_+) may be a function of temperature (T); indeed Seeger (1975) found a $T^{-1/2}$ dependence for diffusion governed

by acoustic phonon scattering, except at the lowest temperatures where it became temperature independent. However, the position is not clear : both theoretically and experimentally, conflicting results have been reported. Some recent theoretical work by McMullen (1977) has predicted that the positron trapping rate should be independent of temperature ; and we (Rice-Evans, Chaglar and El Khangi 1978 a) have confirmed this for defects in plastically deformed lead over the range 4–100 K. In the absence of convincing evidence to the contrary, determinations of monovacancy formation enthalpies (H_{1v}) usually assume that σ is temperature independent. Seeger (1973 b) estimated that the errors in H_{1v} would amount to 0·01, 0·02 and 0·03 eV for experiments with a maximum sensitivity at 300, 600 and 900 K, respectively : i.e. not large.

§ 4. Measurements

In the experiment the lead specimens were derived from 99·9995% pure rod from Johnson–Matthey. The samples consisted of lead discs, initially 3·00 mm thick and 10 mm diameter, which were etched in dilute nitric acid. The positron source, 90μC, carrier-free ^{22}NaCl solution, was evaporated directly on to a central region of 3 mm diameter on one side of each of the two discs. The samples in a sandwich configuration were then mounted in a cryostat regulated to within 1 K by an Oxford Instrument controller in conjunction with a gold–iron/chromel thermocouple (Rice-Evans, Hlaing and Chaglar 1976 a). The annealed samples were conditioned by maintaining them in a furnace at 520 K for 42 hours in a vacuum below 10^{-6} torr.

Three plastically deformed samples were prepared from annealed discs. The first (A) received a (20%) compression at room temperature, but as the results will show, the defects rapidly annealed out at this temperature. The second (B) received a 15% thickness reduction at 77 K ; care was taken to ensure the sample did not rise in temperature above 120 K in being swiftly (2 min) transferred to the cryostat. The third specimen (C) similarly received an intermediate (5%) compression.

Figure 1 shows a sketch of the apparatus. At each temperature setting, the multichannel analyser accumulated pulses from the detector over a period of 2 hours. In this way each 511 keV photopeak contained approximately 900 000 counts. Simultaneously, a source of monoenergetic 497 keV gamma-rays, ^{103}Ru, placed outside the cryostat, also contributed to the spectrum. The narrow 497 keV peak was used to monitor each run ; any significant electronic drift in the system would cause a broadening of this peak, and hence the run could be rejected.

The line parameter F, referred to in § 2, is defined in our customary fashion (Rice-Evans *et al.* 1976 b) ; here, it is the number of counts in the central 18 channels divided by the counts in the whole line totalling 150 channels. In figs. 5 and 6, F is plotted as a function of temperature, for annealed and deformed specimens.

Twenty years ago it was thought that the character of positron annihilation-radiation might be affected when a metal enters the superconducting state. Shafroth and Marcus (1956) found no evidence for this in lead in two-photon coincidence measurements ; and no significant change is here observed in the Doppler-broadening graphs at 7·2 K (figs. 5 and 6).

Fig. 4

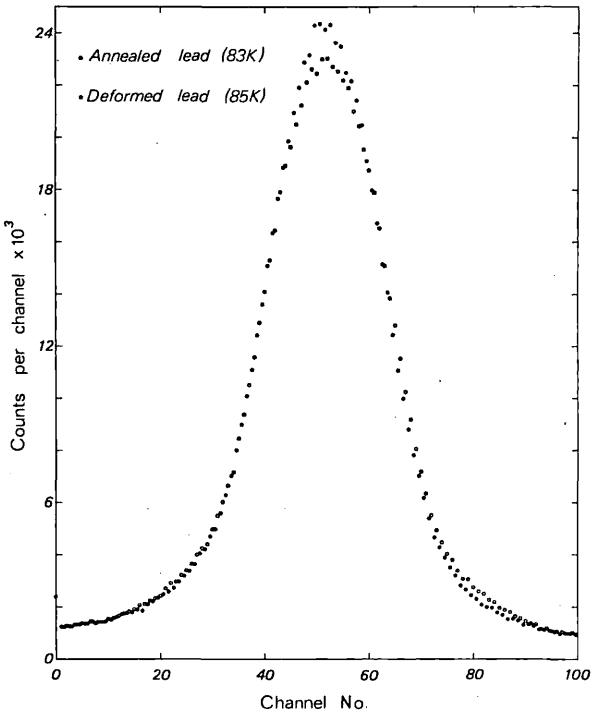

A comparison of two 511 keV annihilation lines. The narrower line for the deformed sample reflects the trapping of positrons at defects and hence more annihilations with conduction electrons.

Fig. 5

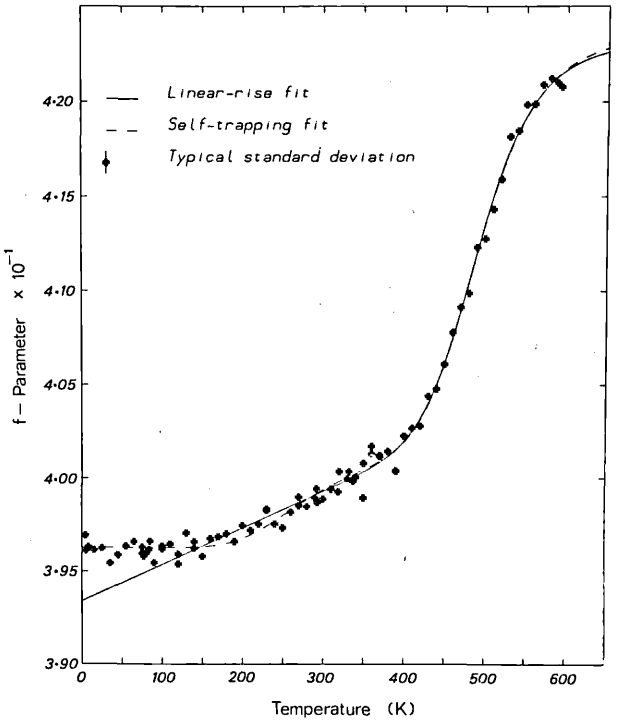

The variation of the F parameter with temperature for the annealed specimen of lead. The steep rise above 400 K is associated with the thermal creation of monovacancies.

Fig. 6

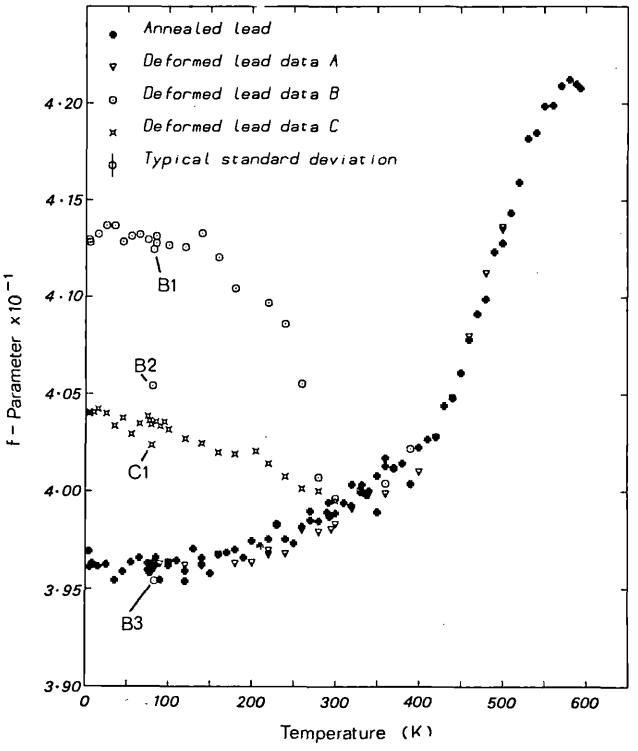

F values for the three deformed samples of lead, contrasted with those for the annealed sample. In data B, the sharp decline above 160 K shows the annealing of the defects. Some return points are shown: B1 was taken immediately after run B (140 K), B2 after B (260 K), B3 after B (390 K), and C1 after C (200 K).

§ 5. Thermal creation of monovacancies

According to statistical thermodynamics (see Seeger 1973 a, b), the atomic concentration of vacancies in thermal equilibrium in a crystal is given by:

$$C_{1v} = \exp(-G_{1v}/kT). \tag{6}$$

The Gibbs free energy of monovacancy formation G_{1v} may be expressed as

$$G_{1v} = H_{1v} - TS_{1v}, \tag{7}$$

where the enthalpy H_{1v} is the work done under conditions of constant temperature and pressure in creating a single vacancy in a crystal, keeping the total number of atoms in the crystal constant. The entropy of monovacancy formation S_{1v} results from changes in the vibration spectrum of the crystal associated with the introduction of a vacancy, and is positive. Hence

$$C_{1v} = \exp(S_{1v}/k) \exp(-H_{1v}/kT). \tag{8}$$

The positron-annihilation-peak parameter F, referred to in the second section, may be used linearly to indicate the proportion of positrons trapped. For monovacancies, we write for a measured value of F :

$$F = F_f P_f + F_{1v} P_{1v}, \tag{9}$$

where F_f corresponds to 100% positron annihilations in the free state, and F_{1v} to 100% annihilations in the trapped state, with $P_f + P_{1v} = 1$. We expect F_{1v} to exceed F_f because positrons trapped in vacancies will be more likely to annihilate with conduction electrons. From (4) and (6) we have

$$C_{1v} = \frac{1}{\sigma\tau_f} \frac{F - F_f}{F_{1v} - F}, \tag{10}$$

and with (8) we obtain

$$\frac{F - F_f}{F_{1v} - F} = (\sigma\tau_f) \exp(S_{1v}/k) \exp(-H_{1v}/kT). \tag{11}$$

In principle, the positron annihilation data can be fitted with this equation, and a value of H_{1v} determined. In fig. 5, the rise in F for temperatures above 430 K indicates the increasing concentration of vacancies, and hence the increasing number of positrons being trapped.

Two other clear features are seen. There is an almost linear rise in F with temperature in the pre-vacancy region, 150→430 K, and below 150 K the graph is flat. In fitting the high-temperature data (> 430 K) an important question is whether the pre-vacancy slope in F should be assumed to continue, and hence should be extrapolated and suitably accounted for.

Considerable controversy surrounds the interpretation of this pre-vacancy slope. Originally it was considered to be simply associated with changing electron densities as a result of thermal expansion. (Triftshaüser and McGervey 1975, Jamieson, McKee and Stewart 1974). However, this explanation has been thwarted by the discovery for cadmium by Lichtenberger, Schulte and MacKenzie (1975) that the slope did not continue as the temperature diminished. In lead too, there is a break : fig. 5 shows it to be at about 150 K.

Another interpretation exists—but this too has been disputed (see § 7). The sensible approach would seem to be to fit the data in accord with the different models, and then to consider the differences in the calculated parameters.

With the assumption that the pre-vacancy slope essentially concerns the free positron in the lattice, we can write $F_f = F_f^\circ(1 + \beta T)$ for the region above 150 K. Equation (11) becomes

$$F = \frac{F_f^\circ(1 + \beta T) + F_{1v} A \exp(-H_{1v}/kT)}{1 + A \exp(-H_{1v}/kT)}. \tag{12}$$

This expression has been fitted to the curve for annealed lead (fig. 5) and the best values of the parameters are displayed in the table. It is assumed that F_{1v} is independent of temperature. The absence of a plateau at high temperatures in fig. 5 almost certainly indicates either less than 100% trapping of

The results of fitting the parameter F for the annealed specimen of lead, according to several theoretical models.

Analysis	F_t (0 K)	F_{1v}	$(\mu/\lambda)\exp(s/k)$	H_{1v} (eV) ($\pm 0{\cdot}02$)	χ^2/κ 80 points
(1) Simple model F_t = constant 320→593 K	0·4003	0·4244	$1{\cdot}56\times10^5$	0·51	1·18 (34 points)
(2) Monovacancies plus linear rise above 150 K	0·3929	0·4233	$10{\cdot}9\times10^5$	0·60	1·05
(3) Monovacancies plus divacancies plus linear rise above 150 K	0·3929	0·4231	$14{\cdot}2\times10^5$	0·61	1·07
(4) Monovacancies plus self-trapping	0·3963	0·4236	$6{\cdot}02\times10^5$	0·56	1·16
(5) Monovacancies plus divacancies plus self-trapping	0·3963	0·4237	$5{\cdot}09\times10^5$	0·56	1·03

positrons or, perhaps, increasing divacancy trapping. Although it is conceivable that F_{1v} might vary with temperature, one would then expect other types of defect to show a similar variation. There is no evidence for this at low temperatures (see fig. 6).

§ 6. Thermal creation of divacancies

In principle, neighbouring single vacancies may bind together to form divacancies. In an f.c.c. crystal with coordination number z there are $\frac{1}{2}z$ possible orientations of such a nearest-neighbour divacancy. Thermodynamic arguments (see Seeger 1973 a, b, Nanao, Kuribayashi, Tanigawa and Doyama 1973) allow one to write for the concentration of divacancies :

$$C_{2v}=\tfrac{1}{2}z\exp(-G_{2v}/kT), \tag{13}$$

where the Gibbs free energy of divacancy formation is

$$G_{2v}=H_{2v}+TS_{2v}. \tag{14}$$

Ignoring higher vacancies, the total vacancy concentration

$$C_v=C_{1v}+2C_{2v}. \tag{15}$$

Introducing the Gibbs free energy of divacancy binding, we have

$$G_{2v}{}^B=2G_{1v}-G_{2v}=H_{2v}{}^B+T\Delta S_{2v}, \tag{16}$$

where the divacancy binding enthalpy is defined by

$$H_{2v}{}^B=2H_{1v}-H_{2v}, \tag{17}$$

and the association entropy of divacancies ΔS_{2v} is equated with the negative of the binding entropy

$$\Delta S_{2v} = S_{2v} - 2S_{1v} = -S_{2v}{}^{B}. \tag{18}$$

Hence

$$C_{2v} = \tfrac{1}{2} z \exp(\Delta S_{2v}/k) \exp(H_{2v}{}^{B}/kT)(C_{1v})^2. \tag{19}$$

Intuitively, one would expect the larger volume of a divacancy to result in the photon line shape parameter F_{2v}, corresponding to 100% trapping of positrons in divacancies, being larger than F_{1v}. In this event one may analyse the data of fig. 5 to search for divacancies.

Extending eqn. (9) to include divacancies (in accord with Nanao *et al.* 1973)

$$F = F_f P_f + F_{1v} P_{1v} + F_{2v} P_{2v} \tag{20}$$

and substituting eqns. (3), (4), (8), (13) and (14) :

$$F = \frac{\begin{array}{r} F_f + F_{1v}(\sigma_{1v}\tau_f)\exp(S_{1v}/k)\exp(-H_{1v}/kT) \\ + F_{2v}(\sigma_{2v}\tau_f)(z/2)\exp(S_{2v}/k)\exp(-H_{2v}/kT) \end{array}}{\begin{array}{r} 1 + (\sigma_{1v}\tau_f)\exp(S_{1v}/k)\exp(-H_{1v}/kT) \\ + (\sigma_{2v}\tau_f)(z/2)\exp(S_{2v}/k)\exp(-H_{2v}/kT) \end{array}}, \tag{21}$$

where the trapping rates (σ_{1v}) and (σ_{2v}) refer to monovacancies and divacancies. This equation has been fitted to the data on the annealed specimen (fig. 5) and the results are displayed in the table.

§ 7. Metastable states and self-trapping

Lichtenberger *et al.* (1975) first observed for Cd that the pre-vacancy behaviour of F cannot be correlated directly with thermal lattice expansion. This has also been noted in indium and gold (Rice-Evans, Chaglar and El Khangi 1978 b) ; and in the lead data (fig. 5) a significant change of slope is seen at about 150 K. In their discussion, Lichtenberger *et al.* argued that the intermediate sloping region might be the result of phonon-assisted trapping by transient dilatations.

An alternative explanation for the change of F in the intermediate temperature region has been given by Seeger (1975). He suggested that a polarization of the lattice as a result of the strong positron interaction with acoustic phonons would cause the positron to be self-trapped in states of negative binding energy —i.e. metastable states. This would be analogous to Landau self-trapping of positive holes in ionic crystals, recently developed in the theory of polarons.

Specifically, Seeger concluded the probability (P_{st}) for self-trapping will be given by

$$P_{st}(T) = \frac{1}{1 + B^{-1}T^{3/2}\exp[\epsilon(\kappa_0)/kT]}, \tag{22}$$

where $\epsilon(\kappa_0)$ is an energy given by

$$\epsilon(\kappa_0) = \frac{3\hbar^2\kappa_0{}^2}{2m_+} - \tfrac{1}{2}\frac{\epsilon_d{}^2\kappa_0{}^3}{K}, \tag{23}$$

where κ_0 is an upper cut-off of the wavenumber, m_+ is the band mass, K is a combination of elastic constants, ϵ_d is the positron deformation potential parameter ; and where

$$B = \prod_j \frac{\nu_j}{\nu'_j} (2\hbar^2/m_+k)^{3/2}/\Omega. \tag{24}$$

Ω is the atomic volume and ν_j, ν'_j are the vibrational frequencies of the crystal with free or self-trapped positrons.

We have applied the self-trapping model to our measurements on lead. With the assumption that trapping by vacancies will always predominate, one would expect the parameter F to be related to P_{st} by

$$F = F_{1v}P_{1v} + \{F_f(1-P_{st}) + F_{st}P_{st}\}(1-P_{1v}). \tag{25}$$

Hence we can write

$$F = \frac{F_f + (F_{st}-F_f)\{1+B^{-1}T^{3/2}\exp(\epsilon/kT)\}^{-1} + F_{1v}A\exp(-H_{1v}/kT)}{1+A\exp(-H_{1v}/kT)}. \tag{26}$$

Theoretical arguments have been advanced against the possibility of positrons being self-trapped. Leung, McMullen and Stott (1976) conceived of two sorts of positron self-trapping in metals :

(*a*) extended self-trapping, where the positron might be trapped by a weakly distorted lattice that has retained much of its periodic character ; and

(*b*) compact self-trapping, formed by a gross ionic re-arrangement of the lattice which destroys the periodic character.

They described extended self-trapping with an harmonic elastic continuum model but found that the positron–phonon coupling strength was inadequate by a factor of two or three for self-trapping to occur. As for compact self-trapping, although energetically it might be possible in some metals, the ionic re-arrangements envisaged would require times considerably in excess of the positron lifetime ($\sim 10^{-10}$ s). Hence Leung *et al.* (1976) concluded that self-trapping was unlikely to occur in metals.

Hodges and Trinkhaus (1976) have also investigated this problem : using lattice theory without a wavenumber cut-off, they found that for most metals the positron–lattice coupling strength somewhat below that necessary for self-trapping. However, lead is apparently one of the few cases where metastable self-trapping is predicted.

In view of the unresolved nature of the argument, the sensible approach would appear to be to keep an open mind and to look for evidence in the data. We have, therefore, fitted our data on lead with the expression (26) ; the values are presented in § 8.

§ 8. Results

The expressions derived in the previous sections have been fitted to the data by the University of London computer, using a least-squares minimization-routine. Reasonable results were obtained in all cases, and they are shown in the table.

In the first case, no assumptions were made for an underlying variation in F_f. The simple model (eqn. (11)) was fitted to the points above 320 K.

In the second case, F_f was taken as constant below 150 K, but for all temperatures above this a linear rise was accepted. With $F_f = F_f^0(1+\beta T)$, the calculated slope $\beta = 53 \times 10^{-6}$ K^{-1}.

The third case was similar to the second, except that divacancies were sought in addition to monovacancies. In eqn. (21), with $F_f = F_f^0(1+\beta T)$, the best values were $\beta = 53 \times 10^{-6}$ K^{-1}, $A_{2v} = 70 \times 10^4$, $F_{2v} = 0{\cdot}4235$ and $H^B = 0{\cdot}044$ eV.

In the fourth case, evidence for self-trapping (eqn. (26)), was sought. The best parameters were $F_{st} = 0{\cdot}4026$, $\epsilon = 0{\cdot}156$ eV and $B = 21 \times 10^5$ K$^{3/2}$.

Finally, in the fifth case, both self-trapping and divacancies were allowed for. In eqn. (21), with $F_f \equiv F_f + (F_{st} - F_f)(1 + B^{-1}T^{3/2} \exp(\epsilon/kT))^{-1}$, the best values were $F_{st} = 0{\cdot}4026$, $F_{2v} = 0{\cdot}4230$, $\epsilon = 0{\cdot}148$ eV, $B = 1{\cdot}53 \times 10^6$, $A_{2v} = 1{\cdot}16 \times 10^6$, and $H^B = 0{\cdot}21$ eV.

§ 9. Conclusions

An alternative method for determining vacancy formation energies is to compare dilatometric measurements with X-ray lattice measurements. Any differences detected in samples undergoing thermal expansion are attributable to the creation of vacancies: the monovacancy concentration at a given temperature T is given by the expression

$$\frac{\Delta N}{N} = 3\left(\frac{\delta L}{L_0} - \frac{\delta a}{a_0}\right),$$

where L_0 and a_0 are values of length and lattice parameter at a low reference temperature T_0, and δL and δa are the increases associated with a rise in temperatures to T.

Feder and Nowick (1967) applied this technique to pure (5N) lead, choosing $T_0 = 20$°C, and they obtained a vacancy concentration at the melting point of $\Delta N/N = 1{\cdot}7 \times 10^{-4}$. They estimated the monovacancy formation energy to be $0{\cdot}49 \pm 0{\cdot}10$ eV, and the formation entropy to be $0{\cdot}7 \pm 2{\cdot}0\,k$.

Our simple analysis of points above 320 K gives a value for the monovacancy formation energy of $0{\cdot}51 \pm 0{\cdot}02$ eV. This is almost identical with the $0{\cdot}49 \pm 0{\cdot}03$ eV obtained for lead by McKee *et al.* (1972) in a positron-annihilation angular-correlation experiment for a temperature range above 300 K. It is striking that both these values agree with the dilatometric value, although a rather large error, 0·1 eV, is quoted for the latter.

It is unfortunate that the dilatometric measurements were not extended below 20°C to observe whether anything analogous to the prevacancy rise is seen. Incidentally, the dilatometric data for cadmium (Feder and Nowick 1972) give little grounds for hope.

In cases (2) and (3) we have assumed the underlying linear rise is continued to high temperatures as one might expect if thermal expansion were the origin of the rise at intermediate temperatures. However, the flat graph for F below 150 K endows no confidence in this interpretation. And if the effects of thermal lattice expansion were significant we would not expect the discrepancy between the estimated 0·60 eV and the dilatometric value to be so large. We

therefore remain sceptical, in spite of the quality of the fit to the data. One point to note is that the slope β, 53×10^{-6} K^{-1}, is nearly twice the coefficient of linear expansion, 28×10^{-6} K^{-1}.

The self-trapping model is considered in cases (4) and (5). The resulting H_{1v}, 0·56 eV, is higher than the 0·49 eV dilatometer value but it is within the quoted error. Of course, positron self-trapping would not be seen in dilatometer experiments ; at any instant only one positron could exist in the sample! The fit over the full range of 80 points is very reasonable. Hence on the basis of positron annihilation alone, we conclude that the self-trapping model is the most plausible, and hence the value of $0{\cdot}56 \pm 0{\cdot}03$ eV is best. After all it would be absurdly arbitrary just to take points above 320 K with a constant F_t.

Case (5) includes provision for divacancies. Although a fair fit is obtained, the estimated ratio of divacancies to monovacancies is not more than 0·3% at the melting point. This is hardly convincing.

There is a temptation to apply Occam's razor to the positron annihilation results : ' it is vain to do with more what can be done with fewer '. In estimating monovacancy formation energies one is faced with a dilemma : whether to believe the absolute, but relatively crude dilatometer measurements, or alternatively, the sensitive, but somewhat insecure values obtained with the positron self-trapping model. For the present we would be wise to adopt a Cartesian position and await confirmation of the interpretation. Eventually there can be little doubt that the sensitive positron technique will be transcendent.

§ 10. Annealing of deformed samples

Annealing experiments on electron-irradiated pure lead have been reported by Birtcher, Lwin and Koehler (1974) and Schroeder and Schilling (1976). With electrical resistivity measurements, recovery stages 1–V concerning the migration and annihilation of vacancies and interstitials, have been investigated over temperatures ranging down to 1·5 K (for a review, see Schilling and Sonnenberg 1973). They found that up to 50% of the radiation damage annealed out below 5 K.

The positron annihilation technique is valuable in the study of concentrations of defects. For example, Petersen, Nielsen and Evans (1976) have identified the stages of isochronal annealing in plastically deformed molybdenum on the basis of lifetime and Doppler-broadening data.

The nature of a particular defect will be associated with a characteristic value of the parameter F. Hence a study of changing values of F in the recovery stages of a defected sample can indicate the defects involved and their relative concentrations. For example, Hautojärvi, Vehanen and Mikhalenkov (1976) have shown that the traps in deformed iron at room temperature are dislocations.

In principle, one might expect each type of defect to have a characteristic Doppler lineshape ; hence a careful analysis of a single experimental line into components might reveal the relative concentrations if more than one type of defect were present. The method is not yet sufficiently refined to do this. Nevertheless, changes in defect concentrations—e.g. in annealing of dislocations and in recrystallization—can be monitored in a sequence of lineshape measurements.

In the present experiment, three plastically deformed lead samples have been studied. Unlike electron irradiation, compression results in high concentrations of a variety of defects, especially dislocations. The results are shown in fig. 6. Sample A was deformed at room temperature and one can see that virtually all the defects have rapidly disappeared. Specimens (B) and (C) were compressed at 77 K. The approach adopted was first to reduce the temperature to 4·2 K, and then to accumulate the photon spectrum over 2 hour intervals, in a series of increasing temperatures. Twenty minutes were required between runs to record the data and raise the temperature to a new value.

Specimen B shows only the slightest annealing in the range up to 130 K ; thereafter the rate increases speecially above 200 K. The point (B2) at 77 K was taken immediately after the point (B, 260 K) ; incidentally, the equal values of F suggest that our previous finding (Rice-Evans *et al.* 1978 a), that the positron trapping rate is independent of temperature, is valid up to 260 K. Complete recovery apparently occurs at about 300 K. The lightly (5%) deformed specimen (C) shows a similar annealing curve for a lower concentration of defects.

A fourth deformed sample was subjected to a 25% compression at 77 K. The resulting value of F was 0·4141 at 77 K. When we compare this with $F = 0{\cdot}4129$ at 77 K for sample (B), we can conclude that the trapping of positrons in sample (B) approaches saturation, i.e. 100%, at low temperatures.

One might expect in the annealing curves to see some structure corresponding to changes in the defects ; for example, clustering in a narrow temperature range might result in different F values and this would become apparent in the graphs. However, in the present measurements it is possible that the statistical fluctuations are large enough to mask these effects. There can be little doubt that positron annihnilation, and especially the Doppler-broadening technique, will in future be refined to allow an identification of defect categories and a close examination of their behaviour with rising temperatures.

Acknowledgments

It is a pleasure to thank Professor E. R. Dobbs for his support. One of us (F.A.R.El.K) would like to thank the Sudanese Atomic Energy Commission for the award of a scholarship. We are grateful to the Science Research Council for financial aid.

References

Birtcher, R. C., Lwin, Y., and Koehler, J. S., 1974, *Phys. Rev. Lett.*, **33**, 899.
Carbotte, J. P., and Arora, H. L., 1967, *Can. J. Phys.*, **45**, 388.
Cotterill, M. J., Petersen, K., Trumpy, G., and Traff, J., 1972, *J. Phys.* F, **2**, 459.
Feder, R., and Nowick, A. S., 1967, *Phil. Mag.*, **15**, 805 ; 1972, *Phys. Rev.* B, **5**, 1244.
Frank, W., and Seeger, A., 1974, *Appl. Phys.*, **3**, 61.
Hautojärvi, P., Vehanen, A., and Mikhalenkov, V. S., 1976, *Appl. Phys.*, **11**, 191.
Hodges, C. H., and Trinkhaus, H., 1976, *Solid St. Commun.*, **18**, 857.
Jamieson, H. C., McKee, B. T. A., and Stewart, A. T., 1974, *Appl. Phys.*, **4**, 79.

KUBICA, P., and STEWART, A. T., 1975, *Phys. Rev. Lett.*, **34,** 852.
LEUNG, C. H., MCMULLEN, T., and STOTT, M. J., 1976, *J. Phys.* F, **6,** 1063.
LICHTENBERGER, P. C., SCHULTE, C. W., and MACKENZIE, I. K., 1975, *Appl. Phys.*, **6,** 305.
LYNN, K. G., URE, R., and BYRNE, J. G., 1974, *Acta metall.*, **22,** 1075.
MCKEE, B. T. A., TRIFTSHÄUSER, W., and STEWART, A. T., 1972, *Phys. Rev. Lett.*, **28,** 358.
MCMULLEN, T., 1977, *J. Phys.* F, **7,** 2041.
MOGENSEN, O., PETERSEN, K., COTTERILL, R. M. J., and HUDSON, B., 1972, *Nature, Lond.*, **239,** 98.
NANAO, S., KURIBAYASHI, K., TANIGAWA, S., and DOYAMA, M., 1973, *J. Phys.* F, **3,** L225.
PETERSEN, K., NIELSEN, B., and EVANS, J. H., 1976, *Phil. Mag.*, **34,** 685.
RICE-EVANS, P., CHAGLAR, I., and EL KHANGI, K., 1978 a, *Phys. Lett.* A, **64,** 450 ; 1978 b, *Phys. Rev. Lett.*, **40,** 716.
RICE-EVANS, P., HLAING, T., and CHAGLAR, I., 1976 a, *Phys. Rev. Lett.*, **37,** 1415.
RICE-EVANS, P., HLAING, T., and REES, D. B., 1976 b, *J. Phys.* F, **6,** 1079.
SCHILLING, W., and SONNENBERG, K., 1973, *J. Phys.* F, **3,** 322.
SCHROEDER, H., and SCHILLING, W., 1976, *Radiat. Effects*, **30,** 243.
SEEGER, A., 1973 a, *Crystal Lattice Defects*, **4,** 221 ; 1973 b, *J. Phys.* F, **3,** 248 ; 1975, *Appl. Phys.*, **7,** 85.
SHAFROTH, S. M., and MARCUS, J. A., 1956, *Phys. Rev.*, **103,** 585.
TRIFTSHÄUSER, W., and MCGERVEY, J. D., 1975, *Appl. Phys.*, **6,** 177.
WEST, R. N., 1973, *Adv. Phys.*, **22,** 263.

On the Temperature Dependence of Positron Annihilation in a Single Crystal of Cadmium

P. Rice-Evans, I. Chaglar and F.A.R. El Khangi,
Department of Physics, Bedford College, University of London,
Regent's Park, London, NW1 4NS. Great Britain.

The Doppler-broadened photon spectra arising from positrons annihilating in a single crystal of cadmium have been studied over the temperature range from 4.2 K to its melting point. A comparison is made with data from annealed and deformed cadmium samples. Line-height parameters indicate peculiar behaviour at low temperatures and in the prevacancy region. Line shape analysis provides good evidence for zero-point motion of positrons trapped in vacancies.

In a recent paper [1] we reported on Doppler-broadening positron-annihilation measurements in polycrystalline cadmium for temperatures ranging from 4 K to 590 K. Many questions remained unresolved, and for clarification we have turned our attention to annihilation in a single cadmium 6 N crystal.

The germanium detector has a resolution of 1.15 keV at 514 keV. Each point in the figures corresponds to a 511 keV line containing 900,000 counts, accumulated in two hours. After spark-cutting, etching and electropolishing, the two crystal elements sandwiching the directly deposited ^{22}NaCl each had a diameter of 10 mm and thickness 1.1 mm. The line-height parameter F was defined in [1].

Figure 1 shows the F-parameter plotted over the full temperature range. A new feature emerges: a definite plateau between 280 and 310K. We have repeated this region several times: Figure 2 shows the plateau for another run with all points taken in the cryostat. The slope ($\beta = \Delta F/F_o \Delta T$) of the approximately linear rise in the region 160-280K is 17.5 10^{-5} K^{-1}, i.e. 50% greater than the corresponding slope (11.2 x 10^{-5} K^{-1}) found in annealed polysrystalline cadmium [1], although the overall magnitudes of the rise are similar. The prevacancy effect therefore appears to be partially suppressed below 280K in the polycrystal.

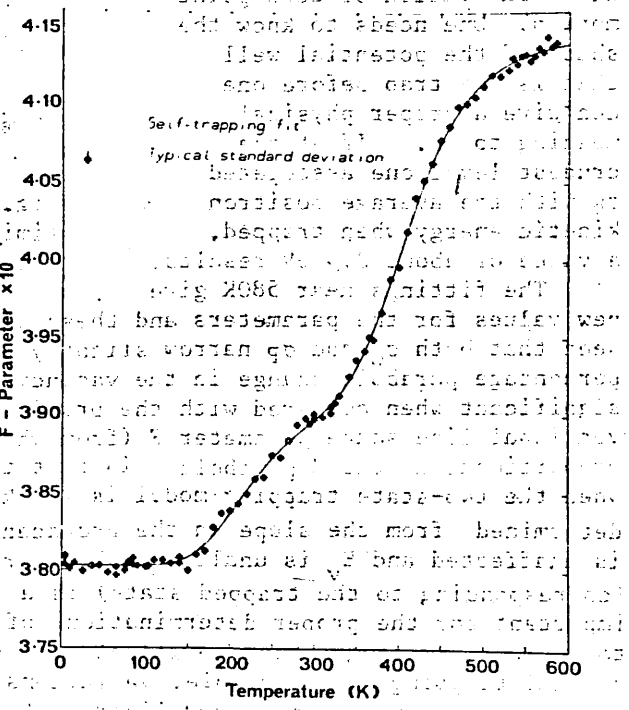

Fig.1. The variation of F with temperature.

The existence of a plateau undermines one's faith in a prevacancy rise continuing in the vacancy region [2]. The

The self-trapping model [3] appears more promising, although the angles of the plateau are a little sharp. With self-trapping employed in the fitting, the monovacancy formation energy (E_v) is 0.40 ± 0.02 eV.

We performed our customary analysis of the line shapes into a Gaussian and a parabolic component by fitting the expression:

$$f(X)=A\int_{-\infty}^{+\infty}\exp\left[-(x'-\bar{x})^2/2\sigma_G^2\right]R(x-x')dx' + B\int_{\sigma_p\sqrt{2}}^{\sigma_p\sqrt{2}}\left(1-\frac{(x'-\bar{x})^2}{2\sigma_p^2}\right)R(x-x')dx'$$

The fittings are satisfactory up to about 350K with χ^2/ν about unity. The parameters of percentage parabola, Gaussian width and parabola width are shown in Figs. 3 and 4. Above 350K χ^2/ν rises to 1.5 at 550K.

A worsening χ^2/ν in the vacancy region might be due to the zero-point motion of positrons trapped in vacancies. For some points, at the highest temperatures with saturation trapping assumed, we have convoluted an additional Gaussian broadening function with our instrumental resolution, prior to the usual analysis. (With a similar approach, Jackman et al. [4] reduced their χ^2/ν to 3.5.) The best width (σ_B) is given by the minimum χ^2/ν. In Fig.5 we see χ^2/ν reduced to unity with σ_b= 3.6 channels (at 94 eV/channel). We take this to be a clear indication of zero-point motion. One needs to know the shape of the potential well that is the trap before one can give a proper physical meaning to σ_b. If at the crudest level one associated σ_b with the average positron kinetic energy when trapped, a value of about 0.4 eV results.

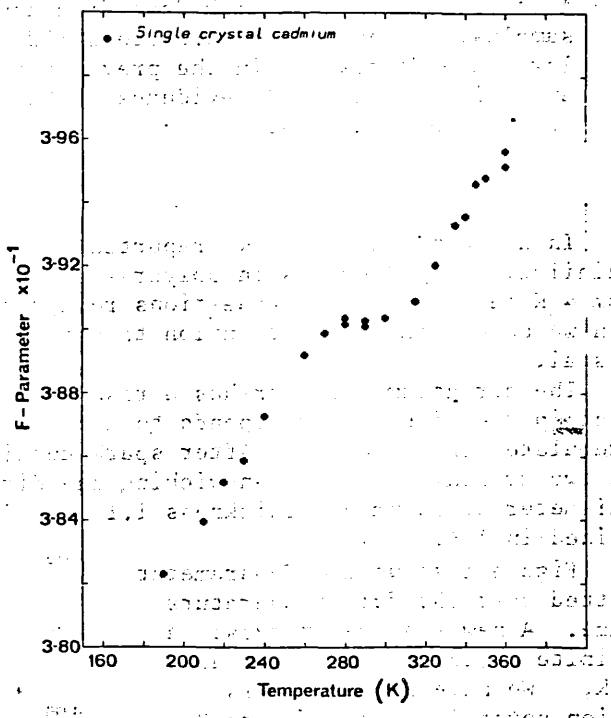

Fig.2. The variation of F over a limited range of temperature. All points taken in the cryostat.

The fittings near 580K give new values for the parameters and these are shown in Figs. 3 and 4. It is seen that both σ_G and σ_p narrow slightly with increasing temperature. The percentage parabola change in the vacancy region from 45% to 59% is most significant when compared with the previous change of 45→51%. But the conventional line shape parameter F (from which values of E_v are derived) is proportional to the % parabola. In fact this itself is of no consequence when the two-state trapping model is invoked. The underlying background, determined from the slope in the prevacancy region (e.g. Fluss et al [5]), is unaffected and E_v is unaltered. However the question of whether F_v (corresponding to the trapped state) is a function of temperature is important for the proper determination of E_v. In the near future we plan to improve our programming to include zero-point motion in regions of partial trapping. In principle, variations in the widths σ_G and σ_p for the trapped component may shed light on $F_v(T)$ and whether values for E_v

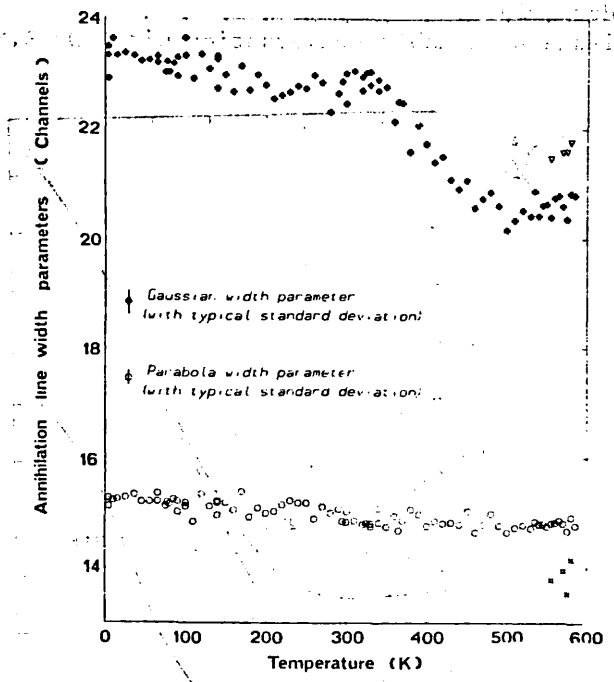

Fig.3. The parameters $\sqrt{2}\sigma_G$ and $\sqrt{2}\sigma_P$ from the simple (P+G) analysis. The additional points near 580K refer to fittings with allowance for zeropoint motion.

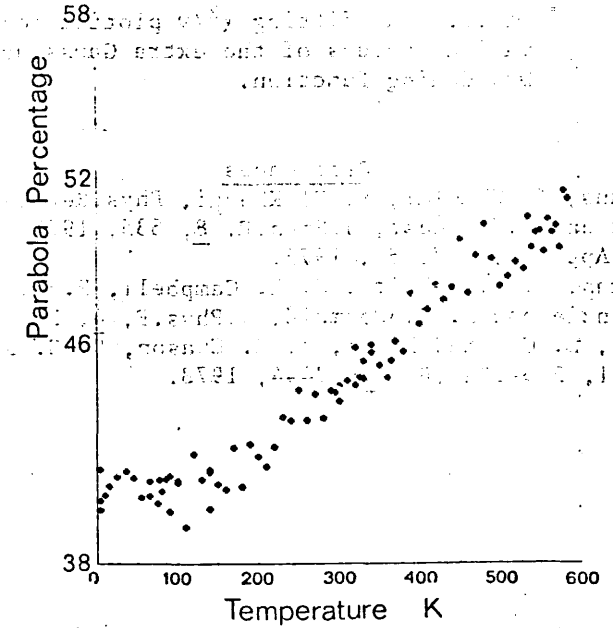

Fig.4. The percentage parabola for the simple (P+G) analysis. The high points near 580K include allowance for zero point motion.

need to be redetermined.

We acknowledge a valuable conversation with Dr R.N.West.

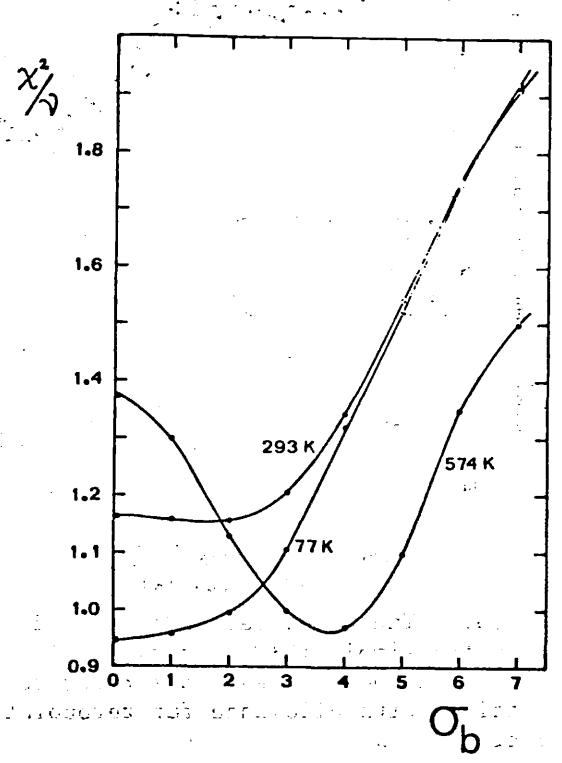

Fig.5. The fitting χ^2/ν plotted for various values of the extra Gaussian broadening function.

References

[1] P. Rice-Evans, I. Chaglar, F. El Khangi, Phys.Rev.Lett., 40, 716, 1978.
[2] M. J. Stott and R. N. West, J.Phys.F. 8, 635, 1978.
[3] A. Seeger, Appl.Phys. 7, 85, 1975.
[4] T. E. Jackman, C. W. Schulte, J. L. Campbell, P. C. Lichtenberger, I. K. MacKenzie and M. R. Wormald, J.Phys.F, 4, L1, 1974.
[5] M. J. Fluss, L. C. Smedskjaer, M. K. Chason, D. G. Leguini and R. W. Siegel, Phys.Rev.B, 17, 3444, 1978.

Proc. 5th Int. Conf. Positron Annihilation (Japan, 1979) 9A-V-3'

On Defects in Polycrystalline Cadmium

P. Rice-Evans, I. Chaglar, F.A.R. El Khangi and M.A. Moghimi
Department of Physics, Bedford College,
University of London,
Regent's Park, London, NW1 4NS. Great Britain.

Positron trapping by defects in polycrystalline cadmium has been investigated with Doppler broadening. The annihilation lines have been analysed into Gaussian and parabolic components with the additional feature of a Gaussian broadening applied to the intrinsic resolution function to account for zero-point motion of positrons in traps. The findings shed light on the nature of the defects.

In 1978 we reported on positron annihilation measurements on plastically deformed cadmium [1]. We presented Doppler-broadening line-height parameters (F) as a function of temperature for a number of cases.

We have always analysed our line shapes into Gaussian and parabolic components, but recently we have added an additional Gaussian broadening function to account for the zero-point motion of positrons in traps (for details see our paper on a single crystal of cadmium at this Tokyo Conference). Tentatively, we think our findings shed light on some prevailing questions in positron annihilation studies.

Fig. 1 shows the variation of the F-parameter over the temperature range 4-590K. Of particular interest is the narrowing of the line (i.e. increase in F) below about 20K for both annealed and defected specimens. This effect is little understood apart from the finding that it seems to disappear when the positrons annihilate in a single crystal.

As already reported, at least two types of defect are seen in the plastically deformed samples. When a sample is severely (50%) compressed at 77K, and not allowed to warm up, high values of R result (A). These begin to anneal out at about 150K. The graph of F descends to meet the annealed curve at about 330K. If the sample is then cooled again, the value of F is roughly maintained (at X).

Also, if a sample be deformed at room temperature its F value is the same as an annealed sample at

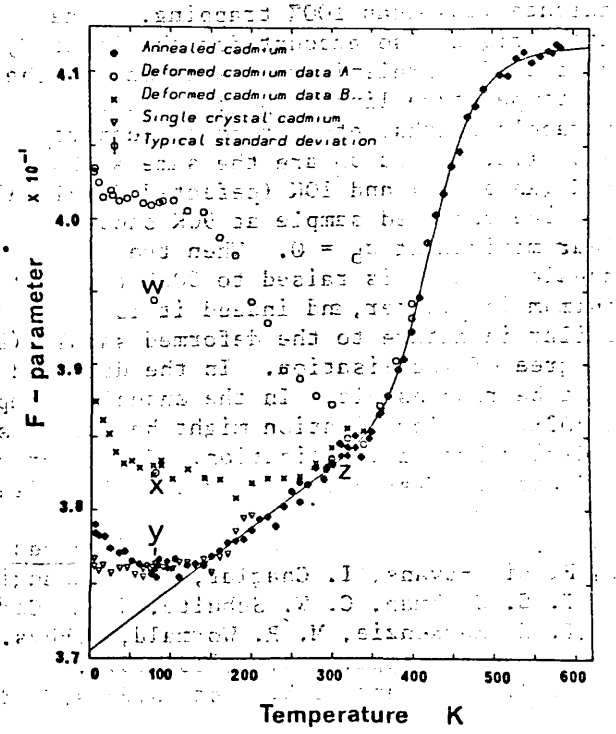

Fig.1. Variation of the line-height parameter as a function of temperature.

this temperature. However, if this deformed sample is reduced in temperature a roughly horizontal line on the graph is followed down to X, rather than the diminishing line for the annealed sample. The horizontal nature of the line ZX, compared with the sloping annealed line, suggests saturation (100%) trapping. Clearly this defect must be different from the predominant defects produced by deformation at 77K.

We have analysed our spectral lines at a few points, basically into a Gaussian and a parabolic component. However, rather than rely on the intrinsic line shape obtained with a 514 keV gamma ray, we have convoluted the latter with a Gaussian function of various widths σ_b (see Jackman et al [2]). The variation of the fitting χ^2/ν as a function of σ_b is shown in Fig.2.

In the vacancy region (580K) a clear minimum is seen at $\sigma_b \sim 3.8$ channels (at 94 eV/channel) in agreement with our findings in a cadmium single crystal. This we take to be due to zero-point motion of the positron within the trap.

A similar clear minimum is seen for the sample (A) deformed at 77K) at 10K, i.e. $\sigma_b \sim 3.4$. The similarity with vacancies is striking and prompts one to suggest that the defects in this sample have a point like structure - i.e. the positrons are localised to within one atomic cell. The flatter nature of the χ^2/ν curve, and the lower value of σ_b at the minimum χ^2/ν, might indicate less than 100% trapping. The latter might also account for the lower F, and indeed a preliminary assessment of the low temperature line shape parameters (parabola widths, etc.) tend to support this (i.e. σ_p and σ_G are the same at both 580K (Annealed) and 10K (defected Sample A).

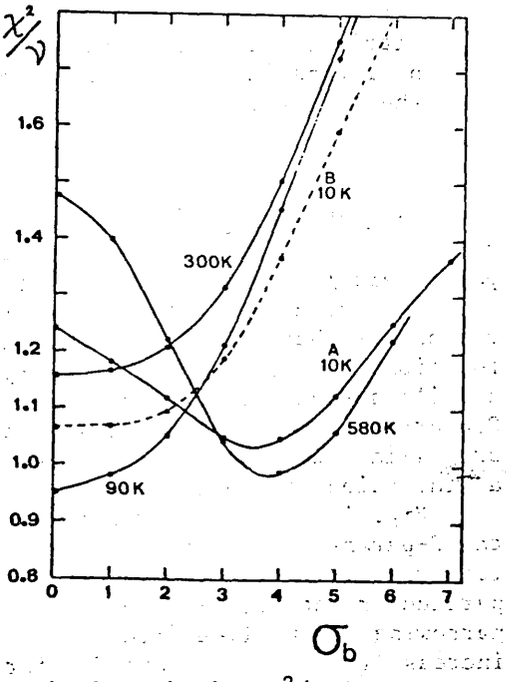

Fig.2. Fitting χ^2/ν for various values of the Gaussian broadening.

The annealed sample at 90K shows a clear minimum at $\sigma_b = 0$. When the annealed sample is raised to 300K the minimum is flatter, and indeed it is similar in nature to the deformed sample (B). These flatter minima suggest a degree of localisation. In the deformed sample (B) line-dislocations might be responsible. In the annealed sample at the prevacancy temperature of 300K, the localisation might be due to self-trapping. Seeger [3] predicted such a localisation. It is not clear whether the alternative model of Stott and West [4] does predict localisation.

References

[1] P. Rice-Evans, I. Chaglar, F. El Khangi, Phys.Rev.Lett. 40, 716, 1978.
[2] T. E. Jackman, C. W. Schulte, J. L. Campbell, P. C. Lichtenberger, I. K. MacKenzie, M. R. Wormald, J.Phys.F.4, L1, 1974.
[3] A. Seeger, Appl.Phys. 7, 85, 1975.
[4] M. J. Stott and R. N. West, J.Phys.F. 8, 635, 1978.

* Work supported by the Science Research Council, London.

BIBLIOGRAPHY

(1) Anderson, C.D., Phys. Rev. 41, 405 (1932)

(2) Wallace, P.R., Solid State Physics, ed. by F. Seitz and D. Turnbull (Academic Press Inc. N.Y. 1960) Vol. 1, Pg. 1.

(3) Gutowsky, H.S., McGarvey, B.R., J. Chem. Phys. 20, 1472 (1952)

(4) Hodges, C.H., Phys. Rev. Lett. 25, 284 (1970)

(5) Damak, A.C., Dienes, G.J., Point Defects In Metals (Gordon and Breach, New York 1963)

(6) Thompson, M.W., Defects and radiation damage in Metals (Cambridge University Press, 1969)

(7) Flynn, C.P., Point defects and diffusion (Clarendon, Oxford, 1972)

(8) Nabarro, F.R.N. Theory of Crystal Dislocations (Clarendon Press, Oxford, 1967)

(9) McKee, B.T.A., Jost, A.G.D., MacKenzie, I.K., Can. J. Phys. 50, 415 (1972)

(10) McKee, B.T.A., Triftshauser, W., Stewart, A.T., Phys. Rev. Lett. 28, 358 (1972)

(11) Mackenzie, I.K. Langstroth, G.F.O.,McKee, B.T.A. White, C.G., Can. J. Phys. 42, 1837 (1964)

(12) MacKenzie, I.K. Khoo, T.L., McDonald, A.B., McKee, B.T.A., Phys. Rev. Lett. 19, 946 (1967)

(13) Nano, S., Kuribayashi, K.K., Tanigawa, S., Doyama, M.,, J. Phys. F: Metal Phys. 3, L225 (1973)

(14) Sueoka, O., J. Phys. Soc. Japan, 36, 464 (1974)

(15) Hautojarvi, P., Tamminen, P., Jauho, P., Phys. Rev. Lett. 24, 459 (1970)

(16) Mackenzie, I.K. Eady, J.A. Gingerich, R.R., Phys. Lett. A33, 279 (1970)

(17) Petersen K., Thrane, N., Cotteril, R.M.J.., Phil. Mag. 29, 9, (1974)

(18) Grosskreutz, J.C., Millel, W.E., Phys. Lett. A28, 621 (1969)

(19) Mogensen, O.E., Petersen, K., Cotteril, R.M.J., Hudson, B., Nature, Lond. 239, 98 (1972)

(20) Cotteril, R.M.J., MacKenzie, I.K., Smedskjaer, L., Trumpy, G., Traff, H.J.O., Nature, Lond. 239, 99, (1972)

(21) Snead, C.L., Hall, T.M., Goland, A., Phys. Rev. Lett. 29, 62 (1972)

(22) Grynszpan, R., Lynn, K.G., Snead, C.L., Goland, A., Phys. Lett. 62A 6 (1977)

(23) Mantel, S., Triftshauser, W., Phys. Rev. Lett. 34, 1554 (1975)

(24) Eldrup, M., Mogenson, O.E., Evans, J.H., J. Phys. F: Metal Phys. 6, 499 (1976)

(25) Lengeler, B., Mantel, S., Triftshauser, W., J. Phys. F: Metal Phys. 8, 1691 (1978)

(26) Triftshauser, W., Appl. Phys. 5, 177 (1974)

(27) Dannefaer, S., Kerr, D.P., Kupca, S., Hogg, B., Madsen, J.W., Cotteril, R.M.J., Can. J. Phys. 58, 270 (1980)

(28) Seeger, A., J. Phys. F: Metal Phys. 3, 248 (1973)

(29) Hood, G.M., Schultz, R.J., J. Phys. F: Metal Phys. 10, 545, (1980)

(30) Gilder, H.M. Lazarus, D., Phys. Rev. B11, 4916 (1975)

(31) Herlach, D., Stott, H., Metz, H., Trost, W., Jackman, T.E., Maier, K., Schaefer, H.E., Seeger, A., Appl. Phys. 12, 59 (1977)

(32) Stott, M.J., Journal of Nucl. Mat. 69 & 70 157 (1978)

(33) Berestetskii, V.B., Lifshitz E.M., Pitaevskii, L.P., Relativistic Quantum Theory (Pergamon, Oxford 1971)

(34) Brandt, W., Paulin, R., Phys. Rev. B15 2511 (1977)

(35) Kubica, P., Stewart, A.T., Phys. Rev. Lett. 34, 852 (1975)

(36) Perkins, A., Carbotte, J.P. Phys. Rev. B1 101 (1970)

(37) Lee-Whiting, G.E., Phys. Rev. 97, 1557 (1955)

(38) Carbotte, J.P., Arora, H.L., Can. J. Phys. 45, 387 (1967)

(39) Kim, S.M, Stewart, A.T., Carbotte, J.P., Phys. Rev. Lett. 18, 385 (1967)

(40) Majumdar, C.K., Phys. Rev. 149, 406 (1966)

(41) Hamann, D.R. Phys. Rev. 146, 277 (1966)

(42) Mills, A.P., Pfeiffer, L., Phys. Rev. Lett. 36, 1389 (1976)

(43) Mills. A.P., Pfeiffer, L. Phys. Lett. A63, 118 (1977)

(44) Bergersen, B., Pajanne, E., Kubica, P., Stott, M.J., Hodges, C.H., Solid State Commun 15, 1377 (1974)

(45) Brandt, W., Appl. Phys. 5, 1 (1974)

(46) Nieminen, R.M. Manninen, M.J. (Topics in Physics, 12, Positrons in Solids, ed. by P. Hautojarvi, Springer-Verlag, Berlin Heidelberg, Germany (1979)

(47) Stott, M.J., Kubica, P., Phys. Rev. B11, 1 (1975)

(48) Kubica, P., Stott, M.J., J. Phys. F: Metal Phys. 4, 1969 (1974)

(49) Stott, M.J., West, R.N., J. Phys. F: Metal Phys. 8, 635 (1978)

(50) Hodges, C.H., Stott, M.J., Phys.Rev. B7, 73 (1973)

(51) Brandt, W., Reinheimer, J., Phys. Lett. A35, 109 (1971)

(52) Kahana, S., Phys. Rev. 129 1622 (1963)

(53) Sjolander, A., Stott, M.J., Phys. Rev. B5, 2109 (1972)

(54) Bhattacaryya, P., Singwi, K.S., Phys. Rev. Lett. 29, 22 (1972)

(55) West, R.N., Solid State Commun. 9, 1417 (1971)

(56) West, R.N., Positron Studies of Condensed Matter (Taylor and Francis Ltd. London 1974)

(57) Gupta, R.P., Siegel, R.W., J. Phys. F: Metal Phys, 9, 2353 (1979)

(58) Carbotte, J.P. Kahana, S., Phys. Rev. 139A, 213 (1965)

(59) Hede, B.B.J., Carbotte, J.P., J. Phys. Chem. Solids, 33, 727 (1972)

(60) Jamieson, H.C., McKee, B.T.A., Stewart, A.T., Appl. Phys. 4, 79 (1974)

(61) Mikeska, H.J., Phys. Lett. A24, 402 (1967)

(62) Kim, S.M., Buyers, W.J.L., J. Phys. F: Metal Phys. 6, L67 (1976).

(63) Singh, K.P., West, R.N., J. Phys. F: Metals Phys. 6, L267 (1976)

(64) Berto Laccini, M., Dupasquier, A., Phys. Rev. B1, 2896 (1970)

(65) Connors, D.C., Crisp, V.H.C., West, R.N., J. Phys. F: Metal Phys, 1, 355 (1971)

(66) Brandt W.,: In "Positron Annihilation" ed. by Stewart A.T., and Roelling, L.O., (Academic Press, New York, 1967) P. 155

(67) Bergersen, B., Stott M.J., Solid State Commun. 7, 1203 (1969)

(68) Connors, D.C., West, R.N., Phys. Lett. A30, 24 (1969)

(69) Seeger, A., Appl. Phys. 4, 183 (1974)

(70) Seeger, A., Appl. Phys. 7, 85 (1975)

(71) Hodges, C.H., J. Phys. F; Metal Phys. 4, L230 (1974).

(72) Peterson, N.L., Journal of Nucl. Materials 69 & 70, 3 (1978)

(73) Siegel, R.W., Journal of Nuclear Materials 69 & 70, 117 (1978)

(74) Bell, R.E., Nucl. Instrum. Methods 55, 1 (1966)

(75) Gedcke, D.A., McDonald, W.J. Nucl. Instrum Methods, 58, 253 (1968)

(76) Gedcke, D.A., Williams, C.W., Ortec Information Sheet-High Resolution Time Spectroscopy. 1. Scintillation Detectors (1968)

(77) Lichtenberger, P.C., Steven J.R., Newton, T.D., Can. J. Phys. 50, 345 (1972)

(78) Crisp. V.H.C., MacKenzie, I.K., West., R.N., J. Phys E6, 1191 (1973)

(79) Stewart, A.T., Can. J. Phys. 35, 168 (1957)

(80) Berko. S., Plaskett, J.S. Phys. Rev. 112, 1877 (1958)

(81) Stewart, A.T., Positron Annihilation, ed. by A.T. Stewart and L.O. Roelling (Academic Press, New York, 1967) P. 17.

(82) Berko, S., Mader, J., Appl. Phys. 5, 287 (1975)

(83) Dirac, P.A.M., Proc. Camb. Phil. Soc. Math. Phys. Sci. 26, 361 (1930)

(84) Hotz, H.P., Mathiesen, J.M., Hurley J.P., Phys. Rev. 170 351 (1968)

(85) Varotsos, P.A., J. Phys. F: Metal Phys. 8, 1373 (1978)

(86) Seeger, A., Appl. Phys. 7, 257 (1975)

(87) Seeger, A., Phys. Lett. 40A, 135 (1972)

(88) Lichtenberger, P.C., Schulte, C.W., Mackenzie, I.K., Appl. Phys. 6, 305 (1975)

(89) Trinkaus, H.,. Hodges, C.H., Journal of Nuclear Materials 69 & 70, 600 (1978)

(90) Hodges, C.H., Trinkaus, H., Solid State Commun. 18, 857 (1976)

(91) Leung, C.H., McMullen, T., Stott, M.J., J. Phys. F: Metal Phys. 6, 1063 (1976)

(92) Segers, D., Dorikens-Vanpraet, L., Dorikens, M., Appl. Phys. 13, 51 (1977)

(93) Lichtenberger P.C., Annihilation Spectrometry of defective metals using Germanium detectors, Ph. D. Thesis, University of Waterloo, 1974.

(94) Rees, D., Positron interaction in metals, M. Phil. Thesis, Bedford College, London University, 1974.

(95) HLaing, T., Positron annihilation in metals. Ph. D. Thesis, Bedford College, London University 1976.

(96) Chaglar, I., Positron annihilation in pure and defected metals, Ph. D. Thesis, Bedford College, London University, 1978.

(97) Kusmiss, J.H., Esseltine, C.D., Snead, C.L., Jr., Goland, A.N., Phys. Lett. A32, 175 (1970)

(98) Snead, C.L., Goland, A.N., Kusmiss, J.H., Huang, H.C., Meade, R., Phys. Rev. B3, 275 (1971)

(99) Bergersen, B., Taylor, D.W., Can. J. Phys. 52, 1594 (1974)

(100) McMullen T.,. Hede, B., J. Phys. F: Metal Phys. 5, 669 (1975)

(101) Seeger, A., Phys. Lett. A41, 267 (1972)

(102) Hall, T.M., Goland, A.N., Jain, K.C., Siegel R.W., Phys. Rev. B12, 1613 (1975)

(103) Mckee B.T.A., Jamieson, H.C., Stewart, A.T., Phys. Rev. Lett. 31, 634 (1973)

(104) Simmons, R.O., Balluffi, R.W., Phys. Rev. 117, 52 (1960)

(105) Simmons, R.O., Balluffi, R.W., Phys. Rev. 119, 600 (1960)

(106) Simmons, R.O., Balluffi, R.W. Phys. Rev. 125, 862 (1962)

(107) Siegel, R.W. Balluffi, R.W., Lie, K.H., Seidman, D.N., Vancancies and Interstitials in Metals, ed. by A. Seeger etal (North-Holland Publ. Co., Amsterdam, 1970) P.125

(108) Lattice Defects in Quenched Metals, ed. by R.M.J. Cotterilétal (Academic Press, London (1965)

(109) Jackman, T.E., Lichtenberger, P.C., Schulte, C.W., Appl. Phys. 5, 259 (1974)

(110) Hood, G.M., McKee, B.T.A., J. Phys. F: Metal Phys. 8, 1457 (1978)

(111) Mackenzie, I.K. Phys. Lett. 30A 115 (1969)

(112) Ramma Reddy, K., Carrigan, R.A., Nuovo Cimento LXVIB,105 (1970)

(113) Schultz, P.J., Lynn, K.G., Mackenzie, I.K., Jean, U.C., Snead, C.L., Phys. Rev. Lett. 44, 1629, (1980)

(114) Coleman, C.F., Appl. Phys. 19, 87 (1979)

(115) Fano, W., Phys. Rev. 72, 26 (1947)

(116) Shizuma, K., Nucl. Instrum. Methods 150, 447 (1978)

(117) Dauwe, Ch., Dorkins-Vanpaet, L., Dorkins L., Solid State Commun. 11, 717 (1972)

(118) Dannefaer S., Kerr, D.P., Nucl. Instrum and Methods 131, 119 (1975)

(119) Feder, R., Nowick, A.S., Phys. Rev. B5, 1244 (1972)

(120) Janot, C., George, B., Phys. Rev. B12, 2212 (1975)

(121) Simon, J.P., Vostry, P., Hillairet, J., Levy, V., Phil. Mag. 31, 145 (1975)

(122) West, R.N., (Topics in Physics, 12 Positrons in Solids, ed. by P. Hautojarvi, Springer-Verlag, Berlin Heidelberg, Germany, 1979(P.113.

(123) MacKenzie, I.K., Lichtenberger, P.C., Appl. Phys. 9, 331 (1976)

(124) Minchin, P., Meyer, A., Young, W.H., J. Phys. F: Metal 4, 2117 (1974)

(125) Singh, K.P. Goodbody, C.S., West, R.N., Phys. Lett. 55A 237 (1975)

(126) Kupca, S., Hogg, B.G., Kerr, D.P., Phys. Lett. 77A, 281 (1980)

(127) Smedskjaer, L.C., Legnini, D.G., Siegel, R.W., J. Phys. F: Metal. Phys. 10, L1 (1980)

(128) Tam, S.W., Singh, S.K., Siegel, R.W., Journal of Nuclear Materials 69 & 70, 596 (1978)

(129) Mackenzie, I.K. Phys. Lett. 77A, 476 (1980)

(130) Lynn, K.G., Snead, C.L., Hurst, J.J., J. Phys. F: Metal Phys. 10, 1753 (1980).

(131) Solid State Physics, N.W. Ashcroft and A.D. Merunin (Holt, Rinehart and Winston New York, 1976)

(132) Introduction to Solid State Physics, C. Kittel, (John Wiley and Sons Inc. New York) 5th Edition 1976

(133) Sharp J.V., Mitchell, A., Christian J.W., Acta. Met. 13 965 (1965)

(134) Doyama, M., Cotteril, R.M.J. 1979 Proc. 5th Int. Conf. on Positron Annihilation, Japan 1979 ed. by R.R., Hasiguti and K. Fujiwara (Sendai; Japan Inst. Metals) P. 89

(135) Gould, A.G. West, R.N., Hogg, B.G., Can. J. Phys. 50, 2294 (1972)

(136) Manninen, M., Nieminen, R., Hautojarvi, P., Phys. Rev. B12 4012 (1975)

(137) Triftshauser, W., Phys. Rev. B 12, 4634 (1975)

(138) Schulte, C.W., Campbell, J.L., Appl. Phys. 19 269 (1979)

(139) Buescher, B.J., Gilder, H.M., Shea, N., Phys. Rev. B 7, 2261 (1973)

(140) Dickman, J.E., Jeffery, R.N., Gustafson, D.R., Phys. Rev. B 16, 3334 (1977)

(141) Samara, G.A., Phys. Rev. Lett. 44, 670 (1980)

(142) Dickey, J.E., Acta. Met. 7, 350 (1959)

(143) Ott, A., Nortten-ott, J., Appl. Phys. 42, 3745 (1971)

(144) McKee, B.T.A., McMullen, T., J.Phys. F: Metal Phys. 8, 1175 (1978)

(145) Smedskjaer, L.C., Manninen, M., Fluss, M.J., J. Phys. F: Metal Phys. 10, 2237 (1980)

(146) Kerr, D.P., Dannefaer, S., Dean, G.W., Hogg, B.G., Can. J. Phys. 56, 1453 (1978)

(147) Hautojarvi, P., Solid State Commun. 11, 1049 (1972)

(148) Campbell, J.L., Appl. Phys. 13, 365 (1977)

(149) Campbell, J.L., Schulte, C.W., Appl.Phys.21,19(1980)

(150) Kerr, D.P., Fellows, P.D., Sullivan, D.J., West, R.N., Phys. Lett. 61A, 418 (1977)

(151) Kusmiss, J.H., Stewart, A.T., Adv. Phys. 16, 471 (1967)

(152) Dedoussis, S.P., Charalambous, S.,Chardalas, M., Phys. Lett. A62, 359 (1977)

(153) Mogensen, O.E., Trumpy, G., Phys. Rev. 188, 639 (1969)

(154) Kontrym-Sznajd, G., Paper B6, 4th Int. Conf. on Positron Annihilation, Helsingor, 1976

(155) Coston,C., Nachtrieb, N.H., J. Phys. Chem. 68, 2219 (1964)

(156) Stroud, D., Ehrenreich, H., Phys. Rev. 177, 399 (1968)

(157) Okada, T., Sekizawa, H.L., Shiotani, N., J. Phys. Soc. Japan 41, 830 (1976)

(158) Mader, J., Berko, S., Krakauer, H., Bansil, A., Phys. Rev. Lett. 37, 1232 (1976)

(159) Lynn, K.G., MacDonald, J.R., Boie, R.A., Feldman, L.C., Gabbe, J.D., Robbins, M.F., Bonderup, E., Golovchenko, J., Phys. Rev. Lett. 38, 241 (1977)

(160) Arponen, J., Hautojarvi, P., Nieminen, R.M., Pajanne, E., J. Phys. F: Metal Phys. 3, 2092 (1973)

(161) Mori, G., J. Phys. F: Metal Phys. 7, L89 (1977)

(162) Hall, T.M., Goland, A.N., Snead, C.L., Phys. Rev. B10, 3062 (1974)

(163) Kim, S.M., Buyers, W.J.L., Martel P., Hood, G.M., J. Phys. F: Metal Phys. 4 343 (1974)

(164) Dlubeck G., Brummer, O., Meyendorf, N., Appl. Phys. 13, 67 (1977)

(165) Fluss, M.J., Smedskjaer, L.C., Chason, M.K., Legnini, D.G., Siegel, R.W., Phys. Rev. B 17, 34444 (1978)

(166) Popovic, Z.D., Carbotte, J.P., Piercy, G.R., J. Phys. F: Metal Phys. 4, 351 (1974)

(167) Cotterill, R.M.J., Petersen, K., Trumpy, G., Treff, J., J. Phys. F: Metal Phys. 2, 459 (1972)

(168) Von Guerard, B., Peisl, H., Zitzmann, R., Appl. Phys. 3, 37 (1974)

(169) Tzanetakis, P., Hillairet, J., Revel, G., Phys. Stat Sol 6 75 433 (1976)

(170) Furukawa, K., Takamura, J., Kuwana, N., Tahara, R., Abe, M.J., Phys. Soc. Japan, 41, 1584 (1976)